IMMUNOMAGNETIC SEPARATION AND RAPID ELECTROCHEMICAL DETECTION STRATEGIES FOR MICROBIAL PATHOGENS

By

Emma B. Setterington

A THESIS

Submitted to
Michigan State University
in partial fulfillment of the requirements
for the degree of

MASTER OF SCIENCE

BIOSYSTEMS ENGINEERING

2010

ABSTRACT

IMMUNOMAGNETIC SEPARATION AND RAPID ELECTROCHEMICAL DETECTION STRATEGIES FOR MICROBIAL PATHOGENS

By

Emma B. Setterington

Biodefense, food safety, and water quality require the means to efficiently screen large volumes of samples for low concentrations of microbial pathogens. Rapid, sensitive, and field-ready detection methods are essential, but must also include a means to specifically extract and concentrate the target pathogen from a complex matrix. This thesis outlines three proof-of-concept approaches for rapid electrochemical detection of microbial pathogens, each beginning with immunomagnetic separation (IMS) of the target organism. Additionally, the development of an improved IMS methodology and its use in an electrochemical detection method are described.

In the first approach, target cells were detected directly by means of their ability to impede electrical current. *Bacillus cereus* (as a surrogate for *B. anthracis*) and *E. coli* O157:H7 were detected from pure culture with limits of 40 CFU/ml and 6 CFU/ml, respectively, in 65 min. In the second approach, Bovine Viral Diarrhea Virus (BVDV) from bovine serum samples was detected by means of an electroactive label, in 80 min. In the third approach, *E. coli* O157:H7 cells were electroactively labeled, magnetically positioned, and detected from pure culture with a limit of 70 CFU/ml (corresponding to 7 CFU present on the sensor) in 70 min.

Finally, an improved IMS methodology was developed for *E. coli* O157:H7 using two magnetic nanoparticle (MNP) types, and its specificity was initially evaluated against *E. coli* O55:H7 and *Shigella boydii*. The method, optimized in terms of antibody concentration, MNP concentration, and conjugation conditions, required only 35 min and yielded antibody-conjugated MNPs that were stable for up to 60 days.

ACKNOWLEDGMENTS

This research was funded in part by the U.S. Department of Homeland Security through the National Center for Food Protection and Defense under Grant R9106007101, and in part by the U.S. Environmental Protection Agency through award number RD83300501. These funding sources had no involvement in the actual research or writing of this report. The contents of this publication do not necessarily reflect the position or policy of the Federal Government.

Dr. Sudeshna Pal is acknowledged for the original development of the electrically active magnetic nanoparticles and associated immunomagnetic separation procedure. The author would like to thank Dr. Parul Jain for developing and supplying the carboxylate- and amine-functionalized magnetic nanoparticles, for aiding with transmission electron microscopy studies, and for providing consultation regarding the chemical synthesis and immunofunctionalization procedures for the non-magnetic polyaniline nanostructures. The author would like to thank Dr. Barbara C. Cloutier for her extensive contributions as a co-researcher in the immunomagnetic separation study, and for taking the lead in microbiological methods and statistical analyses. Jessica M. Ochoa and Ashley K. Cloutier are acknowledged as valuable undergraduate contributors to this study as well.

Additionally, Dr. Daniel Grooms and the MSU Large Animal Clinical Sciences Department provided bovine serum samples and anti-BVDV antibodies, Dr. Deng Zhang supplied synthesized gold nanoparticles, Dr. Reza Loloee assisted with magnetization measurements, Dr. Paul Bartlett and the MSU Center for Statistical Training and Consulting assisted with statistical analyses, Dr. Julie Funk and Dr. Shannon Manning provided bacterial cultures and advice on microbiological methods, Dr. John Linz and Dr. Elliot Ryser offered consultation on best practices in food microbiology.

Finally, the author would like to thank Dr. Evangelyn C. Alocilja for guiding this research, for advising the author's graduate program, and for providing support and encouragement throughout the author's undergraduate and graduate academic career.

TABLE OF CONTENTS

LIST OF TABLES

LIST OF FIGURES

KEY TO ABBREVIATIONS

AMNP: Amine-functionalized Magnetic Nanoparticle

AP: Alkaline Phosphatase

APS: Ammonium Persulfate

AuNP: Gold (Au) Nanoparticle

BVDV: Bovine Viral Diarrhea Virus

CMNP: Carboxylate-functionalized Magnetic Nanoparticle

CFU: Colony-Forming Unit

CV: Cyclic Voltammetry

DI: De-Ionized

EAMNP: Electrically Active Magnetic Nanoparticle

EHEC: Enterohemorrhagic *E. coli*

EIS: Electrochemical Impedance Spectroscopy

HCl: Hydrochloric acid

HRP: Horse Radish Peroxidase

IDAM: Interdigitated Array Microelectrode

IMB: Immunomagnetic Bead

Immuno-AMNP: Immunofunctionalized Amine Magnetic Nanoparticle

Immuno-CMNP: Immunofunctionalized Carboxylate Magnetic Nanoparticle

Immuno-EAMNP: Immunofunctionalized Electrically Active Magnetic Nanoparticle

Immuno-MNP: Immunofunctionalized Magnetic Nanoparticle

Immuno-PANI: Immunofunctionalized Polyaniline Nanostructures

IMS: Immunomagnetic Separation

MNP: Magnetic Nanoparticle

Nano-PANI: Polyaniline Nanostructures

PBS: Phosphate-Buffered Saline

SPCE: Screen-Printed Carbon Electrode

SPAuE: Screen-Printed Gold Electrode

ΔQ: Charge Transfer

INTRODUCTION: RESEARCH OBJECTIVES

The two primary objectives of the research contained in this thesis are as follows: (1) to develop electrochemical methods for rapid microbial pathogen detection using immunomagnetic separation (IMS) of the target organism as the starting point; and (2) to develop an improved IMS methodology for microbial pathogens and demonstrate its use in a rapid electrochemical detection method.

To meet the first objective, three distinct electrochemical detection methods were demonstrated, on a proof-of-concept basis, for various microbial pathogens. These include impedance-based detection of *E. coli* O157:H7 and *Bacillus cereus* (Chapter 2), on-chip electroactive label-based detection of Bovine Viral Diarrhea Virus (Chapter 3), and off-chip electroactive label-based detection of *E. coli* O157:H7 (Chapter 4). Each method begins with immunomagnetic separation of the target organism from its sample matrix, using either a previously developed immunomagnetic particle and IMS procedure, or a commercially available immunomagnetic particle. To meet the second objective, a new IMS methodology was developed for two different types of synthesized magnetic nanoparticles (Chapter 5), and applied to the electroactive label-based detection of *E. coli* O157:H7 (Chapter 6).

This research is significant for two main reasons. First, standard culture methods for identifying microbial pathogens are unable to provide results fast enough for perishable food screening, drinking water monitoring, or emergency detection of bio-threats. There is a tremendous need for rapid and sensitive methods of microbial detection, such as those presented in Chapters 2 through 4. Second, food safety, water quality, and biosecurity require the means to efficiently screen large quantities of food, water, or other material for microbial pathogens. Most rapid detection methods cannot handle complex matrices, and many also require lengthy

enrichment steps. Immunomagnetic separation, as presented and demonstrated in Chapters 5 and 6, is a means of quickly and specifically extracting target pathogens from their sample matrices and concentrating them prior to detection, thus eliminating both pre-enrichment steps and matrix interferences in many rapid detection schemes. Potential applications for the electrochemical detection methods and IMS methodology presented in this thesis include biosecurity and biodefense, food and water safety, agriculture and animal health, environmental protection, and point-of-care medical diagnostics.

CHAPTER 1

LITERATURE REVIEW

1.1 Microbial Pathogen Targets

1.1.1 *Escherichia coli* O157:H7

Escherichia coli O157:H7, a type of enterohemorrhagic *E. coli* (EHEC), is a highly infective food and water borne pathogen. Symptoms of infection with *E. coli* O157:H7 include abdominal cramps, bloody diarrhea, nausea, vomiting, headache, and (in 2-7% of cases) life-threatening hemolytic uremic syndrome, characterized by kidney failure and hemolytic anemia (WHO 2006). The pathogen is a fecal contaminant commonly found in raw or undercooked meat, unwashed produce, unpasteurized milk, and sewage-tainted waters.

The U. S. Food & Drug Administration estimates that the infectious dose of *E. coli* O157:H7 is 10 to 100 cells (FDA 2009). Therefore, it is not acceptable for this pathogen to be present at any level in food or water intended for human use. The World Health Organization states that to verify the safety and quality of water intended for drinking or for public distribution, *E. coli* must not be detectable in any 100-ml sample. The presence of *E. coli*, even non-pathogenic strains, is evidence of recent fecal contamination, and provides sufficient grounds to quarantine the water source for further investigation (WHO 2006). Also, the United States Centers for Disease Control and Prevention (CDC) and the National Institute of Allergy and Infectious Diseases (NIAID) classify *E. coli* O157:H7 as a "Category B" (second-highest priority) pathogen for biodefense, because of its ease of dissemination in water and food sources (NIAID 2009; CDC 2010).

The CDC cites at least nine confirmed food-linked outbreaks of *E. coli* O157:H7 infection in the U.S. from 2006 to 2009 (CDC 2010), and estimates that 70,000 *E. coli* O157:H7 infections occur each year in the U.S. alone (CDC 2008). These facts indicate a vital need for improved disease surveillance, diagnostic methodologies, prevention strategies, and food and water monitoring techniques.

The standard method of identifying *E. coli* O157:H7 from unknown samples is through enrichment in selective media, followed by growth on differential agar to isolate sorbitol non-fermenting colonies. These are identified phenotypically and serologically, and tested for Shiga toxin genes by PCR, a process lasting several days. For applications that require faster results and high throughput, *E. coli* O157:H7 can be identified (after selective enrichment) by real-time PCR, which provides a negative or positive result within 24 h. But three days are still required to confirm presumptive positive results by culture methods and PCR. With an enrichment medium that can effectively suppress non-target flora growth while allowing growth of viable *E. coli* O157:H7 cells, the standard method is able to detect <1 colony-forming unit (CFU) per gram in foods (FDA 2009).

1.1.2 *Bacillus cereus*

Bacillus cereus, a gram-positive bacterium, is a common foodborne pathogen able to cause diarrhea and abdominal pain with an infectious dose of about 10^6 organisms per gram of food (FDA 2009). Although the high infectious dose and non-fatal symptoms make this bacteria an unlikely candidate for a biological weapon, *B. cereus* is phenotypically very similar to *Bacillus anthracis*. This research utilizes *B. cereus* as a surrogate (model) organism for *B. anthracis*, a gram-positive, spore-forming bacterium which is the causative agent of anthrax.

Anthrax infection in humans takes on three forms: respiratory, gastrointestinal, and cutaneous. Respiratory anthrax is contracted by inhalation of aerosolized spores, and without treatment, is fatal in 97% of cases. The lethal dose ranges from 8,000 to 40,000 spores, or one breath at a location where the pathogen has been released (CDC 2001). Gastrointestinal anthrax is contracted by ingesting contaminated food or water, and is fatal in up to 60% of cases. Cutaneous anthrax occurs when cells or spores penetrate the skin, and is fatal in 20% of cases. *B. anthracis* is able to form spores can withstand harsh conditions, including heat, radiation, and chemicals, for long periods of time and remain infectious, making the organism an ideal agent for biological warfare (Edwards, Clancy et al. 2006). The CDC and the NIAID classify *B. anthracis* as a "Category A" priority pathogen in biodefense, because of its ease of dissemination and transmission, environmental stability, disease severity and high mortality rate, the potential for a major public outbreak or disturbance, and the need for public health action and emergency preparedness (NIAID 2009; CDC 2010).

The remarkable genetic similarity within the *Bacillus* genus makes specific detection of *B. anthracis* challenging. An unknown microorganism can be easily identified as a *Bacillus* species by standard culture methods and biochemical tests within 24 hours, but definitive identification of *B. anthracis* may require another 1-2 days (Edwards, Clancy et al. 2006).

1.1.3 Bovine Viral Diarrhea Virus

Bovine Viral Diarrhea Virus (BVDV) is a term used to describe two distinct species of virus, BVDV1 and BVDV2, which can infect not only cattle, but a wide variety of domestic and wild ruminants and pigs. BVDV1 and BVDV2 are of the genus *Pestivirus* of the family

Flaviviridae. *Pestivirus* virions consist of an envelope and a nucleocapsid, and are spherical with diameter ranging from 40 to 60 nm (ICTVdB 2006).

Acute BVDV infections can produce respiratory and reproductive symptoms as well as enteric symptoms such as diarrhea, and nearly always lead to immune suppression, making the animal vulnerable to secondary infections. Some BVDV strains can also cause long term persistent infections, which may not exhibit active symptoms, and are a major source of introduction of BVDV into herds. The United States Department of Agriculture (USDA) states that "reduction of BVDV infections in the national herd requires effective surveillance programs… and reliable means to detect both persistent and acute infections." In order to achieve this, the USDA cites the need for "robust field-ready tests that both detect and differentiate viral pathogens" (Ridpath 2010). Bovine blood serum, containing 10^3 to 10^5 virons per mL if the animal is infected, is usually used for BVDV diagnosis (Saliki, Fulton et al. 1997).

1.2 Electrochemical Biosensors for Rapid Microbial Detection

Standard culture methods for identifying pathogenic bacteria or viruses cannot provide results fast enough to be useful for perishable food screening or emergency detection as in a biological attack. There is a tremendous need for rapid and sensitive methods of microbial detection for food and water safety, animal health, environmental stewardship, and biodefense or biosecurity applications.

A biosensor is an analytical device which employs a biological element (such as antibodies, enzymes, or nucleic acids) to detect the analyte in close proximity to a transducer. A transducing mechanism is required to transform the interaction between the biological element and the analyte into a signal that can be quantified by associated electronics or signal processors.

Biosensors can be categorized based on their transducing mechanisms, the most common of which are optical, mass, electrochemical, magnetic, micromechanical, and thermal methods. Of these, electrochemical biosensors have emerged as the ideal choice for applications requiring low cost, miniaturization, and portability. In general, they require simpler equipment, are more easily integrated with electronic readout devices, and are less susceptible to environmental effects and contaminants than other analytical techniques (Palchetti and Mascini 2008).

1.2.1 Use of Conductive Polymers in Electrochemical Biosensors

Conducting polymers have found widespread application in electrochemical biosensors, since they are electrically active, compatible with biological molecules, simple to synthesize, and environmentally stable (Rahman, Kumar et al. 2008). Electrochemical biosensors most often employ conducting polymers in the form of a thin film deposited onto the working electrode, for signal amplification and/or as a platform for immobilization of biological compounds (enzymes, antibodies, or nucleic acids). One of the most studied conducting polymers is polyaniline, because its various physical, chemical, and electronic states can be controlled and exploited for various purposes. Polyaniline can be switched from the electrically insulating (semiconducting, emeraldine base) form to the conducting (metallic, emeraldine salt) form by doping with a protonic acid, and de-protonated again by addition of a base (Sarno, Manohar et al. 2005). Furthermore, polyaniline has well-defined, reversible redox chemistry, and is easily recognized in cyclic voltammetry by its characteristic oxidation and reduction peaks (Prakash 2002).

1.2.2 Use of Screen-Printed Electrodes in Electrochemical Biosensors

Traditional electrochemistry is performed in solution in a three-electrode electrochemical cell. In this system, the *working electrode* is the site at which current is measured. A potential is applied to this electrode relative to a second *reference electrode*, also in contact with the test solution, in order to create a potential at the interface between the working electrode and the solution. The *counter electrode* is part of a feedback system which can supply current to the test solution when necessary, to maintain the correct electrode-solution potential (monitored by the reference electrode) (Daniels and Pourmand 2007). An important advance in biosensor technology has been the miniaturization of electrochemical systems, which reduces sample and reagent volumes, reduces response time due to faster diffusion, makes the sensor more economical, and is more conducive to portability.

Most electrochemical biosensors today use micrometer to millimeter sized electrodes on compact sensing chips to perform electrochemistry on a small scale. The "electrochemical cell" in these miniaturized systems is simply a reaction well, which can range in volume from a few microliters to one milliliter, in contact with two electrodes (the reference and counter electrodes are usually combined in miniaturized systems). The small sensing chips often consist of screen-printed electrodes on a glass or plastic substrate. Screen-printing involves deposition of metallic or semiconductive ink to form electrodes of a specific shape and size, with constant thickness. Screen-printed electrode sensors are mass-produced, inexpensive, and often designed to be disposable, which decreases the possibility of electrode fouling, cross-contamination between samples, and irreproducibility (Palchetti and Mascini 2008). Screen-printed carbon (Obuchowska 2008; Shabani, Zourob et al. 2008) and gold (Susmel, Guilbault et al. 2003; Escamilla-Gómez, Campuzano et al. 2009; Gamella, Campuzano et al. 2009) electrodes have been recently applied to impedance-based detection of *E. coli* and other bacterial targets. Also, conductive

nanoparticles are sometimes coated onto screen printed electrodes in electrochemical biosensor assays, for signal transduction and amplification purposes. Gold is the most common choice in conductive nanoparticle for facilitating electron transfer at electrode surfaces (Lin, Chen et al. 2008). In addition to gold, other nanoparticles employed for electrochemical biosensor enhancement include silver, platinum, copper, and silicon dioxide (Wang and Hu 2009).

1.2.3 Impedance-Based and Label-Based Electrochemical Biosensors

Common electrochemical measurement techniques employed in biosensors include amperometry and voltammetry, in which a constant (amperometric) or varying (voltammetric) potential is applied between the electrodes and the resulting current flow is measured. Electrochemical impedance spectroscopy (EIS) is a technique in which an alternating current is applied at constant or varying frequency and the impedance of the electrode system is measured. Impedance is opposition to current flow due to energy dissipation (resistance) and energy storage (capacitance) by the elements in the system. Impedance is calculated as the ratio of applied voltage to response current, and can provide information about the physical and chemical phenomena occurring at the electrode-solution interface and in the bulk solution (Daniels and Pourmand 2007).

A wide variety of impedance-based biosensors have been designed for the detection of chemicals, toxins, DNA, proteins, and whole microorganisms. Typical impedance biosensors consist of a small electrode or pair of interdigitated electrodes, modified with a biological receptor (e.g., antibody, enzyme, or nucleic acid probe). The modified electrodes are immersed in solution containing the analyte, and binding of analyte to receptor creates a measurable impedance change (Zourob, Elwary et al. 2008). In faradaic impedance biosensors, a redox

couple is added to the test solution and is alternately oxidized and reduced corresponding to the applied potential, by exchanging electrons across the interface between the working electrode and the solution. A non-faradaic impedance biosensor, on the other hand, has no redox couple and is generally simpler to operate and more conducive to portability, since fewer reagents are required (Daniels and Pourmand 2007).

An important advantage of impedance biosensors is that, unlike many biosensing methods, it does not necessitate a label. A labeling step adds complexity, time, and expense to any detection assay. Since EIS can directly detect receptor-analyte binding on an electrode surface, no further labeling or modification of the bound analyte is needed. Some impedance biosensors do employ a label, however, to enhance sensitivity or selectivity (Daniels and Pourmand 2007). What follows is a survey of impedance-based biosensors for rapid pathogen detection which have been reported in the literature in recent years. Both label-based and label-free assays are discussed.

In 2003, Susmel et al. captured *B. cereus* and *L. monocytogenes* on a screen-printed gold electrode (SPAuE) functionalized with antibodies. Cells bound to the SPAuE impede or electrostatically repel the ferrocyanide redox probe from the electrode surface, as measured by chronocoulometry (in which charge is measured over time in the presence of a constant applied potential) and cyclic voltammetry (CV). The bacteria were detected at 10^3 to 10^4 CFU/ml from pure culture in about 1.5 h (Susmel, Guilbault et al. 2003).

In 2004, Yang et al. captured *E. coli* O157:H7 on an indium-tin oxide interdigitated array microelectrode (IDAM) functionalized with antibodies. Cells bound to the IDAM increased the impedance of the system in the presence of ferri-/ferrocyanide redox couple, as measured by

both EIS and CV. A detection limit 10^6 CFU/ml was achieved from pure culture in less than 1 h (Yang, Li et al. 2004).

In 2004 and 2005, Radke and Alocilja captured *E. coli* O157:H7, *E. coli* K12, and *Salmonella* on a gold IDAM functionalized with antibodies. Cells bound to the IDAM increased the impedance of the system as measured by EIS, with no redox probe. The bacteria were detected at 10^4 CFU/ml from pure culture, or 10^7 CFU/ml from romaine lettuce, in only 5 to 10 min (Radke and Alocilja 2004; Radke and Alocilja 2005; Radke and Alocilja 2005).

In 2007, Li et al. captured *E. coli* O157:H7 on a gold electrode functionalized with antibodies via a protein A monolayer. Cells bound to the electrode increased the impedance of the system in the presence of ferri-/ferrocyanide redox couple, as measured by both EIS and CV. *E. coli* O157:H7 was detected at 10^3 CFU/ml from pure culture in only 10 min (Li, Wang et al. 2007). In 2008, the same group improved the detection limit of this system to 10^2 CFU/ml from pure culture by measuring capacitance rather than impedance (Li, Wang et al. 2008).

In 2008 Obuchowska captured bacteria (*E. coli* and other species) nonspecifically on an unmodified screen-printed carbon electrode (SPCE) simply by immersing it into the cell solution Immobilized cells were lysed by the addition of lysozyme, and released proteins which fouled electrode, leading to an increase in impedance in the presence of ferricyanide redox probe, as measured by CV. Unlysed cells, did not affect the impedance signal. *E. coli* was detected at 10^4 CFU/ml from pure culture and environmental water, in about 1 h (Obuchowska 2008).

In 2008 Shabani et al. functionalized an SPCE microarray with a bacteriophage, which acted as both a receptor to capture *E. coli* cells from solution, and a lysing agent, to lyse captured cells. Ions released from lysed cells increased the solution conductivity and therefore decreased

the impedance of the system as measured by EIS, with no redox probe. *E. coli* was detected at 10^4 CFU/ml from pure culture in about 30 min (Shabani, Zourob et al. 2008).

In 2008, Laczka et al. captured *E. coli* and *Salmonella* on a gold IDAM functionalized with antibodies. Cells bound to the IDAM decrease the capacitance of the system, in the absence of a redox probe, as measured by EIS. *E. coli* was detected at 10^4 CFU/ml from pure culture in about 1 h (Laczka, Baldrich et al. 2008).

In 2008, Geng et al. captured *E. coli* on a gold electrode functionalized with antibodies. Cells bound to the electrode increased the impedance of the system in the presence of ferri-/ferrocyanide redox couple, as measured by both EIS and CV. *E. coli* was detected at 10^3 CFU/ml from pure culture and river water in a little more than 1 h (Geng, Zhang et al. 2008).

In 2008, Kim et al. captured *Salmonella* on a gold IDAM functionalized with antibodies. Cells bound to the IDAM increased the impedance of the system as measured by EIS, with no redox probe. *Salmonella* was detected at 10^3 CFU/ml from pork meat extract in only 10 min (Kim, Morgan et al. 2008).

In 2008 Mantzila et al. captured *Salmonella* cells on a gold electrode functionalized with antibodies. Cells bound to the electrode increased the impedance of the system in the presence of ferri-/ferrocyanide redox couple, as measured by both EIS and CV. Enrichment (increased incubation time of functionalized electrode in cell solution) was required in order to achieve adequate sensitivity. *Salmonella* was detected at 10^2 CFU/ml from pure culture, requiring 2 h, and from milk, requiring 10 h. The sensor displayed good specificity against *E. coli* cells (Mantzila, Maipa et al. 2008).

In 2009 Gamella et al. bound *E. coli* cells with lectin (protein) in solution, and adsorbed the bacteria-lectin complexes onto a SPAuE (cells not bound by lectin did not adsorb). Cells adsorbed onto the electrode increased the impedance of the system in the presence of ferri-/ferrocyanide redox couple, as measured by both EIS and CV. *E. coli* was detected at 10^3 CFU/ml from pure culture in a little more than 1 h (Gamella, Campuzano et al. 2009).

In 2009 Escamilla-Gómez et al. captured *E. coli* on a SPAuE functionalized with antibodies. Cells bound to the electrode increased the impedance of the system in the presence of ferri-/ferrocyanide redox couple, as measured by both EIS and CV. *E. coli* was detected at 10 CFU/ml from pure culture, tap water, and river water in a little more than 1 h (Escamilla-Gómez, Campuzano et al. 2009).

In 2009, Barreiros dos Santos et al. captured *E. coli* O157:H7 on a gold electrode functionalized with antibodies. Cells bound to the electrode increased the impedance of the system as measured by both EIS and CV, with no redox probe. *E. coli* O157:H7 was detected at 10 to 100 CFU/ml from pure culture, in a few minutes (Barreiros dos Santos, Sporer et al. 2009).

From 2005 to 2009, a number of different researchers (Garifallou 2007, Tsekenis 2008) have employed as similar impedance-based assay for detection of bacterial cells, proteins, pharmaceuticals, and antibiotics. SPCEs were coated with a conductive polymer (polypyrrole or polyaniline) film with antibody immobilized in the film. Antigen which bound to the modified SPCE while it was immersed in sample increased the impedance of the system in the presence of ferri-/ferrocyanide redox couple, as measured by EIS (Grant, Davis et al. 2005; Garifallou, Tsekenis et al. 2007; Barton, Davis et al. 2008; Tsekenis, Garifallou et al. 2008; Barton, Collyer et al. 2009). *S. aureus* and *C. difficile* were detected at 10 to 100 CFU/ml and 1000 CFU/ml, respectively, from pure culture in about 30 min (ELISHA 2010).

In 2005, Suehiro et al. employed an applied electric field (positive dielectrophoretic force) to precisely position negatively-charged *E. coli* K12 cells in the inter-electrode spaces of an unmodified interdigitated chrome microelectrode. A very high pulse voltage was then briefly applied to electropermeabilize (perforate) the cell membranes, releasing ions from the cytoplasm. EIS measurements indicated a significant increase in conductance due to electropermeabilization of the electrophoretically positioned cells. This non-specific assay achieved a detection limit of 10^2 CFU/ml of *E. coli* K12 in a 3 h (Suehiro, Hatano et al. 2005). In 2006 the same group modified the assay for specific bacterial detection by immobilizing anti-*E. coli* antibodies onto the microelectrode (Suehiro, Ohtsubo et al. 2006).

In 2007 and 2008, Maalouf et al. captured *E. coli* on a gold electrode functionalized with antibodies, and on antibody-functionalized paramagnetic nanoparticles which were magnetically adhered to the electrode. Bound cells increased the impedance of the system in the presence of ferri-/ferrocyanide redox couple, as measured by CV. EIS measurement showed the same result with no redox probe. *E. coli* was detected with an apparent detection limit of 10 CFU/ml from pure culture in a little more than 1 h. Magnetic nanoparticles add an extra benefit to this system in that they allow the sensor to be easily regenerated. Removal of the magnetic field will immediately release particles, antibodies, and cells from the electrode surface (Maalouf, Fournier-Wirth et al. 2007; Maalouf, Hassen et al. 2008).

In 2007, Varshney and Li captured *E. coli* O157:H7 from solution with immunomagnetic nanoparticles, which were then applied to an unmodified gold IDAM and pulled to the surface via magnetic field. Bound cells decreased the impedance of the system (because cell walls and cytoplasm, as well as ions that leak out of cells, act like conductors in the non-conductive testing medium) as measured by EIS, with no redox probe. *E. coli* O157:H7 was detected at 10^4

CFU/ml from pure culture and 10^5 CFU/ml from ground beef, in 35 min (Varshney and Li 2007). Later this assay was incorporated into a microfluidic device, in which case bound cells increased the impedance of the system, leading to an improved detection limit of detected at 10^2 CFU (absolute number) from pure culture and 10^3 CFU from ground beef, in 35 min (Varshney, Li et al. 2007).

The final three examples of electrochemical biosensors for pathogen detection reported in the literature are assays which employ a label (in these cases, an enzyme) either for enhancement of impedance-based detection (via enzymatic precipitate) or for amperometric or voltammetric detection of an electroactive enzymatic product.

In 2002 and 2005, Ruan and Yang et al. developed an impedance biosensor for detection of *E. coli* O157:H7, which also employed an enzymatic label. *E. coli* O157:H7 cells were captured on an indium-tin oxide IDAM functionalized with monoclonal antibodies, and then labeled with a second (polyclonal) antibody to *E. coli* which was conjugated with the enzyme alkaline phosphatase (AP). Cells bound to the IDAM increased the impedance slightly, but the action of the AP enzymatic label on a substrate (5-bromo-4-chloro-3-indolyl phosphate, added in solution), resulting in a precipitate settling on the electrode surface, created a much more significant increase in impedance, as measured by both EIS and CV in the presence of ferri-/ferrocyanide redox couple. *E. coli* O157:H7 was detected at 10^3 CFU/ml from pure culture in about 1 h. The capture efficiency of the immobilized antibodies was estimated to be 16% (Ruan, Yang et al. 2002; Yang and Li 2005).

Also in 2002, Ruan et al. demonstrated immunomagnetic capture of *E. coli* O157:H7 from pure culture, chicken carcass wash water, ground beef, and fresh broccoli. The

immunomagnetically captured cells were then labeled with an AP-conjugated anti-*E. coli* O157:H7 antibody, then combined with phenol phosphate and allowed to produce phenol production via enzymatic reaction. H_2O_2 was added and the solution was introduced into a flow injection analysis system, containing working electrodes which were modified with two enzymes, tyrosinase and horse radish peroxidase (HRP). Within the electrochemical cell, HRP acted on H_2O_2 to produce oxygen, and the presence of oxygen allows tyrosinase to oxidize phenol, which was measured by amperometry. *E. coli* O157:H7 was detected at 10^2 to 10^3 CFU/ml in about 2 h (Ruan, Wang et al. 2002).

Another enzymatic labeled-based impedance assay was reported by Gehring et al. in 1999 and 2005. In the enzyme-linked immunomagnetic electrochemical assay, they demonstrated immunomagnetic capture of *E. coli* O157:H7 from pure culture, pH-adjusted apple juice, and porcine carcass wash water. The immunomagnetically captured cells were labeled with an AP-conjugated anti-*E. coli* O157:H7 antibody, and deposited onto screen-printed graphite ink electrodes and held to the surface with a magnetic field. The substrate (1-naphthyl phosphate) was added and the electroactive product (1-naphthol) of the enzyme-substrate reaction was measured by square-wave voltammetry. *E. coli* O157:H7 was detected at 10^3 CFU/ml from each of the three sample matrices in 80 min (Gehring, Brewster et al. 1999; Gehring and Tu 2005).

It is evident from the literature survey that of the few label-based electrochemical biosensors for pathogen detection reported, most employ an enzymatic label. To our knowledge, a conducting polymer has not previously been employed as a label in an electrochemical detection assay. Chapters 4 and 6 present the novel use of polyaniline nanostructures as electroactive labels for bacterial detection.

In conclusion, impedance-based sensing and other forms of electrochemical detection are rapid and inexpensive techniques, and the instrumentation can be made small and portable, thus it is amenable to on-site, high-throughput testing. However a key challenge in the development of field-ready impedance-based sensors is to obtain adequate specificity. When a complex sample matrix (containing high levels of non-analyte components) is introduced to the sensor, the response signal should result from the analyte species *only*, but in reality the response is often significantly affected by the presence other species, leading to false positive and negatives (Daniels and Pourmand 2007). In a few of the assays discussed above, immunomagnetic separation was employed as a practical means of extracting and purifying the analyte from the sample matrix prior to detection, in order to avoid the problem of non-specificity. This method will be addressed further in the next section.

1.3 Immunomagnetic Separation for Rapid Microbial Extraction and Concentration

1.3.1 Immunomagnetic Separation (IMS) Technique

The most practical and field-ready pathogen detection methods begin with extraction, purification, and concentration of target cells, in order to eliminate lengthy enrichment steps and interference from the sample matrix during detection. Rapid detection methods are only effective if the target pathogen can first be extracted from its sample matrix, otherwise severe matrix effects are encountered. Additionally, many rapid detection methods are not sensitive enough to detect low levels of microorganisms without a lengthy pre-enrichment step, but if the target could be both extracted and concentrated prior to detection, the enrichment period could be eliminated. Immunomagnetic separation (IMS) is a rapid method for extracting a target analyte

from its sample matrix and concentrating it in a testing medium, and is an ideal starting point for nearly any detection technique.

In IMS, micro- or nanometer scale magnetic particles are immunofunctionalized with antibody, incubated with the sample to bind target cells, and separated from the sample matrix through application of a magnetic field. The magnetic particle-bound target can then be washed and suspended at a higher concentration in the testing medium. The possibility of concentrating target cells prior to detection can eliminate the need for time-consuming pre-enrichment steps. In comparison to centrifugation, filtration, or capture of target on an immunofunctionalized surface, IMS is simpler and generally results in higher capture efficiency due to the greater surface area available for target binding.

1.3.2 Sample Matrices and Detection Methods Paired with IMS

IMS has been paired with a wide variety of biosensors for rapid detection of bacterial pathogens (Jaffrezic-Renault, Martelet et al. 2007; Yang, Li et al. 2008). As mentioned above, several assays have employed IMS as an initial step in enzymatic label-based electrochemical detection of *E. coli* O157:H7, from a variety matrices including apple juice (Gehring and Tu 2005), porcine carcass wash water (Gehring, Brewster et al. 1999), chicken carcass wash water, ground beef, and fresh broccoli (Ruan, Wang et al. 2002). IMS has been paired with label-free amperometric detection of *E. coli* O157 by flow injection analysis (Perez, Mascini et al. 1998). Immunomagnetic beads have also been used to capture bacteria while already adhered (either chemically or magnetically) to an electode surface, for enhanced capture surface area and signal amplification (Hnaiein, Hassen et al. 2008; Maalouf, Hassen et al. 2008). Varshney et al. developed an immunomagnetic nanoparticle and demonstrated its use in immunomagnetic

separation of *E. coli* O157:H7 from ground beef with a capture efficiency of 74% (Varshney, Yang et al. 2005), before combining it with impedance-based detection (Varshney and Li 2007; Varshney, Li et al. 2007).

Pal et al. synthesized electrically active magnetic nanoparticles (EAMNPs) for immunomagnetic separation and electrical detection of bacterial cells, using a core/shell format in which a "shell" of conducting polyaniline was chemically polymerized around an iron oxide "core." The nanoparticles were employed for immunomagnetic separation of *Bacillus anthracis* and also functioned as the transducing material in an electrical biosensor. The EAMNP-cell complexes were captured on a membrane functionalized with a second antibody, where the EAMNPs formed conductive "wires" between two silver electrodes on either side of the membrane, resulting in a decrease in electrical resistance. *B. anthracis* was detected at 10^2 to 10^3 spores/ml from pure culture, milk, lettuce, and ground beef, in approximately 1.5 hours (Pal, Setterington et al. 2008; Pal and Alocilja 2009).

Besides electrochemical sensors, IMS has also been combined with optical pathogen detection assays. Cheng et al. synthesized unique amine-functionalized magnetic nanoparticles and coated them with antibodies in two ways, for immunomagnetic separation of *E. coli* from tap water, pasteurized milk, pasteurized apple juice, and ground beef. Captured cells were detected via ATP bioluminescence (Cheng, Liu et al. 2009). Varshey et al. performed IMS on *Salmonella* cells and then labeled the captured cells with an enzyme, which was detected optically via chemiluminescence reaction (Varshney, Li et al. 2003). Tu et al. reported a sandwich assay consisting of immunomagnetic bead-based separation and fluorescent bead-based labeling of *E. coli* O157:H7. In this way they extracted and fluorescently detected the pathogen from pure culture and from ground beef (Tu, Golden et al. 2005).

CHAPTER 2

IMPEDANCE-BASED DETECTION OF *ESCHERICHIA COLI* O157:H7 AND *BACILLUS CEREUS*

The first objective of this research was to develop electrochemical methods for rapid microbial pathogen detection using immunomagnetic separation (IMS) of the target organism as the starting point. The development of a novel electrically active magnetic nanoparticle (EAMNP) for both IMS and electrical transducing applications in biosensors has been previously reported by this laboratory (Pal, Setterington et al. 2008; Pal and Alocilja 2009). The magnetic and conductive nanoparticle consists of an iron oxide core, imparting magnetic functionality, and a polyaniline shell, imparting electronic activity. In this chapter, the previously-developed EAMNP is employed for IMS, for magnetic positioning of target bacterial cells on a SPCE sensor, and as a mediator for current flow. A brand new impedance-based electrochemical detection technique is presented, in which the presence of EAMNP-bound target cells inhibits current response in cyclic voltammetry. The technique enables rapid detection of *B. cereus* and *E. coli* O157:H7 at low concentrations (40 CFU/ml and 6 CFU/ml, respectively). The versatility of IMS makes this method applicable to a wide variety of target organisms and sample matrices. The system could potentially become fully portable and be deployed in government facilities, military zones, airports and public transit, or food and water supply centers, for routine monitoring or emergency detection of bacterial pathogens.

2.1 Materials and Methods

2.1.1 Reagents and Materials

Iron (III) oxide (γ-Fe_2O_3) nanopowder, aniline monomer, hydrochloric acid (HCl),

ammonium persulfate, methanol, and diethyl ether were used for synthesis of EAMNPs. Polysorbate-20 (Tween-20), phosphate buffered saline (PBS), trizma base, casein from bovine milk, and sodium phosphate (dibasic and monobasic) were used in conjugation of antibodies to nanoparticles and in capture of bacterial cells from culture media. All of the above reagents were purchased from Sigma-Aldrich (St. Louis, MO). Potassium ferricyanide (Spectrum Chemical Mfg. Corp, Gardena, CA) was used for validation of SPCE electroactivity.

Polyclonal anti-*Bacillus* antibodies and monoclonal anti-*E. coli* O157:H7 antibodies were obtained from Meridian Life Science, Inc. (Saco, ME). *Bacillus cereus* strain R4 and a strain of *E. coli* O157:H7 were obtained from the collection of the Nano-Biosensors Laboratory at Michigan State University, and grown in tryptic soy broth (BD Biosciences, MD) at 37° C for 24 h. Cells were serially diluted in 0.1% w/v peptone water (Fluka-Biochemika, Switzerland) prior to detection. Viable cells were enumerated by microbial plating (20 h incubation at 37° C) on trypticase soy agar II (BD Biosciences, MD).

All solutions and buffers used in this study were prepared in de-ionized (DI) water (from Millipore Direct-Q system) as follows: phosphate buffer (100mM sodium phosphate, pH 7.4), blocking buffer (100mM tris buffer, pH 7.6, with 0.01% w/v casein), PBS buffer (10mM PBS, pH 7.4), and wash buffer (10mM PBS, pH 7.4, with 0.05% Tween-20). Magnetic separations were performed with a commercial magnetic separator (FlexiMag, SpheroTech Inc, IL). Hybridization reactions were carried out on a rotisserie-style tube rotator (Labquake, Thermo Fisher Scientific Inc, MA).

2.1.2 Detection Apparatus

Cyclic voltammetric measurements were performed with a 263A potentiostat/galvanostat

(Princeton Applied Research, MA) connected to a personal computer. Data collection and analysis were controlled with the PowerSuite electrochemical software operating system (Princeton Applied Research, MA). Screen-printed carbon electrode (SPCE) sensors (Gwent Inc., UK) are shown in Figure 1. The sensor is composed of two electrodes: the inner carbon/graphite working electrode, having a diameter of 4 mm, and the outer silver/silver chloride counter/reference electrode. A 200-µl capacity sample well is defined by insulating foam. Every SPCE sensor was rinsed with sterile DI water and allowed to dry before test solution was applied. Sensors were disposed of after single use.

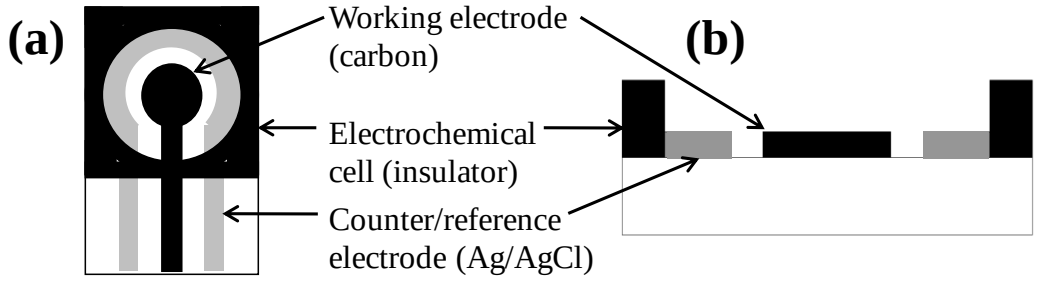

Figure 1. Schematic of the SPCE sensor: (a) top view; (b) cross-sectional view.

2.1.3 Synthesis and Characterization of Electrically Active Magnetic Nanoparticles

EAMNPs were synthesized by polymerization and acid doping of aniline monomer around gamma iron (III) oxide (γ-Fe_2O_3) nanoparticles (Sharma, Lamba et al. 2005), as previously reported (Pal, Setterington et al. 2008; Pal and Alocilja 2009). Briefly, commercial γ-Fe_2O_3 nanoparticles were dispersed in 50 ml of 1M HCl, 10 ml DI water, and 0.4 ml aniline monomer by ultrasonication at 0° C for 1 h. The γ-Fe_2O_3 to monomer weight ratio was fixed at

1:0.6. Oxidant (1 g ammonium persulfate in 20 ml DI water) was added drop-wise while the mixture was stirred at 0° C. Color change from rust brown to dark green indicated formation of electrically-active (green) polyaniline over the smaller (brown) γ-Fe_2O_3 nanoparticles. The reaction continued with constant stirring at 0° C for 4 h. Finally the solution was filtered, washed with 1M HCl, 10% methanol, and diethyl ether, and dried for 18 h. The resulting solid was ground into fine powder and stored in a vacuum desiccator. A schematic of EAMNP synthesis is given in Figure 2(a).

These electrically-active magnetic/polyaniline EAMNPs have been previously characterized and compared with unmodified γ-Fe_2O_3 nanoparticles (Pal, Setterington et al. 2008; Pal and Alocilja 2009). A 200 kV field emission transmission electron microscope (JEOL 2200 FS) was used to investigate structural properties and size distribution. A Four Point Probe (Lucas/Signaton Corp., Pro4, CA) was used to measure solid state electrical conductivity at room temperature. Magnetic properties were evaluated with a superconducting quantum interference device (Quantum Design MPMS SQUID) magnetometer. Hysteresis magnetization was measured with field cycling between +15 and –15 kOe, at a constant temperature of 300 K.

2.1.4 Immunomagnetic Separation of Microorganism

The electrically active EAMNPs were conjugated with antibodies by direct physical adsorption as previously described and confirmed (Pal and Alocilja 2009). Polyclonal anti-*Bacillus* antibodies (50 μg/ml) were mixed with EAMNPs (10 mg/ml) in phosphate buffer and hybridized for 1 h at room temperature with rotation. The bio-modified particles (immuno-EAMNPs) were magnetically separated to remove any unbound antibody in the supernatant, washed twice with blocking buffer (tris buffer with casein), resuspended in phosphate buffer, and

stored at 4° C. A schematic of antibody adsorption onto EAMNPs is shown in Figure 2(b).

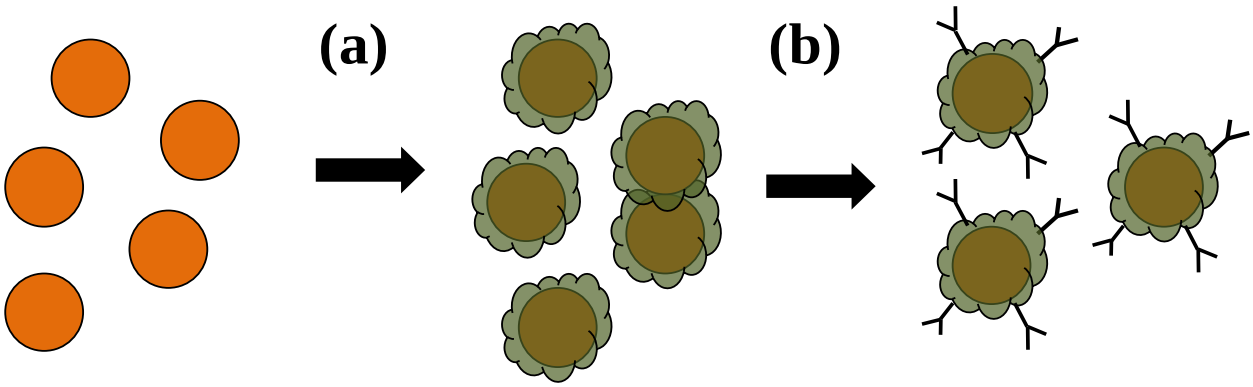

Figure 2. Synthesis and immunofunctionalization of EAMNPs: (a) polymerization of aniline over iron oxide core; (b) antibody adsorption onto polyaniline surface. For interpretation of the references to color in this and all other figures, the reader is referred to the electronic version of this thesis.

The immuno-EAMNPs were used to isolate from target cells from pure culture. Serial dilutions of *B. cereus* and *E. coli* O157:H7 cultures grown overnight in trypticase soy agar were prepared independently of one another in 0.1% w/v peptone water. Immuno-EAMNPs and an aliquot of the appropriate bacterial dilution (containing serially diluted cells and culture media) were combined in PBS buffer (for a final EAMNP concentration of 1 mg/ml), and hybridized for 30 min at room temperature with rotation. The immuno-EAMNP-cell complexes were magnetically separated and the supernatant removed. Complexes were washed twice with wash buffer (PBS with Tween-20) and resuspended in PBS buffer. The immuno-EAMNP-cell solutions, and also pure bacterial dilutions, were plated to determine the number of viable cells present. Capture efficiency was calculated as the number of viable cells captured divided by the number of viable cells in the original dilution. The immunomagnetic separation procedure is depicted in Figure 3. Upon completion of immunofunctionalization of EAMNPs and immunomagnetic separation of target cells, the polyaniline shell of the EAMNPs visibly changes color from dark green to dark blue.

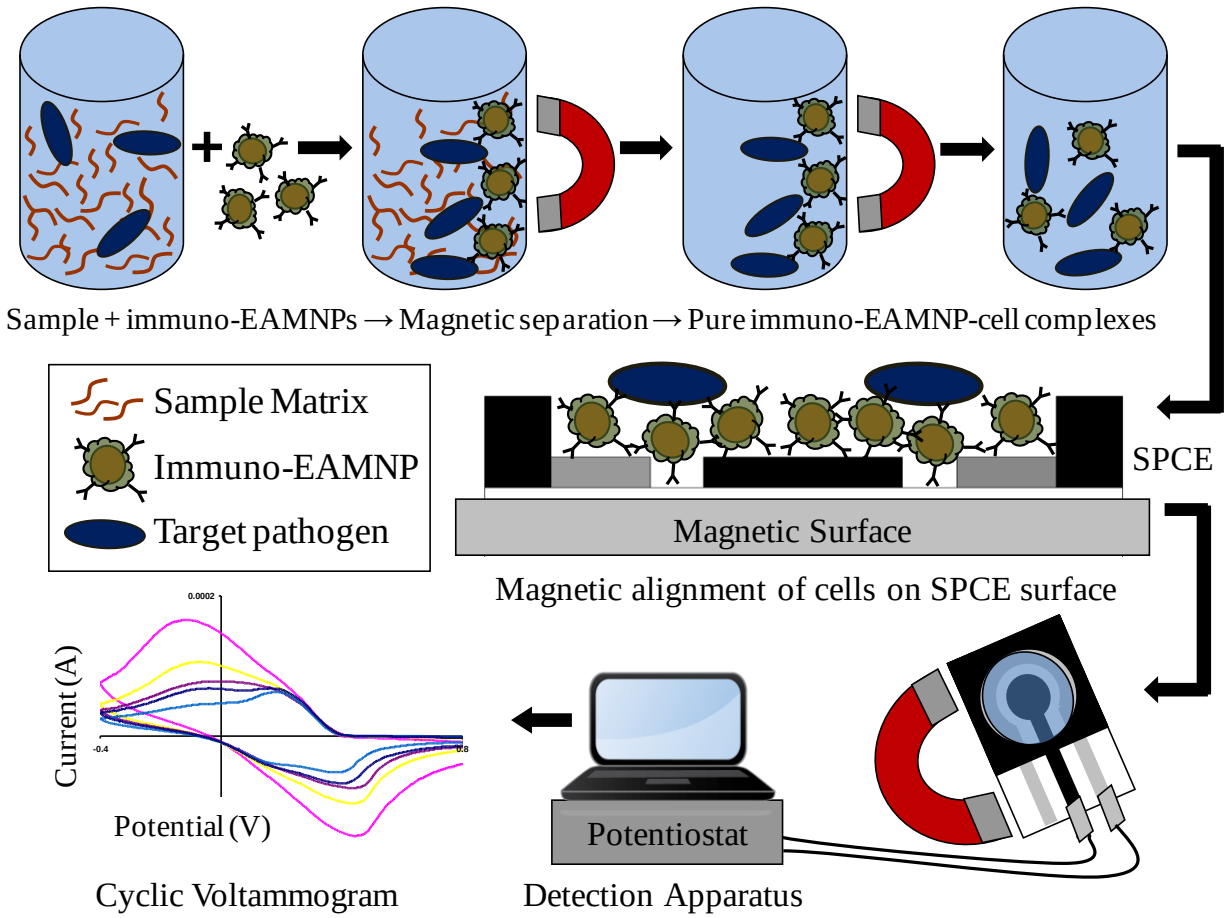

Figure 3. Immunomagnetic separation from sample matrix, magnetic alignment on SPCE surface, and electrochemical detection of *B. cereus* and *E. coli* O157:H7 cells.

2.1.5 Electrochemical Detection of Microorganism

The immuno-EAMNP-cell complexes were magnetically separated from the supernatant (PBS buffer) and resuspended in 0.1M HCl for 20 min in order to reactivate the polyaniline by acid doping. Upon addition of the acid, the EAMNPs underwent a color change from blue back to green.

The electrochemical detection apparatus is depicted in Figure 3. Immediately following the 20 min incubation period, a volume of 100 µl of the immuno-EAMNP-cell complexes in 0.1M HCl was added to the sample well of the SPCE sensor, and the sensor was placed on a

magnetic platform in order to attract and orient the immuno-EAMNP-cell complexes tightly onto the sensor surface (Figure 3), where the electrochemical effect of the cells is maximized. The SPCE sensor was connected to the potentiostat/galvanostat with specially adapted electrical connector clips, and a voltammetric cycle between -0.4 V and +1.0 V was applied at a scan rate of 50 mV/s. Each sensor was scanned with three complete, consecutive cycles, and for each cycle the response current data and the value of total charge transfer (ΔQ) were recorded. The third cycle was chosen for analysis because it showed the most pronounced differences in current flow for different samples. Cyclic voltammetric tests were performed in the same way for pure *B. cereus* and *E. coli* O157:H7 cells suspended in 0.1M HCl.

2.2 Results and Discussion

2.2.1 Synthesis and Characterization of Electrically Active Magnetic Nanoparticles

Characterization studies (Pal and Alocilja 2009) of the EAMNPs indicated a value of 3.3 S/cm in room temperature solid state electrical conductivity, whereas unmodified γ-Fe_2O_3 nanoparticles showed a conductivity of 3.4 x 10^{-5} S/cm. The high conductivity of the synthesized EAMNPs confirmed the presence of electrically-active polyaniline. Both the EAMNPs and the unmodified γ-Fe_2O_3nanoparticles demonstrated superparamagnetic behavior, meaning they only became magnetized when exposed to an external magnetic field. At an applied field of 15 kOe, EAMNPs displayed a room temperature saturation magnetization value of 44.1 emu/g. Although lower than the saturation magnetization of unmodified γ-Fe_2O_3 nanoparticles (64.4 emu/g under the same conditions), the magnetization of the EAMNPs is more than sufficient for the intended applications of IMS and magnetic positioning of target cells. Transmission electron microscopy

studies indicated an average diameter of 20 nm for unmodified γ-Fe_2O_3 nanoparticles and a range in diameter from 50 to 100 nm in synthesized magnetic/polyaniline EAMNPs.

2.2.2 Electrochemical Characterization of Nanoparticles

Cyclic voltammograms of pure (nonmagnetic) polyaniline nanoparticles, synthesized EAMNPs, and immuno-EAMNPs in 0.1M HCl solution are shown in Figure 4.

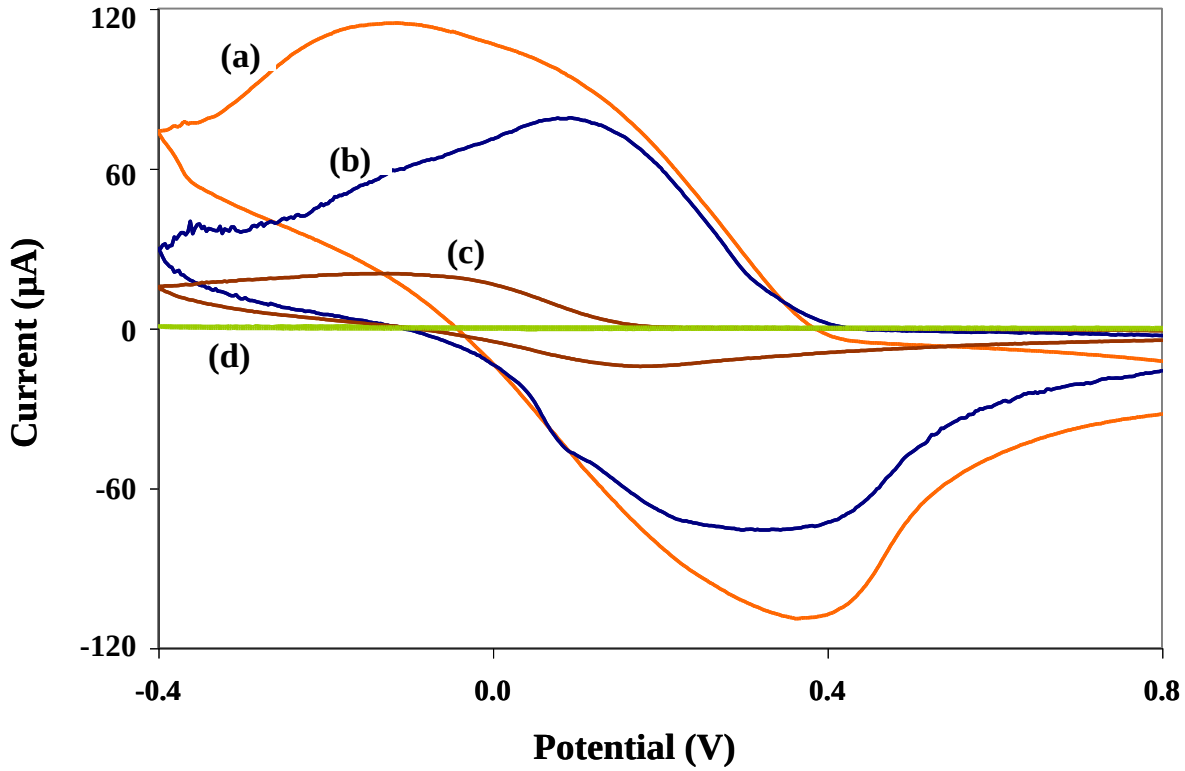

Figure 4. Cyclic voltammograms of (a) 1 mg/ml EAMNPs, (b) 0.1 mg/ml polyaniline nanoparticles, (c) 1 mg/ml immuno-EAMNPs, each suspended in 0.1M HCl solution, and (d) 0.1M HCl solution alone.

The HCl solution alone produces a very low background signal (Figure 4 curve d). The presence of polyaniline nanoparticles (curve b) results in a characteristically-shaped

voltammogram for pure electroactive polyaniline at slightly acidic pH values (Prakash 2002). Pure polyaniline nanoparticles were tested at a lower concentration (0.1 mg/ml) than EAMNPs (1 mg/ml) for ease of display in a single figure. The EAMNPs (curve a) also show the characteristic electroactive polyaniline shape, although a higher concentration (1 mg/ml) of particles is needed to produce a current response with approximately the same magnitude as that of pure polyaniline (at 0.1 mg/ml). This is to be expected, since the greater portion of the EAMNP mass is iron oxide, not polyaniline (weight ratio of iron oxide to aniline monomer during EAMNP synthesis is 1:0.6). Immunofunctionalization significantly decreases the electroactivity of the EAMNPs, as shown by the attenuated current response in curve c. This is likely due to the immobilized antibodies and casein blocking protein inhibiting electron transfer at the polyaniline surface.

2.2.3 Immunomagnetic Separation of Microorganism

The green color of the synthesized EAMNPs indicates the presence of the electroactive (protonated) form of polyaniline, which is expected to result from the acidic chemical polymerization method employed here. Throughout the immunofunctionalization and target extraction procedures, which were carried out in slightly basic conditions (pH 7.4-7.6), the shell of the EAMNPs became at least partially de-protonated to the emeraldine base form of polyaniline, as evidenced by the color change from green to blue. This pH-induced redox reversibility is a well-characterized property of polyaniline (Liu, Kumar et al. 1998; Prakash 2002). Incubation in HCl and the accompanied color change from blue back to green ensures that the polyaniline is fully doped and conducting prior to electrochemical tests.

Immunofunctionalization of EAMNPs was carried out by physical adsorption of

antibodies onto the polymer shell. Electrostatic interactions between the negatively charged Fc portion of the antibodies and the positively charged polyaniline surface are thought to play a role in adsorption and orientation of the biomolecules on the EAMNPs (Pal and Alocilja 2009).

Successful immunomagnetic extraction of *B. cereus* and *E. coli* O157:H7 cells was confirmed by microbial plating. Table 1 shows the capture efficiencies (%) obtained at several different original concentrations of each pathogen. Since a 100 μl (0.1 ml) aliquot of each immuno-EAMNP-cell solution was applied to the SPCE, the estimated number of cells (CFU) actually present on the SPCE during electrochemical detection can be estimated by dividing the captured cell concentration (CFU/ml) by a factor of ten. These values are also given in Table 1 for each original cell concentration. The final column in Table I reports ΔQ values obtained during cyclic voltammetry of each test solution. Each reported value in Table 1 is the mean of three identical trials ± 1 standard deviation.

Table 1 indicates that capture efficiency is quite consistent at 22 to 32% for both bacteria. The only exceptions to this are the very lowest original cell concentrations. In the case of *B. cereus*, no cells were captured (at least, as indicated by plate counts) at an original concentration of 4×10^0 CFU/ml. However since the original cell concentration was so low, it is very possible that 22 to 32% (approximately 1 CFU/ml) was indeed captured, but was not present in the aliquot plated. While the mean ΔQ value corresponding to this low *B. cereus* concentration is not statistically different from the mean ΔQ value of the blank test, it is considerably lower, suggesting that in at least one of the three identical trials, a cell or two may have indeed been captured and applied to the SPCE for detection. The concentration of *B. cereus* one order of magnitude greater (4×10^1 CFU/ml) however, does result in a ΔQ value significantly different from the blank test, indicating a detection limit of 40 CFU/ml of *B. cereus*, which corresponds to

approximately 1 CFU (estimated) present on the SPCE sensor.

Table 1. Capture of *B. cereus* and *E. coli* O157:H7 cells by immuno-EAMNPs. Capture volume was 0.5 ml and volume applied to SPCE was 0.1 ml.

Original Viable Cell Concentration, estimated (CFU/ml)	Mean Captured Viable Cell Concentration (CFU/ml) ± S.D. (n = 3)	Capture Efficiency ± S.D. (n = 3)	Mean Viable Cell Number (CFU) on SPCE, estimated ± S.D. (n = 3)	Mean ΔQ (mC) ± S.D. (n = 3)
B. cereus				
0 (Blank)	0	---	0	1.4 ± 0.20
4×10^0	$(0 \pm 0) \times 10^0$	(0 ± 0) %	0 ± 0	1.1 ± 0.15
4×10^1	$(1 \pm 1) \times 10^1$	(26 ± 26) %	1 ± 1	1.1 ± 0.03
3.9×10^2	$(1.2 \pm 0.31) \times 10^2$	(32 ± 8) %	12 ± 3	1.0 ± 0.06
E. coli O157:H7				
0 (Blank)	0	0	0	1.5 ± 0.07
6×10^0	$(7 \pm 6) \times 10^0$	(113 ± 98) %	0.7 ± 0.6	1.2 ± 0.12
6×10^1	$(1 \pm 0.6) \times 10^1$	(23 ± 10) %	1 ± 0.6	0.94 ± 0.03
5.9×10^2	$(1.7 \pm 0.12) \times 10^2$	(28 ± 2) %	17 ± 1.2	0.97 ± 0.26
5.9×10^3	$(1.6 \pm 0.81) \times 10^3$	(28 ± 14) %	160 ± 81	2.6 ± 0.51
5.9×10^4	$(1.3 \pm 0.36) \times 10^4$	(22 ± 6) %	1300 ± 360	2.2 ± 0.37

In the case of *E. coli* O157:H7, the calculated capture efficiency from pure culture was greater than 100% at an original concentration of 6×10^0 CFU/ml. Once again, the low original cell concentration results in greater variability in the capture efficiency value. The high standard deviation (98%) accurately expresses the uncertainty associated with the mean capture efficiency value at this concentration. In this case, the mean ΔQ value corresponding to this low *E. coli* O157:H7 concentration was statistically different from the mean ΔQ value of the blank test. This

suggests a detection limit of 6 CFU/ml of *E. coli* O157:H7, which corresponds to ≤1 CFU (estimated) present on the SPCE sensor.

These issues of uncertainty in capture efficiency arise at low cell concentrations with small volumes (100 µl) applied to either the culture plate or the SPCE sensor for electrochemical detection. For practical purposes, however, any unknown sample should be both diluted and concentrated (via IMS) by several orders of magnitude, and each of the resulting dilutions and concentrations tested independently. This will ensure that if a sample is positive, at least one of the dilutions or concentrations of the original sample will fall within the range of detectable concentrations, and yield a positive reading in the electrochemical detection step. Any presumptive positive sample would undergo further analysis to confirm the result.

Improving the capture efficiency is an important future objective for optimization of this biosensing method. If the current capture efficiency could be doubled, then the detection limit of the biosensor could also be improved by about 50%. One potential way to achieve better capture efficiency is to alter the method of immobilizing antibodies onto EAMNPs. Uniform orientation of antibodies with the constant (Fc) region bound to the nanoparticle surface and the antigen-binding (Fab) region outward can be achieved via biotin-avidin coupling (Varshney, Yang et al. 2005; Cheng, Liu et al. 2009) or Protein A-/G-mediated immobilization (Widjojoatmodjo, Fluit et al. 1993; Aybay 2003; Wang and Jin 2003).

2.2.4 Electrochemical Detection of Microorganism

From each electrochemical test, cyclic voltammograms (plot of response current vs. applied potential) were recorded. The third scan (of three consecutive scans performed) was chosen for analysis because it shows the most pronounced differences in current flow for

different samples. Figure 5 depicts cyclic voltammograms and charge transfer values for pure (a) *B. cereus* and (b) *E. coli* O157:H7 cells suspended in 0.1M HCl. The presence of cells has no effect on the electrochemical response, except at the highest cell concentrations tested, which are 10^6 and 10^7 CFU/ml. The increase in charge transfer observed at this high concentration can be explained by the conductivity of bacterial cell membranes and cytoplasm (Varshney and Li 2007). If the cells are packed densely enough, their membranes could form a conductive wire through which current is able to flow. Additionally, leakage of ions and cytoplasm out of the cells into the surrounding medium, which could be significant at high cell concentrations, increases the conductivity of the bulk solution and thereby increases current flow.

Although a low concentration of *B. cereus* or *E. coli* O157:H7 cells on the sensor surface in PBS buffer or HCl solution does not significantly influence the current response, a small number of cells *complexed* with EAMNPs and in the presence of excess (uncomplexed) EAMNPs has a much more pronounced effect on current flow. The conductivity of intact bacterial cells is on the order of 10^{-3} to 10^{-2} S/cm (Marquis and Carstensen 1973), whereas the conductivity of the electroactive EAMNPs is 3.3 S/cm (Pal and Alocilja 2009). Therefore when cells are bound to and dispersed in EAMNPs, they will function as barriers to current flow. Additionally, an external magnetic field is used to draw EAMNPs to the sensor surface and position cells in a layer directly above the surface (Figure 3), where the electric field is most concentrated (Radke and Alocilja 2004). In this location, the cells create the greatest obstruction to current flow. Therefore magnetic positioning of the immuno-EAMNP-cell complexes is a simple method of signal amplification.

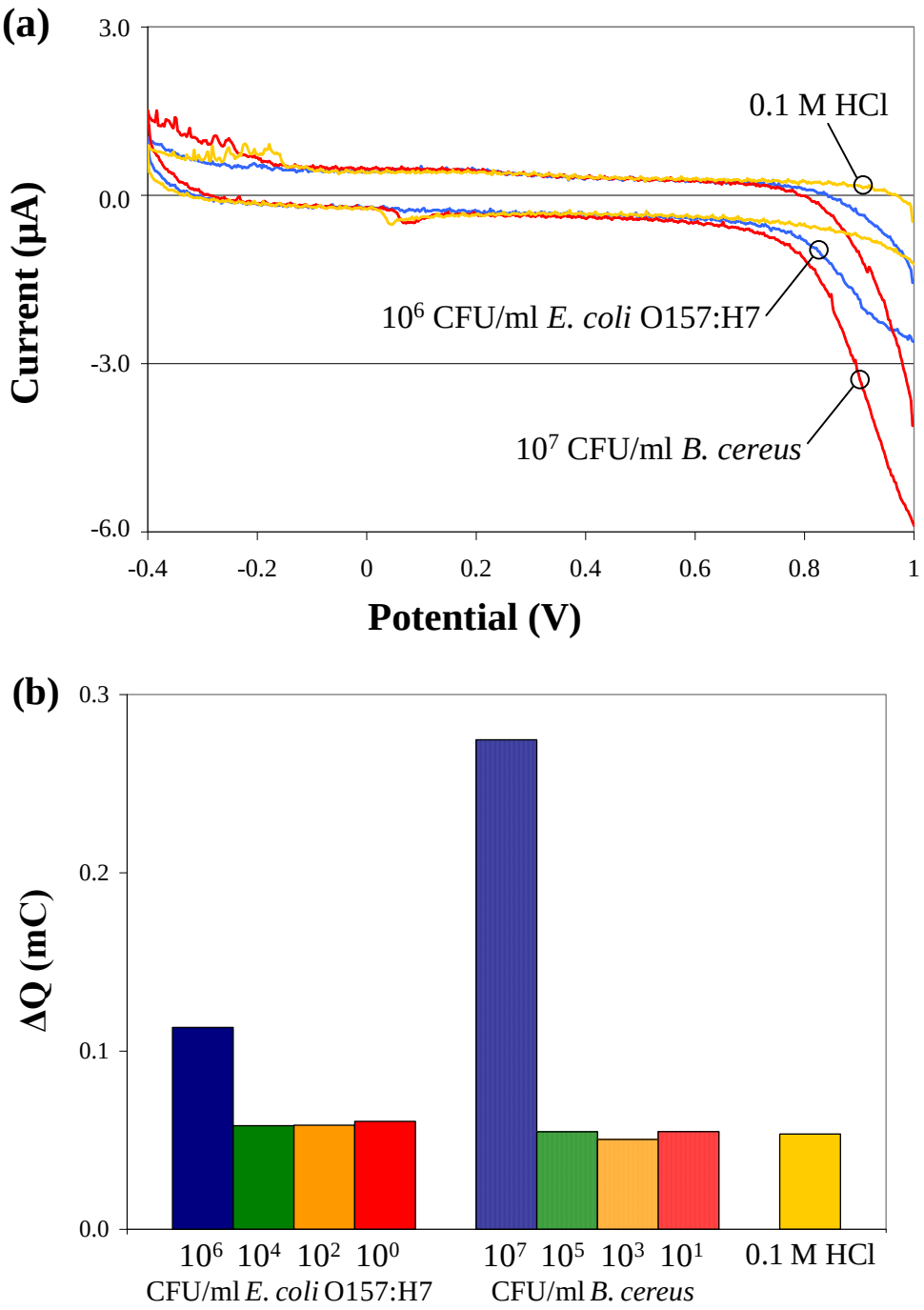

Figure 5. Cyclic voltammograms (a) and charge transfer values (b) for electrochemical tests performed on pure *B. cereus* and *E. coli* O157:H7 cells, suspended at various concentrations in 0.1M HCl solution.

Electrochemical tests were performed on immuno-EAMNP-cell solutions with various concentrations of *B. cereus* and *E. coli* O157:H7 cells. The concentration of EAMNPs was

constant at 1 mg/ml. In all cases, the polyaniline shell of the EAMNPs had been doped prior to testing by incubation in 0.1M HCl. Figure 6 shows the cyclic voltammograms for (a) *B. cereus* and (b) *E. coli* O157:H7, comparing blank tests (no cells) to cell concentrations ranging from 10^0 to 10^2 (*B. cereus*) or 10^4 (*E. coli* O157:H7) CFU/ml. It is evident that the current response decreases with an increasing number of cells present on the sensor, as expected. The only exception to this is at the two highest concentrations of *E. coli* O157:H7, 5.9×10^3 and 5.9×10^4 CFU/ml, which actually result in a current response much larger than that of the blank test.

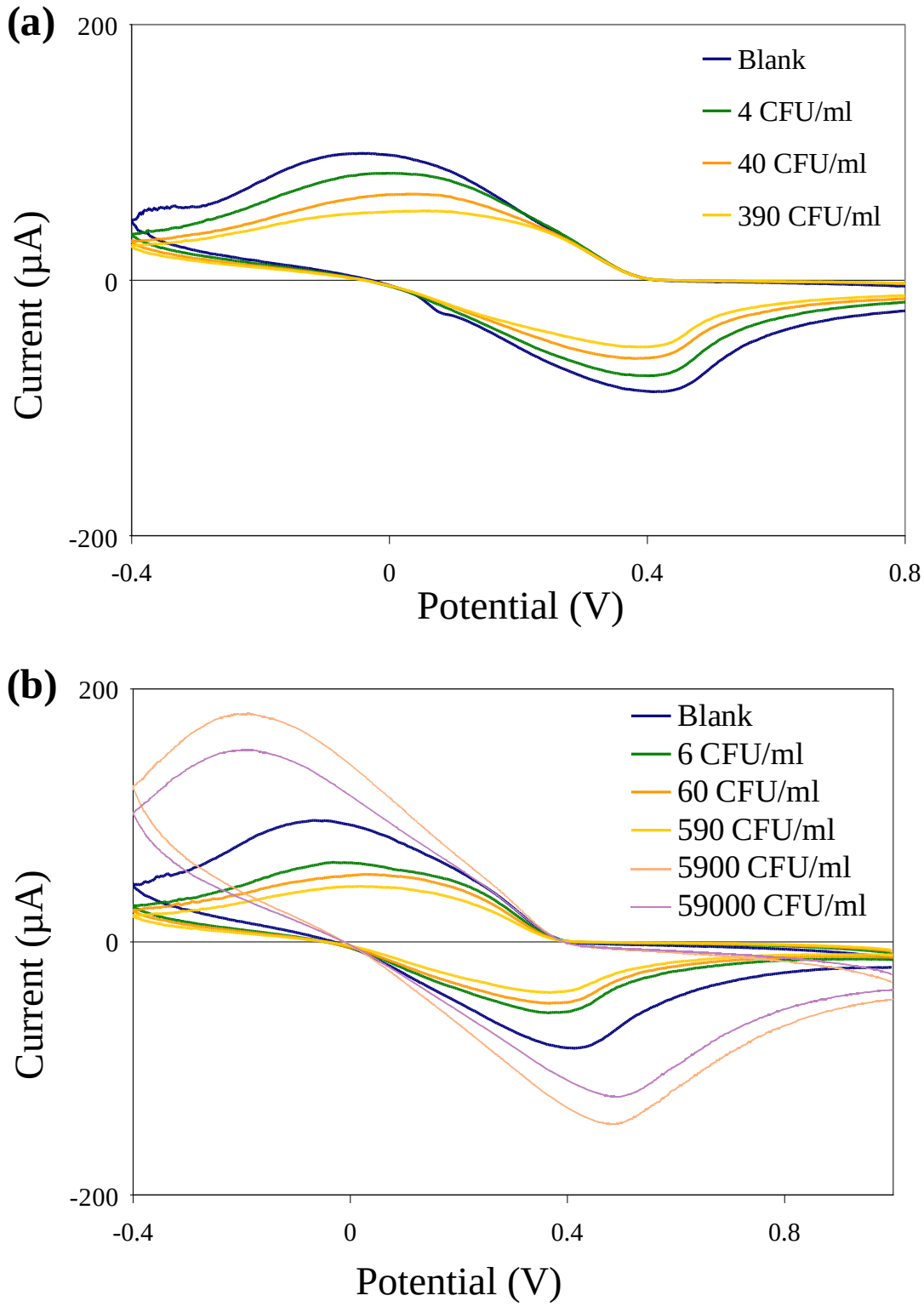

Figure 6. Cyclic voltammograms of immuno-EAMNP-cell solutions: (a) *B. cereus* cell concentrations ranging from 4 to 3.9 x 10^2 CFU/ml, and (b) *E. coli* O157:H7 cell concentrations ranging from 6 CFU/ml to 5.9 x 10^4 CFU/ml.

Figure 7 shows the mean ΔQ values for the same experiment that was depicted in the cyclic voltammograms in Figure 6. Error bars represent ± 1 standard deviation (n = 3). For both bacteria, the differences in ΔQ values between concentration groups are statistically significant with 95% confidence ($\alpha = 0.05$) by a single-factor analysis of variance (ANOVA).

For *E. coli* O157:H7, the system shows an upper detection limit falling between 5.9×10^2 and 5.9×10^3 CFU/ml. Further experiments would be required to determine the upper detection limit for *B. cereus,* if one exists. The larger current responses observed at high cell concentrations (5.9×10^3 and 5.9×10^4 CFU/ml of *E. coli* O157:H7) indicate a concentration-dependent Hook effect, a phenomenon commonly observed in immunoassays, in which the presence of analyte above a certain saturation concentration results in negative test readings. In this case, the increase in current flow at high cell concentrations is probably associated with conductance through the bacterial cell membranes and cytoplasm (Varshney and Li 2007), and cell rupture or leakage, releasing ions into the bulk solution and thereby increasing its conductivity. It is important to note that for applications in biodefense, bacterial pathogens intentionally released as biological weapons would most likely be present at very high concentrations. The Hook effect can be unmasked by diluting the sample, thus it is critical in practical applications to test several dilutions (differing in concentration by orders of magnitude) of any unknown sample, to ensure that at least one dilution of a positive sample will fall within the range of detectable concentrations, so that the sample is flagged for further analysis.

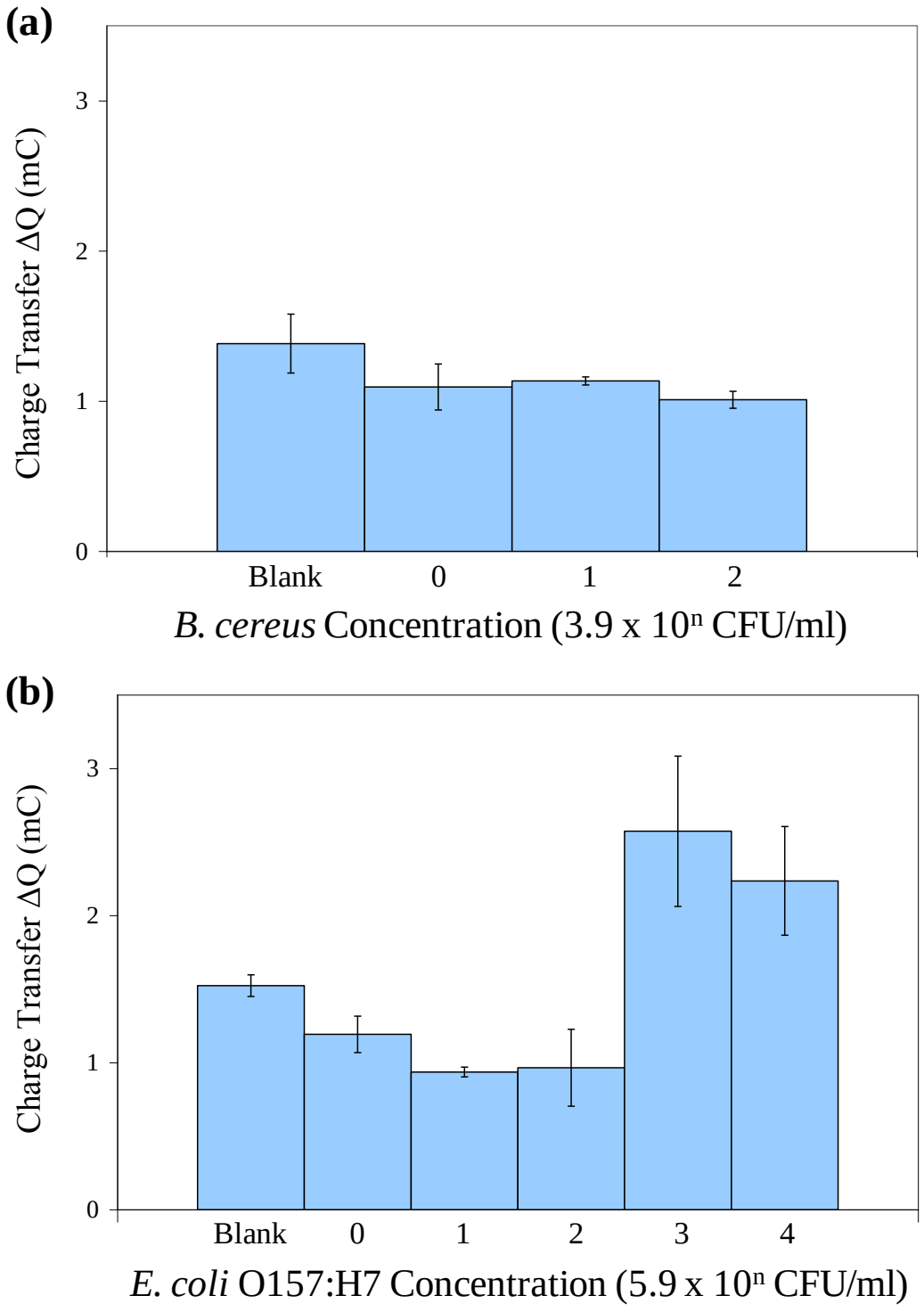

Figure 7. Mean (n = 3) charge transfer values obtained in cyclic voltammetry of immuno-EAMNP-cell solutions: (a) *B. cereus* cell concentrations ranging from 4 to 3.9 x 10^2 CFU/ml, and (b) *E. coli* O157:H7 cell concentrations ranging from 6 CFU/ml to 5.9 x 10^4 CFU/ml. Error bars represent ± 1 standard deviation.

The data displayed in Figure 7 indicate that at levels of 4 x 10^1, or 40 CFU/ml *B. cereus*, and 6 x 10^0, or 6 CFU/ml *E. coli* O157:H7 in pure culture, the sensor signal is statistically different from the blank signal. When capture efficiency and solution volume are taken into consideration, these concentrations may correspond to as few as 1 CFU present on the SPCE sensor during detection (Table 1). Therefore this electrochemical technique is applicable to rapid detection of bacterial pathogens even at trace levels.

2.3 Conclusion

A novel electrochemical detection technique has been presented and applied to *B. cereus* and *E. coli* O157:H7 with detection capability estimated at concentrations as low as 40 CFU/ml and 6 CFU/ml, respectively, from pure culture. Cyclic voltammetry is combined with immunomagnetic separation in a rapid method requiring only 40 min for target recovery (and if necessary, concentration) and 25 min for detection. The method can be easily adapted for different bacterial targets simply by use of a different antibody, and the EAMNP-based magnetic extraction of the target can be performed in a variety of sample matrices (Pal and Alocilja 2009). Future research will include pathogen extraction and detection from food and environmental matrices, specificity and sensitivity tests, and validation of the sensor's performance under non-laboratory environmental conditions. The entire system can be made portable through the use of a handheld potentiostat and laptop PC or PDA. The cost of the assay is not prohibitive, at approximately $1 per disposable SPCE sensor and $0.20 per test for reagents. Applications for this detection system include routine monitoring or emergency detection of bacterial pathogens for biodefense and biosecurity, or water and food safety.

CHAPTER 3

LABEL-BASED DETECTION OF BOVINE VIRAL DIARRHEA VIRUS

This rapid electrochemical method successfully detected Bovine Viral Diarrhea Virus (BVDV) in real bovine serum samples. The virus was isolated from the serum by immunomagnetic separation via antibody-coated EAMNPs. EAMNP-BVDV complexes were then immobilized on the surface of a SPCE sensor, which had been modified with gold nanoparticles and anti-BVDV antibody. Cyclic voltammetry was performed and current flow is proportional to the amount of EAMNP-BVDV complexes present on the sensor (due to the electroactivity of the EAMNP polyaniline shell). The total assay time, including sample and sensor preparation and detection, was approximately 80 minutes.

3.1 Materials and Methods

3.1.1 Reagents and Materials

Iron (III) oxide (γ-Fe_2O_3) nanopowder, aniline monomer, HCl, ammonium persulfate, methanol, and diethyl ether were used for synthesis of EAMNPs. Hydrogen tetrochloroaurate (III) trihydrate and sodium citrate dehydrate were used for the synthesis of gold nanoparticles. Glutaraldehyde was used in SPCE sensor surface modification. Polysorbate-20 (Tween-20), phosphate buffered saline (PBS), trizma base, casein, and sodium phosphate (dibasic and monobasic) were used in conjugation of antibodies to EAMNPs and in capture of virus from serum. All of the above reagents were purchased from Sigma-Aldrich (St. Louis, MO).

All solutions and buffers used in this study were prepared in DI water (from Millipore Direct-Q system) as follows: PBS buffer (10mM PBS, pH 7.4), wash buffer (10mM PBS, pH 7.4, with 0.05% Tween-20), phosphate buffer (100mM phosphate buffer, pH 7.4), casein

blocking buffer (100mM tris buffer, pH 7.6, with 0.01% w/v casein), and glycine blocking buffer (67μM glycine in 10mM PBS, pH 7.4). Magnetic separations were performed with a commercial magnetic separator (FlexiMag, SpheroTech).

Monoclonal anti-BVDV antibodies and bovine serum samples were obtained from the Large Animal Clinical Sciences department at Michigan State University. Fifty serum samples, including BVDV-positive serum (collected from a sick cow) and unknown samples, were stored at -80° C until testing. Serum was confirmed to be BVDV-positive (7 samples) or BVDV-negative (43 samples) by real time PCR (Muhammad-Tahir, Alocilja et al. 2005).

3.1.2 Detection Apparatus

Cyclic voltammetric measurements were performed with a 263A potentiostat/galvanostat (Princeton Applied Research, MA, USA) connected to a personal computer. Data collection and analysis was controlled through the PowerSuite electrochemical software operating system (Princeton Applied Research, MA, USA). SPCE sensors purchased from Gwent Inc. (UK) are shown in Figure 1. Foam and mesh covering was removed from sensors prior to use.

3.1.3 Synthesis and Characterization of Electrically Active Magnetic Nanoparticles

EAMNPs were synthesized and characterized exactly as described in section 2.1.3.

3.1.4 Modification of Screen-Printed Carbon Electrode Sensor

Gold nanoparticles (AuNPs) were synthesized according to a published procedure (Hill and Mirkin 2006). Hydrogen tetrochloroaurate (III) trihydrate aqueous solution (1mM, 50 ml) was heated with stirring on a hotplate. Once it refluxed vigorously, the solution was slowly

titrated with 5 ml of 38.8mM sodium citrate. The solution turned from yellow to clear, to black, to purple and finally deep red. AuNPs have been previously characterized in terms of size (average diameter 15 nm), spectroscopic properties, and magnetic profile (Zhang, Carr et al. 2009).

SPCE sensors were washed with sterile DI water prior to modification. A volume of 25 µl of 2.5mM glutaraldehyde solution was applied to the working area, incubated at 4° C for 1 h, and washed with DI water. A volume of 25 µl of AuNP solution was applied to the glutaraldehyde-treated working electrode, incubated at 4° C for 1 h, and washed with DI water. The working electrode was then incubated with 25 µl of monoclonal anti-BVDV antibodies (5 µg/ml) for 15 min at 37° C, washed with DI water, blocked with 25 µl of blocking buffer (PBS with glycine) for 60 min at 4° C, and washed again with DI water (Lin, Chen et al. 2008). Prepared sensors were stored at 4° C until use.

3.1.5 Immunomagnetic Separation of Microorganism

The electrically active EAMNPs were conjugated with antibodies by direct physical adsorption as described and confirmed by Pal and Alocilja (2009). Monoclonal anti-BVDV antibodies (100 µg/ml) were mixed with EAMNPs (10 mg/ml) in phosphate buffer and incubated for 1 h at 25° C in a rotational hybridization oven (Amerex Instruments, Inc., CA). Following adsorption of antibody the immunofunctionalized nanoparticles (immuno-EAMNPs) were magnetically separated to remove any unbound IgG in the supernatant. Immuno-EAMNPs were washed twice with blocking buffer (tris buffer with casein), and finally resuspended in phosphate buffer and stored at 4° C.

Immuno-EAMNPs were used to isolate BVDV viruses from bovine serum samples. Immuno-EAMNPs (1 mg/ml) were combined with bovine serum (10%) in PBS buffer, and incubated for 30 min at 25° C in a rotational hybridization oven (Amerex Instruments, Inc., CA). The immuno-EAMNP-BVDV complexes were magnetically separated and the serum supernatant removed. Complexes were washed twice with wash buffer (PBS with Tween-20), and finally resuspended in PBS buffer.

3.1.6 Immobilization and Electrochemical Detection of Microorganism

Prepared SPCE sensors (coated with glutaraldehyde, AuNPs, antibodies, and glycine blocker) were electrically characterized with cyclic voltammetry. DI water, 0.1M HCl, 1 mg/ml EAMNPs in DI water, and 1 mg/ml EAMNPs in 0.1M HCl were applied (separately) to four prepared sensors, in volumes of 100 µl each. Solutions covered both the working and counter/reference electrodes. A cyclic voltammetry scan between +1.0 V and -0.4 V was performed on each sensor, at a scan rate of 50 mV/s. Three complete, consecutive cycles were scanned and recorded.

For virus detection tests, a volume of 100 µl of captured virus solution (immuno-EAMNP-BVDV) was applied to the working electrode of the prepared SPCE sensor, incubated for 15 min at 37° C, and washed with DI water. A volume of 100 µl of 0.1M HCl was applied to the surface of the sensor, covering both the working and counter/reference electrodes, and incubated for 5 min at room temperature. A cyclic voltammetry scan between +1.0 V and -0.4 V was begun immediately upon completion of the incubation period, at a scan rate of 50 mV/s. Three complete, consecutive cycles were scanned and recorded for each test. The third scan (of

three consecutive scans performed) was chosen for analysis because it showed the most pronounced differences in current flow for different samples.

3.2 Results and Discussion

3.2.1 Synthesis and Characterization of Electrically Active Magnetic Nanoparticles

The results of EAMNP synthesis and characterization are presented and discussed in section 2.2.1.

3.2.2 Immobilization and Electrochemical Detection of Microorganism

Cyclic voltammograms of prepared sensors with DI water only, HCl only, EAMNPs in DI water, and EAMNPs in HCl are shown in Figure 8. The DI water scan reveals a very low background signal, on the order of 2-3 μA. In HCl, this background signal increases only slightly, but the immobilized AuNPs (activated by the acid) now show characteristic oxidation and reduction peaks at approximately -0.15 V and +0.10 V, respectively. The presence of EAMNPs creates significantly greater current flow, even in DI water, due to the electroactivity of the polyaniline shell. When EAMNPs are suspended in HCl, however, the polyaniline becomes fully doped, current flow increases further, and the cyclic voltammogram shows the characteristic shape of electroactive polyaniline. The two AuNP peaks are still prominent (possibly even accentuated by the conductive polyaniline) as well.

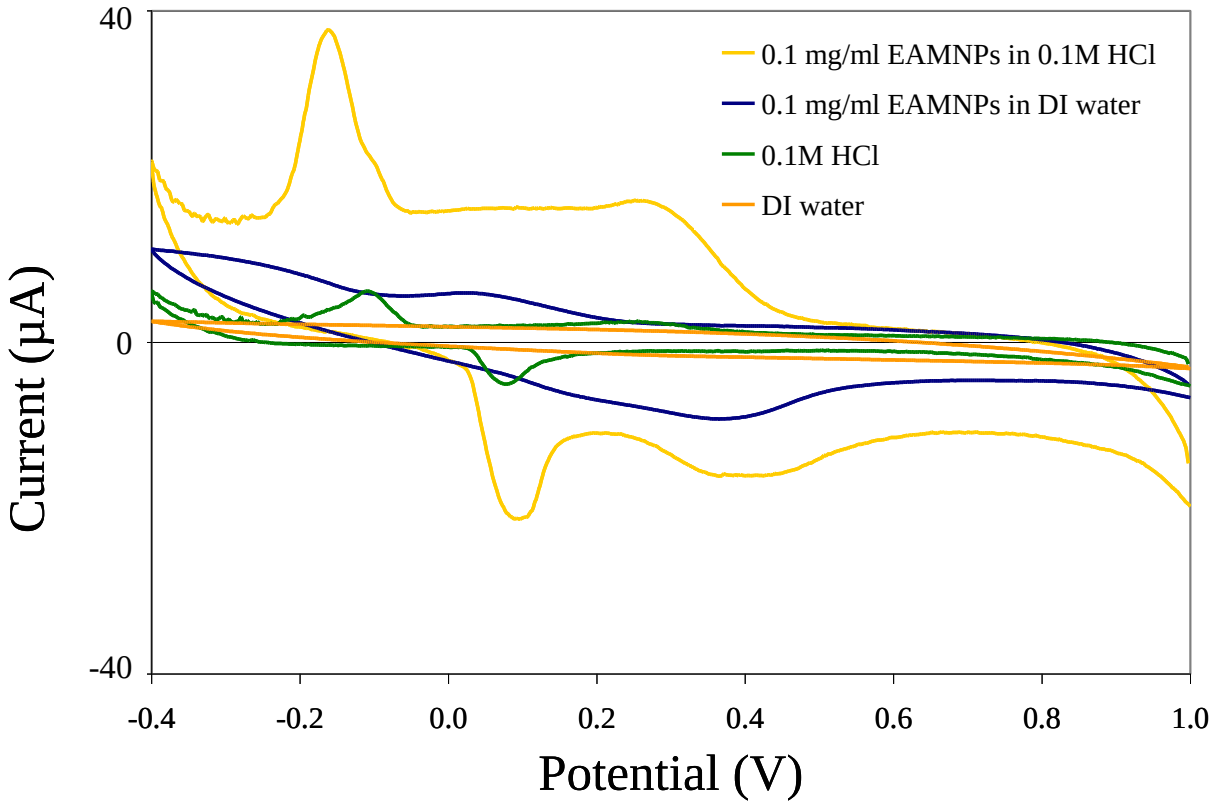

Figure 8. Cyclic voltammograms of DI water alone, 0.1M HCl alone, and EAMNPs at 0.1 mg/ml in DI water and in 0.1M HCl, on SPCE sensors prepared with glutaraldehyde, AuNPs, anti-BVDV antibodies, and blocker.

Figure 9 shows the cyclic voltammetry results of a triplicate test comparing negative control serum (containing no BVDV) and a positive serum sample (containing BVDV). In all cases, the polyaniline shell of the EAMNPs has been doped prior to testing by incubation in HCl. The AuNP peaks at -0.15 V and +0.10 V are barely evident, and the polyaniline oxidation and reduction peaks, at approximately +0.25 V and +0.40 V, respectively, are now dominant. This is likely because the EAMNPs are now specifically bound to the SPCE sensor via the target virus, and thus are in very close proximity to the electrode surface, whereas in Figure 8, the EAMNPs were simply deposited onto the electrode in solution. Also, there may be a higher concentration of EAMNPs specifically bound to the SPCE in Figure 9 than the concentration applied to the

SPCE in Figure 8 (0.1 mg/ml), leading to larger polyaniline peaks in Figure 9. Regardless, the four replicate positive tests result in a much larger current response than the four negative tests (Figure 9). The polyaniline characteristic peaks weakly observed in the negative control tests are caused by EAMNPs which non-specifically bound to the sensor surface in the absence of the target virus.

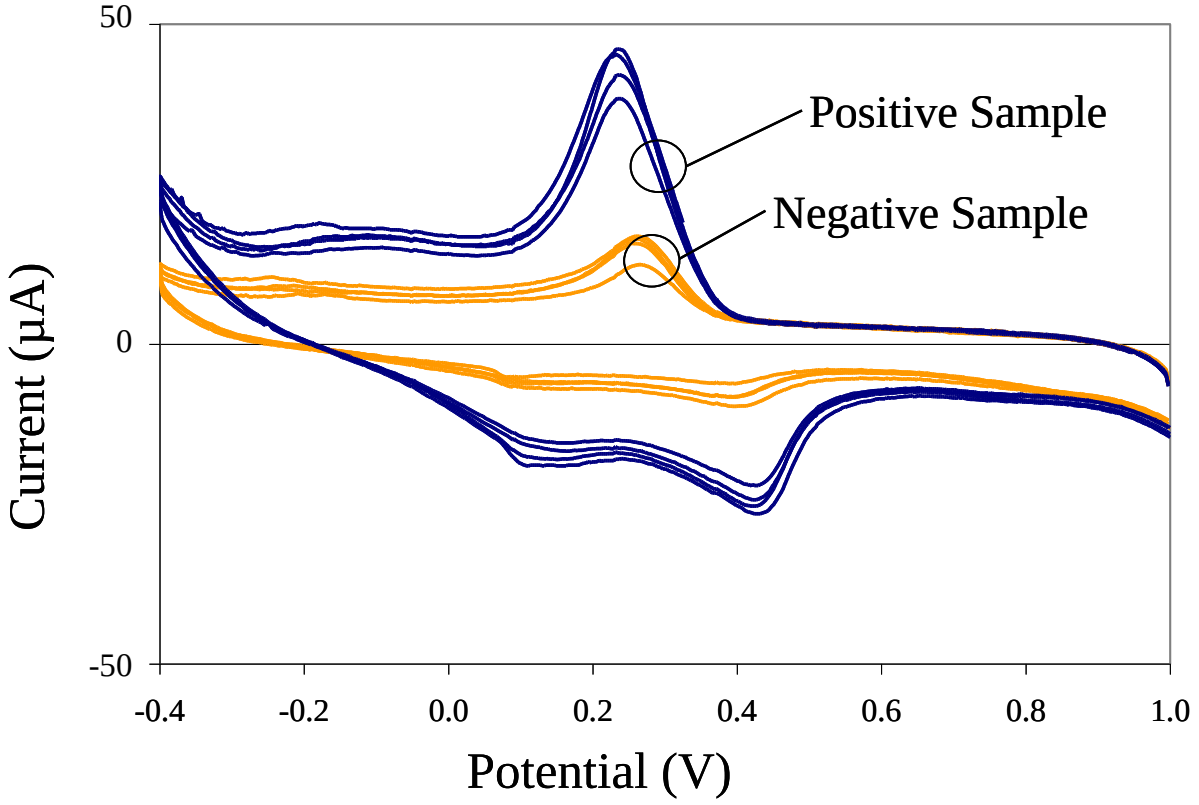

Figure 9. Cyclic voltammogram showing four replicate tests of a negative serum sample and a positive serum sample.

The charge transfer, ΔQ, was computed from the cyclic voltammogram as the integral of current with respect to time (according to the relationship $I = dQ/dt$). Figure 10 shows that the average ΔQ values are 0.634 mC for negative serum and 0.745 mC for positive serum. Error bars represent ± 1 standard deviation (0.017 mC for negative and 0.031 mC for positive), and demonstrate that the value of ΔQ is significantly greater in positive tests than in negative tests.

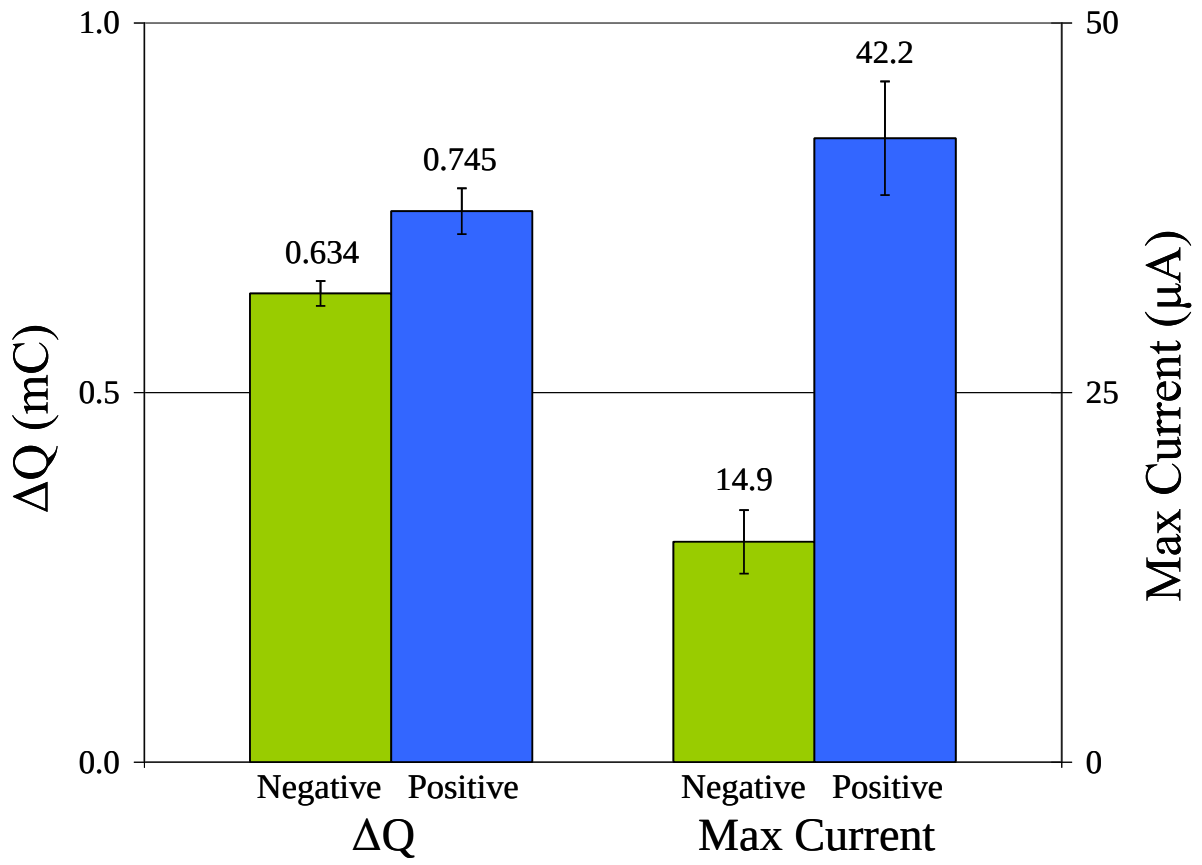

Figure 10. Comparison of average ΔQ values and average maximum current values (n = 3) for negative serum sample and positive serum sample. Error bars represent ± 1 standard deviation.

Maximum current (simply the maximum point on the cyclic voltammogram) was identified as the best single parameter for quantitative comparison of results. Figure 10 shows that the average maximum current values are 14.9 μA for negative serum and 42.2 μA for positive serum. Error bars represent ± 1 standard deviation (2.15 μA for negative and 3.85 μA for positive), and demonstrate that the maximum current value observed is significantly greater in positive tests than in negative tests. It is evident from Figure 10 that maximum current is a better parameter than ΔQ for evaluation of the detection results, since it shows a much more significant difference between positive and negatives tests. This difference was shown to be statistically significant with 95% ($\alpha = 0.05$) confidence by a single-factor analysis of variance (ANOVA).

3.3 Conclusion

In this study we successfully detected BVDV in bovine serum samples. The virus was captured with antibody-coated EAMNPs, and isolated from serum by IMS. Virus-nanoparticle complexes are then immobilized on the surface of a SPCE sensor which has been modified with gold nanoparticles and anti-BVDV antibody. Cyclic voltammetry was performed and current flow was proportional to the amount of EAMNPs present on the sensor (due to the electroactivity of the nanoparticles' polyaniline shell). Thus the occurrence of BVDV on the sensor surface (complexed with electroactive EAMNPs) resulted in increased current flow. Detection required approximately 10 minutes, after 70 minutes of sample and sensor preparation.

CHAPTER 4

LABEL-BASED DETECTION OF *ESCHERICHIA COLI* O157:H7

Setterington, E. B. and E. C. Alocilja (2010). "Rapid electrochemical detection of polyaniline-labeled *Escherichia coli* O157:H7." Biosensors and Bioelectronics In Press, Corrected Proof.

The biosensor presented here employs immunomagnetic separation and electrochemical detection of *E. coli* O157:H7 cells, with detection based on a novel electroactive polyaniline label. To our knowledge, conducting polymers have not previously been employed as electrochemical labels for detection of bacteria or other targets. The polyaniline-labeled *E. coli* O157:H7 cells were detected by cyclic voltammetry on disposable SPCE sensors. An external magnetic field was employed to pull the labeled cells to the electrode surface, in order to amplify the electrochemical signal generated by the polyaniline. The biosensor assay required only 70 min and can detect the presence of as few as 7 CFU of *E. coli* O157:H7 on the SPCE (Setterington and Alocilja 2010).

4.1 Materials and Methods

4.1.1 Reagents and Materials

Aniline monomer, HCl, sodium dodecyl sulfate (SDS), ammonium persulfate, and methanol were used for the synthesis of polyaniline. Polysorbate-20 (Tween-20), Triton X-100, phosphate buffered saline (PBS), trizma base, casein, and sodium phosphate (dibasic and monobasic) were used in immunomagnetic separation and polyaniline labeling of bacteria. All of the above reagents were purchased from Sigma-Aldrich (St. Louis, MO) except SDS, which was purchased from Pierce/Thermo Scientific (Rockford, IL).

Monoclonal anti-*E. coli* O157:H7 antibodies were obtained from Meridian Life Science, Inc. (Saco, ME). Dynabeads® MAX *E. coli* O157 immunomagnetic beads were purchased from Invitrogen Life Science. A strain of *E. coli* O157:H7 was obtained from the Nano-Biosensors Laboratory collection at Michigan State University, and grown in tryptic soy broth (BD Biosciences, MD) at 37° C for 24 h. Viable cells were enumerated by microbial plating (20 h incubation at 37° C) on TSA II trypticase soy agar, modified (BD Biosciences, MD).

All solutions and buffers used in this study were prepared in DI water from Millipore Direct-Q system, as follows: PBS buffer (10mM PBS, pH 7.4), phosphate buffer (100mM phosphate buffer, pH 7.4), blocking buffer (100mM tris buffer, pH 7.6, with 0.01% w/v casein). Magnetic separations were performed with a commercial magnetic separator (FlexiMag, SpheroTech Inc, IL). Centrifugation was performed with an Eppendorf 5415 R microcentrifuge. Hybridization of biological materials was carried out at room temperature with rotation on a tube rotisserie (Labquake, Thermo Scientific, MA).

4.1.2 Detection Apparatus

Cyclic voltammetric measurements were performed with a potentiostat/galvanostat connected to a personal computer. Both the PalmSens handheld potentiostat with PSLite software (PalmSens, Houten, Netherlands), and the VersaStat II potentiostat with PowerCV software (Princeton Applied Research, MA) were used. SPCE sensors (Gwent Inc., UK) are shown in Figure 1. Every SPCE sensor was rinsed with sterile DI water and allowed to dry before test solution was applied. Sensors were disposed of after single use.

4.1.3 Synthesis and Characterization of Conductive Polymer for Target Labeling

Polyaniline nanostructures (nano-PANI) were synthesized by chemical oxidative polymerization in micellar solution (Kim, Oh et al. 2000). Briefly, 0.043M aniline monomer was dispersed in 0.1M HCl containing approximately 0.2M SDS. Ammonium persulfate (APS) dissolved in 0.1M HCl was added dropwise, such that aniline:APS ratio = 2. The solution was stirred at room temperature for 90 min and changed from colorless to dark green, indicating formation of conductive polyaniline emeraldine salt. Methanol was added to quench polymerization. Polyaniline precipitate was collected by centrifugation, washed in 50% methanol, and finally suspended in phosphate buffer containing 0.05% Triton X-100. Very brief (1-2 s) centrifugation was performed to precipitate only the largest polyaniline particulates. The supernatant, consisting of bright green, well-dispersed polyaniline nanostructures, was reserved and used for further experiments. The size and morphology of the nano-PANI was characterized using a 200 kV field emission transmission electron microscope (JEOL 2200 FS). The electrical conductivity of nano-PANI in solution was measured using an Accumet Basic AB30 conductivity meter (Fisher Scientific).

4.1.4 Immunomagnetic Separation of Microorganism

E. coli O157:H7 in pure culture was serially diluted in PBS. Commercial immunomagnetic beads (IMBs), pre-coated with antibody to *E. coli* O157, were combined with the diluted bacteria (20 µl of IMBs per 1 ml of bacterial dilution) and hybridized for 10 min. IMB-*E. coli* complexes were magnetically separated from unbound cells, washed once in PBS containing 0.05% Tween-20, and resuspended in PBS. IMB-based capture of *E. coli* O157:H7 from a complex sample matrix is depicted in Figure 11.

4.1.5 Electroactive Labeling of Microorganism

Monoclonal anti-*E. coli* O157:H7 antibodies were coated onto nano-PANI by direct physical adsorption, as described previously (Pal and Alocilja 2009). Antibodies (0.1 mg/ml, final concentration) were added to nano-PANI suspended in phosphate buffer containing 0.05% Triton X-100, and hybridized for 1 h. Following adsorption of antibody, the bio-modified polyaniline (immuno-PANI) was centrifuged for 3 min at 10,000 rpm to remove unbound antibodies, washed twice with blocking buffer (tris buffer with casein to block unoccupied reactive sites on polyaniline), and finally resuspended in phosphate buffer containing 0.05% Triton X-100, and stored at 4° C. A Shimadzu UV-3101PC spectrophotometer was used to compare protein content (absorbance at 280 nm) of the antibody solution before and after incubation with nano-PANI, in order to confirm hybridization between antibodies and nano-PANI.

Immuno-PANI was added to the immunomagnetically captured *E. coli* O157:H7 (IMB-*E. coli*) solutions at 10% v/v and hybridized for 30 min. IMB-*E.coli*-immuno-PANI complexes were magnetically separated from unbound immuno-PANI, washed twice in PBS containing 0.05% Triton X-100, and finally resuspended in PBS. Polyaniline labeling of immunomagnetically captured *E. coli* O157:H7 cells is depicted in Figure 11.

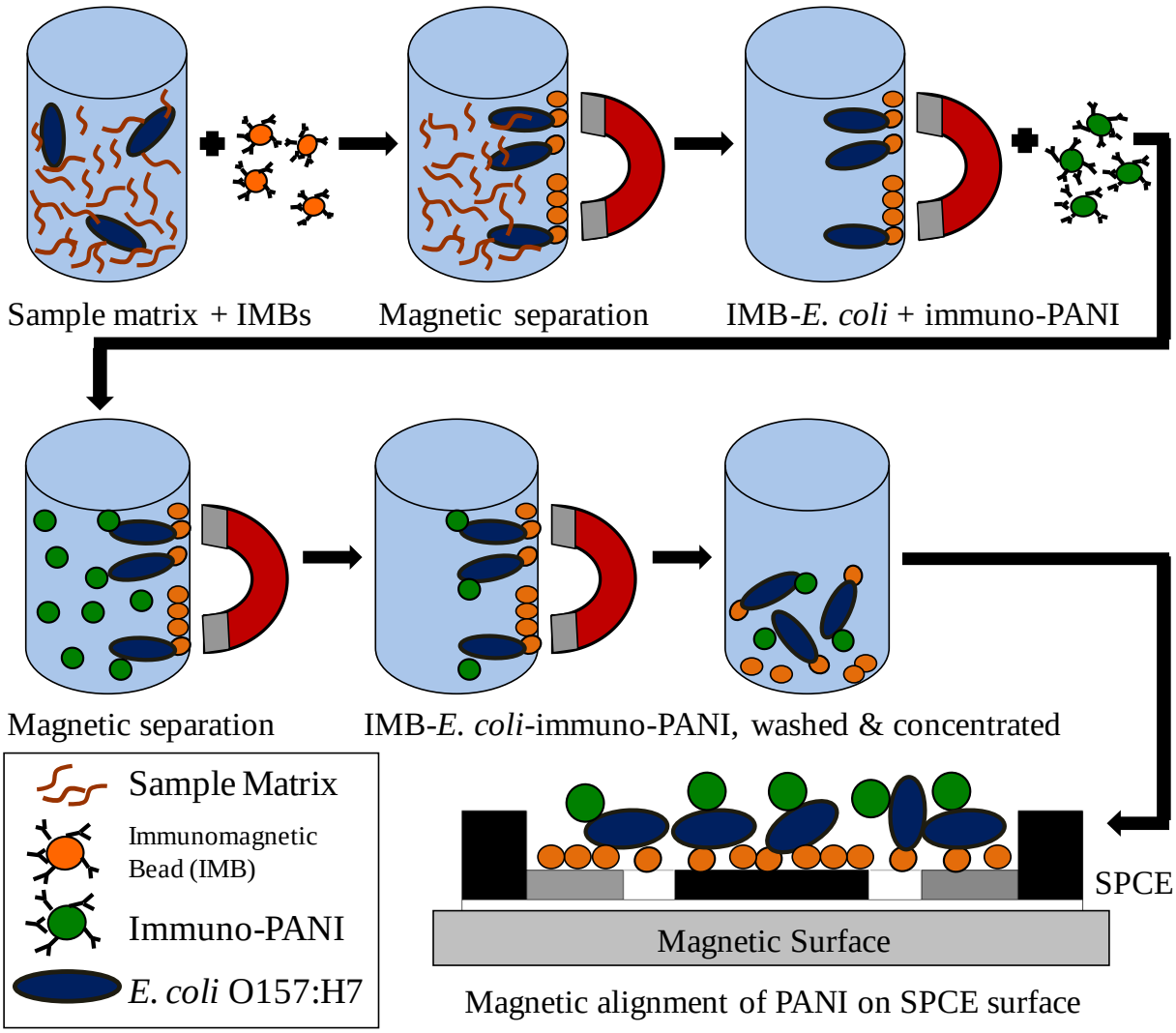

Figure 11. Immunomagnetic separation of *E. coli* O157:H7 cells from a complex sample matrix, followed by labeling with electroactive immuno-PANI, and magnetic alignment of IMB-*E.coli*-immuno-PANI complexes on an SPCE sensor for amplified electrochemical detection.

4.1.6 Electrochemical Detection of Microorganism

The IMB-*E.coli*-immuno-PANI complexes were magnetically separated and suspended in 0.1M HCl for 10 min in order to electrically activate the polyaniline by acid doping. The volume of acid in which complexes were suspended was *half* of the original solution volume, so that the concentration of IMB-*E.coli*-immuno-PANI complexes was doubled prior to detection.

Immediately following the incubation period, a volume of 100 µl of IMB-*E.coli*-immuno-PANI in 0.1M HCl was added to the sample well of the SPCE sensor, and the sensor was placed on a magnetic field in order to attract and position the complexes tightly onto the sensor surface (Figure 11), to amplify the electrochemical signal generated by the polyaniline. The SPCE sensor was connected to the potentiostat/galvanostat, and a voltammetric cycle between +1.0 V and -0.4 V was applied at a scan rate of 100 mV/s. Each sensor was scanned with four complete, consecutive cycles, and for each cycle the response current data was recorded.

4.2 Results and Discussion

4.2.1 Immunomagnetic Separation and Electroactive Labeling of Microorganism

Successful immunomagnetic extraction of *E. coli* O157:H7 was confirmed by microbial plating of the IMB-*E.coli*-immuno-PANI solutions. Percent capture efficiency was calculated as (captured viable cell concentration / original viable cell concentration) x 100. The concentration of captured viable cells (CFU/ml) was also used to estimate the actual number of cells present in the 100-µl sample which was deposited onto the SPCE. For four different concentrations of *E. coli* O157:H7 (blank, 10^1, 10^3, and 10^5 CFU/ml), Table 2 shows the original and captured cell concentrations, the capture efficiency, the estimated number of cells present on the SPCE during detection, and the minimum electrical current signal obtained during detection. Reported values are the mean of three identical trials ± 1 standard deviation. Blank tests were identical to positive tests in every way except that bacteria were absent.

Table 2. Original and captured cell concentrations, capture efficiencies, estimated cell numbers on SPCE sensor for detection, and electrical current signals obtained for four *E. coli* O157:H7 samples.

Original Viable Cell Concentration (CFU/ml)	Mean Captured Viable Cell Concentration (CFU/ml) ± S.D. (n = 3)	Capture Efficiency (%)	Mean Viable Cell Number (CFU) on SPCE ± S.D. (n = 3)	Mean Minimum Current Signal (μA) ± S.D. (n = 3)
0 (Blank)	0	---	0	-2.8 ± 0.75
7.1×10^1	$(3.3 \pm 0.2) \times 10^1$	47.2 ± 32.7	$(7.0 \pm 5.0) \times 10^0$	-5.0 ± 0.40
7.1×10^3	$(3.0 \pm 0.2) \times 10^3$	42.3 ± 3.3	$(6.0 \pm 0.5) \times 10^2$	-6.1 ± 1.1
7.1×10^5	$(3.4 \pm 0.6) \times 10^5$	48.3 ± 8.7	$(6.8 \pm 1.2) \times 10^4$	-7.4 ± 0.42

The capture efficiencies attained here (40 to 50%) were comparable to other published bacterial capture studies using this brand of commercial IMBs (Liu, Yang et al. 2004; Yang, Qu et al. 2007), but improving capture is still an important future objective for optimization of this method. If capture efficiency could be increased, then the detection capability of the biosensor would be improved as well. Other means of immunomagnetic separation are currently being investigated in order to economically attain higher capture efficiency. The minimum current signals displayed in the last column of Table 2 demonstrate that the electrochemical detection results agree with microbial plating results (increasing cell concentration corresponds to increasing absolute value of current signal).

Nano-PANI, investigated by transmission electron microscopy (TEM), consisted of spherical particles less than 50 nm in diameter and clusters of particles ranging in size from approximately 100 to 300 nm (Figure 12). The nano-PANI solution was a bright green color, indicating that it is the conductive emeraldine salt form of polyaniline, which results from the acid-doping polymerization method employed here. Polyaniline has well-characterized pH-induced redox reversibility (Liu, Kumar et al. 1998; Prakash 2002), meaning that in neutral or

basic conditions, loss of electroactivity will occur. The electrical conductivities of nano-PANI suspended in DI water and in 0.1M HCl were determined to be 0.4 mS/cm and 26.4 mS/cm, respectively. Both solutions contained 0.1% v/v Triton X-100 to keep nano-PANI well dispersed during measurement. The conductivity of nano-PANI is significantly increased in the presence of HCl as a dopant (relative to non-doped nano-PANI in neutral DI water). To ensure maximum electroactivity of the polyaniline label used in this assay, the IMB-*E.coli*-immuno-PANI complexes were re-doped in 0.1M HCl for 10 min immediately prior to electrochemical detection.

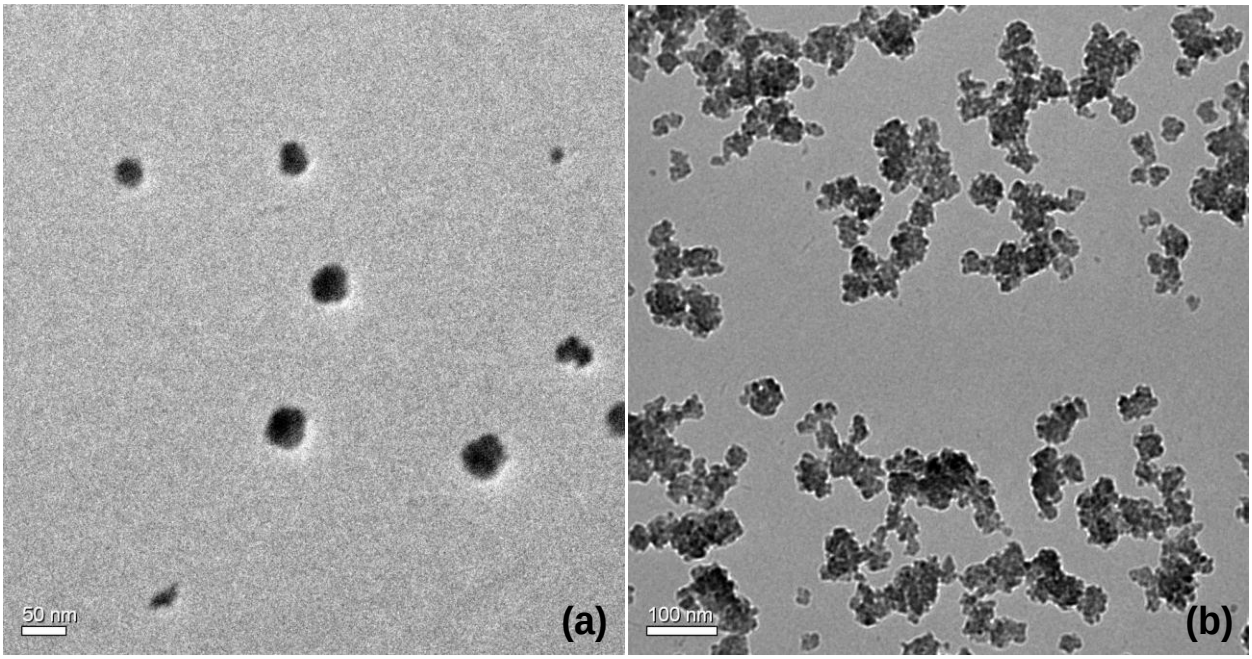

Figure 12. TEM images of synthesized nano-PANI: (a) particles <50 nm in size, (b) clusters ranging in size from 100 to 300 nm.

Immunofunctionalization of nano-PANI was carried out by physical adsorption of antibodies onto the polyaniline surface. Electrostatic interactions between the negatively charged Fc portion of the antibodies and the positively charged polymer are thought to play a role in adsorption and orientation of the biomolecules (Pal and Alocilja 2009). Successful conjugation

of antibodies onto nano-PANI was confirmed by measuring the absorbance of the antibody solution at 280 nm, an indicator of protein content. The measured absorbance of the conjugation supernatant was lower than that of the original antibody solution, demonstrating that antibodies were retained on the nano-PANI during hybridization.

4.2.2 Electrochemical Detection of Electroactively-Labeled Microorganism

From each electrochemical test, cyclic voltammograms (plot of response current vs. applied potential) were recorded for each of the four consecutive scans performed. Figure 13 depicts cyclic voltammograms of nano-PANI, immuno-PANI, and IMB-*E.coli*-immuno-PANI solutions containing various bacterial counts. Also shown are voltammograms of IMBs, *E. coli* O157:H7 cells, and 0.1M HCl solution alone, at concentrations equivalent to those used in the IMB-*E.coli*-immuno-PANI assay.

Figure 13 curve (a), the cyclic voltammogram of nano-PANI, shows three oxidation peaks (having positive current values) and three corresponding reduction peaks (having negative current values), which are characteristic of conducting polyaniline. Oxidation peaks occur at approximately 0.25, 0.45, and 0.6 V. The first of these peaks represents the initial step in oxidation of reduced-form polyaniline (leucoemeraldine to protoemeraldine/emeraldine), the second represents the presence of soluble species arising from degradation of polyaniline, and the third peak represents the final step in oxidation of polyaniline (emeraldine to nigraniline/pernigraniline) (Pruneanu, Veress et al. 1999; Prakash 2002). The fourth cathodic peak, occurring at 0.95 V, is not typically found in cyclic voltammograms of pure polyaniline, and may be associated with the surfactant (SDS) which was incorporated into the nano-PANI during synthesis. Reduction peaks occur at approximately 0.1, 0.4, and 0.5 V. The oxidation and

reduction potentials of polyaniline will vary with scan rate (in this case 100 mV/s) and with the type and concentration of dopant acid (in this case HCl at 0.1M) (Pruneanu, Veress et al. 1999).

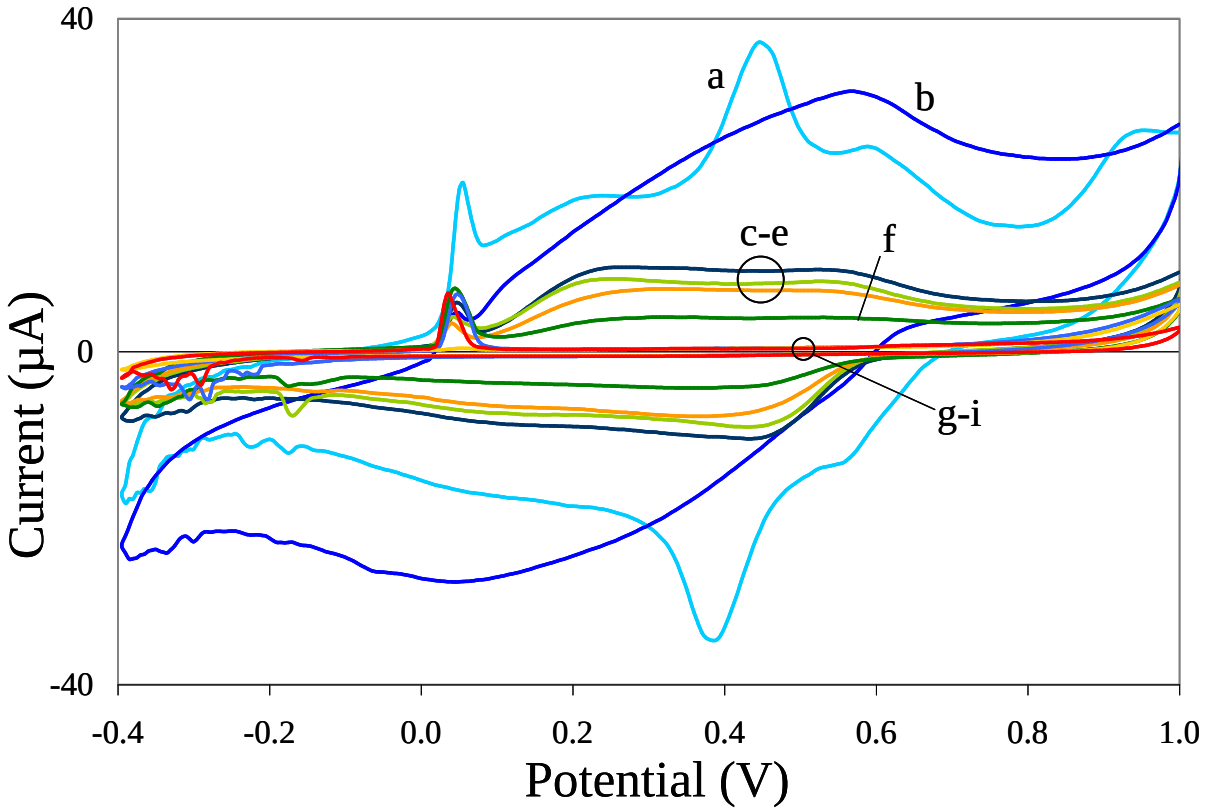

Figure 13. Cyclic voltammograms of samples suspended in 0.1M HCl: (a) nano-PANI; (b) immuno-PANI; (c) IMB-*E.coli*-immuno-PANI, 7 x 10^4 CFU; (d) IMB-*E.coli*-immuno-PANI, 6 x 10^2 CFU; (e) IMB-*E.coli*-immuno-PANI, 7 CFU; (f) IMB-No *E.coli*-immuno-PANI, 0 CFU (blank test); (g) IMBs; (h) *E. coli*, 10^5 CFU; (i) 0.1M HCl alone. Data was obtained in the fourth voltammetric scan performed.

Immunofunctionalization of nano-PANI masks its electroactivity to some extent, as shown by the smaller magnitude and loss of peak resolution in the cyclic voltammogram of immuno-PANI, Figure 13 curve (b). Specifically, the second and third oxidation (and corresponding reduction) peaks merge into one, and overall peak height decreases. Curves (c-e) are the IMB-*E.coli*-immuno-PANI complexes, with bacteria counts ranging from 7 x 10^4 to 7 x

10^0 CFU. These curves exhibited the same shape as that of immuno-PANI, but were smaller in magnitude because excess immuno-PANI had been removed by washing, and only that which was bound to *E. coli* O157:H7 cells remained. Curve (f), the blank test, has a similar shape but significantly lower magnitude. The low level of immuno-PANI present in the blank test was due to *non-specific* interaction with IMBs, which prevented some of the immuno-PANI from being removed during washings. This was considered as the background signal. The fact that the tests containing *E. coli* cells (curves c-e) had significantly higher magnitude than the background signal demonstrated that immuno-PANI was indeed *specifically* binding to *E. coli* O157:H7 cells. The remaining curves (g-i) had very low current magnitude and no polyaniline peaks, demonstrating that HCl, IMBs, and *E. coli* O157:H7 cells alone did not significantly contribute to the magnitude of the signal. The narrow spike occurring around 0.05 V arises from the HCl solution in which all samples were suspended.

For simplicity of comparison, each cyclic voltammogram (plot of response current vs. applied potential) can be represented by a single numeric parameter. Three parameters were evaluated for each voltammogram: the quantity of charge transferred (ΔQ), the maximum current value, and the minimum current value. Charge transfer ΔQ is computed as the integral of the current with respect to time. Maximum current is taken as the *positive* current value occurring at +0.245 V on the cyclic voltammogram (approximate location of the highest oxidation peak). Minimum current is taken as the *negative* current value occurring at +0.420 V on the cyclic voltammogram (approximate location of the lowest reduction peak).

Figure 14 displays the charge transfer values and the maximum and minimum current values obtained from the cyclic voltammograms of test solutions containing 0, 7×10^0, 6×10^2, and 7×10^4 CFU. Values shown are the mean of three replicate trials, and error bars represent ±

1 standard deviation. All data were collected in a single experiment. Two values, confirmed to be outliers with 95% confidence by a two-sided Grubbs' test, were excluded from the data set. The outliers occurred in tests containing 10^2 or 10^4 CFU *E. coli* O157:H7, and were exceptionally high values. Thus even the outlying values were not false negatives (which would be particularly undesirable for food and water safety applications), but only "extreme positive" results, obtained for samples which were indeed positive.

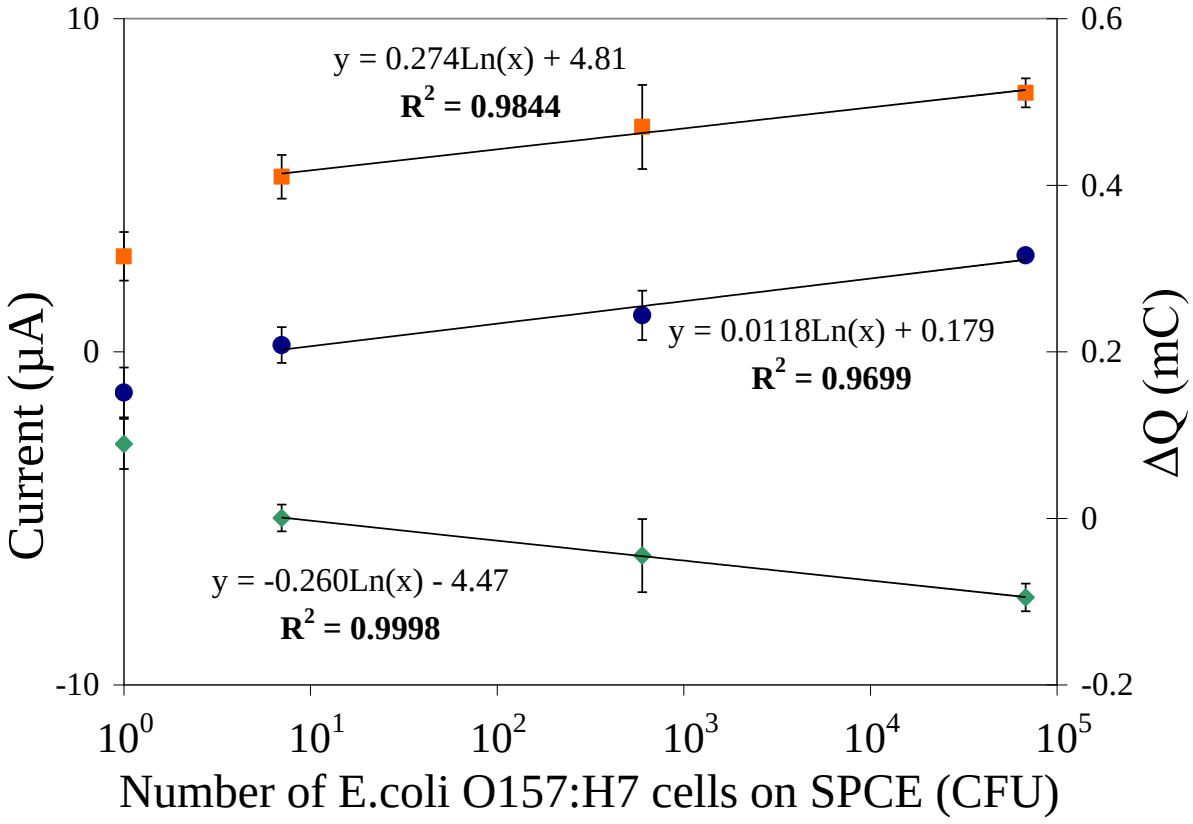

Figure 14. Average ΔQ (●), average maximum current (■), and average minimum current (◆) values obtained in cyclic voltammetry of IMB-*E.coli*-immuno-PANI solutions with cell counts ranging from 7 x 10^0 to 7 x 10^4 CFU. Error bars represent ± 1 standard deviation (n = 3). Data was obtained in the first voltammetric scan performed. Logarithmic regression equations and coefficients for the average values of each parameter are displayed on the figure.

All three sensor response parameters (ΔQ, maximum current, minimum current) were strongly linear across the three cell concentrations tested. Each of the regression coefficients (R^2) were greater than 0.96. Logarithmic regression equations for the average values are displayed in the figure. A single-factor ANOVA test indicated that the ΔQ values obtained for each cell count (7×10^4, 6×10^2, 7×10^0, and 0 CFU) were statistically different from one another with 99% confidence. The same result was obtained for maximum and minimum current values.

Figure 15 depicts the maximum current signal: blank ratios from twenty positive tests carried out in four different experiments, with cell counts ranging from 7×10^0 to 3×10^5 CFU. Signal: blank ratios were obtained by dividing the maximum current value of each positive test by the *average* maximum current value of the blank tests which were performed on the same day. Signal: blank ratios were used because absolute signal values vary from one experiment to the next. This day to day variation in signal magnitude may be attributable to the following causes: (1) the electroactivity of polyaniline is temperature dependent, and (2) batch-to-batch variation in nano-PANI synthesis and immuno-PANI preparation will alter the quality and quantity of polyaniline in test solutions.

The strong linear trend observed in Figure 14, in which all data was collected in a single experiment, indicated a linear dynamic range of 7×10^0 to 7×10^4 CFU (7×10^1 to 7×10^5 CFU/ml). However, the linearity of the sensor response disappeared when data from several different experiments were pooled (Figure 15). Even without linearity, the sensor can still provide a qualitative (positive/negative) result. If quantitative results are desired, a new calibration curve must be constructed for each experiment in which unknown samples are tested. Even so, the biosensor's strong linearity and wide linear range (within one experiment) is an

advantage, showing that it has the potential to be developed into a fully quantitative detection method, if day to day variation in signal values can be reduced. Figure 15 demonstrates that the biosensor results were reproducible for qualitative (yes/no) detection, because all twenty positive tests produced signals much higher than the blank tests (signal: blank ratio ≥1.45).

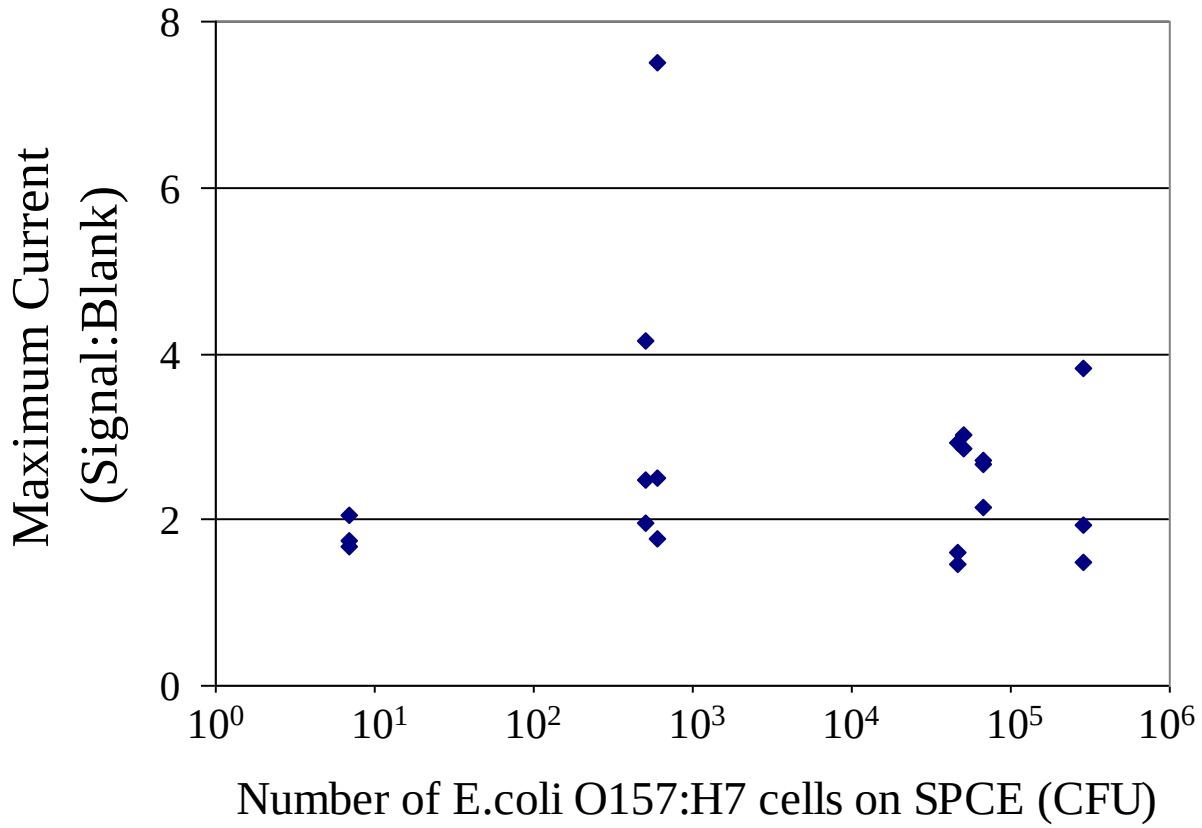

Figure 15. Plot of the maximum current signal: blank ratios of IMB-*E.coli*-immuno-PANI solutions with cell counts ranging from 7 x 10^0 to 3 x 10^5 CFU. Data was obtained in the fourth voltammetric scan performed.

The data displayed in Figures 14 and 15 indicated that an estimated 7 CFU of *E. coli* O157:H7 present on the SPCE sensor (corresponding to an original cell concentration of 70 CFU/ml) can be detected with signal: blank ratio >1.5 (the signal: blank ratios at this cell count are 1.67, 1.74, and 2.05). Slightly lower signal: blank ratios were observed at higher cell counts (1.45 and 1.50 at 4.7 x 10^4 and 2.9 x 10^5 CFU, respectively) which may indicate a slight Hooke

effect. It is important to note, though, that for four of the positive tests, signal: blank ratios were greater than 3, and even as high as 7.5. Future efforts will focus on improving the sensitivity of the sensor until signal: blank ratios greater than 3 can be consistently achieved for all positive samples.

Prior to detection, the IMB-*E.coli*-immuno-PANI complexes were immunomagnetically separated and resuspended in half of the original volume, in order to double the concentration being applied to the SPCE sensor. This resulted in a larger amount of PANI on the sensor, and consequently a stronger electrochemical signal as compared to unconcentrated test solutions (data not shown). A potential way to increase the sensitivity of the system is to use larger sample volumes and immunomagnetically concentrate the test solutions by more than two-fold before they are applied to the SPCE sensor.

Also prior to detection, an external magnetic field was used to draw IMB-*E.coli*-immuno-PANI complexes to the sensor surface (Figure 11), where the electric field is most concentrated (Radke and Alocilja 2004). Magnetically positioning the polyaniline as near as possible to the electrode is a simple way of amplifying the electrochemical signal. Figure 16 shows minimum current values of blank (0 CFU) and positive (5×10^4 CFU) tests performed both in the presence and absence of a magnetic field. The presence of the magnetic field results in current values approximately five times higher than those obtained without the magnetic field. Additionally, the signal: blank ratio is slightly higher in the presence of the magnetic field (signal/blank = 3.2) than in its absence (signal/blank = 3.1).

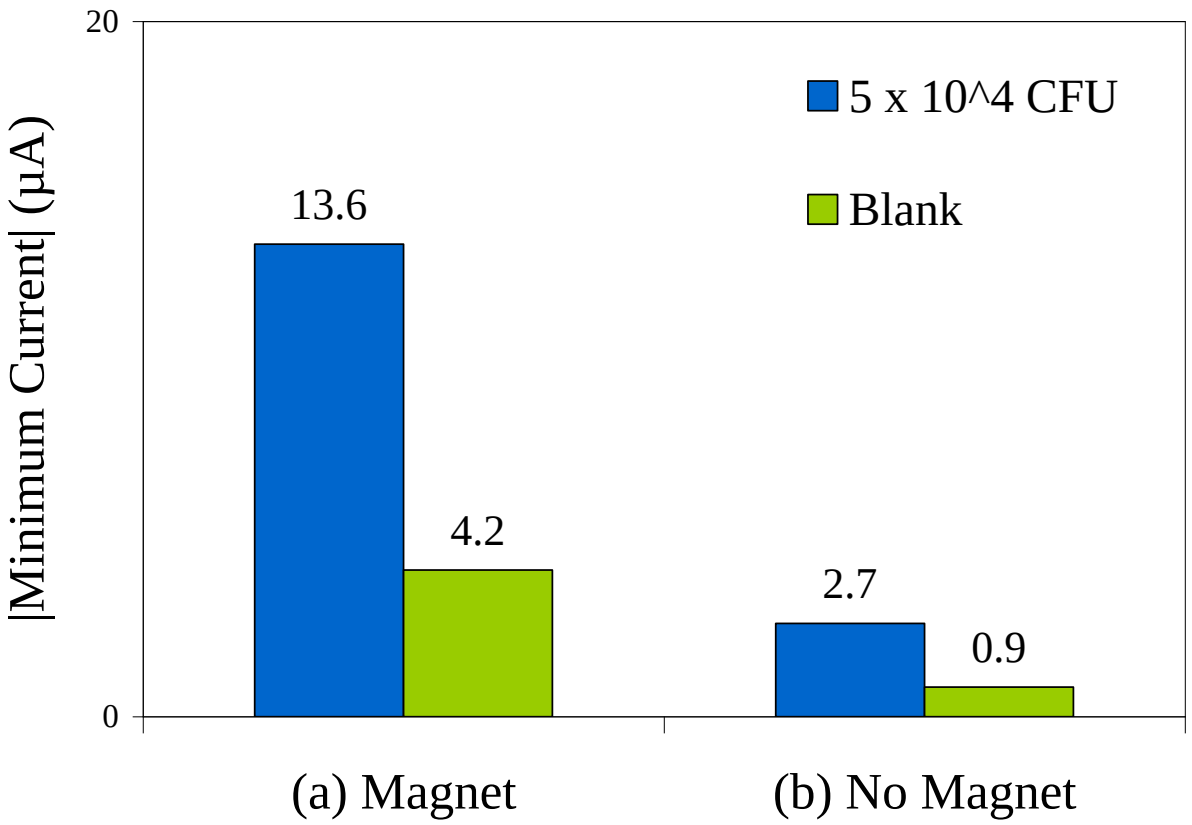

Figure 16. Plot of the (absolute) minimum current values obtained in cyclic voltammetry of IMB-*E.coli*-immuno-PANI solutions (5 x 10^4 CFU and blank), in the presence (a) and absence (b) of a magnetic field beneath the SPCE sensor. Data was obtained in the fourth voltammetric scan performed.

The biosensor was able to detect 7 CFU or 70 CFU/ml, which is lower than the infectious dose of *E. coli* O157:H7 (10 to 100 cells), making it a practical detection method. Table 3 compares this with other biosensors for *E. coli* O157:H7 which also employ IMS and some type of electrochemical detection. The detection limit of the biosensor reported here is one order of magnitude lower than any of the detection levels of similar methods found in the literature, giving this biosensor a clear advantage. The linear range of 7 x 10^1 to 7 x 10^5 CFU/ml observed for this biosensor (in data from a single experiment, Figure 14) is also an advantage. As shown in

Table 3, other IMS-electrochemical detection methods are either not linear at all or have a smaller linear range (≤3 orders of magnitude) than that of our sensor (4 orders of magnitude).

Table 3. Comparison of the analytical performance (detection limit, linear range, and assay time) of several biosensors which employ IMS and electrochemical techniques to detect *E. coli* O157: H7 cells from pure culture.

Biosensor Principle	Detection Limit	Linear Range	Assay Time	Reference
IMS, label-free amperometric detection	10^5 CFU/ml	10^6 to 10^8 CFU/ml	120 min	(Perez, Mascini et al. 1998)
IMS, enzymatic label & amperometric detection	6 x 10^2 CFU/ml	Nonlinear	120 min	(Ruan, Wang et al. 2002)
IMS, enzymatic label & square wave voltammetry detection	5 x 10^3 CFU/ml	10^3 to 10^6 CFU/ml	80 min	(Gehring and Tu 2005)
IMS, label-free electrochemical impedance spectroscopy detection	8 x 10^5 CFU/ml (1.6 x 10^2 CFU)	Nonlinear	35 min	(Varshney, Li et al. 2007)
IMS, conducting polymer label & cyclic voltammetry detection	7 x 10^1 CFU/ml (7 x 10^0 CFU)	10^1 to 10^5 CFU/ml	70 min	This work

The FDA reports that the standard method can detect *E. coli* O157:H7 at <1 CFU/g of food (FDA 2009). Since the biosensor presented here can detect as few as 7 CFU, it theoretically should also be able to detect the pathogen at <1 CFU/g in a typical food sample (≥25 g). It is noted however, that the capture efficiency of immunomagnetic beads usually decreases in complex matrices as compared to pure culture, so the sensitivity of this sensor may be reduced when applied to food samples. Similarly, in theory the sensor will be able to detect the target pathogen *specifically* (due to the monoclonal antibody employed in the cell labeling step), but

specificity cannot be claimed until detection is actually performed in mixed bacterial cultures. Therefore, detection from complex matrices and from mixed cultures is an essential future step in the validation of this biosensor. Another limitation of the sensor is that it is probably not able to distinguish between viable and nonviable cells. Although this has not been experimentally confirmed, it is well known that nonviable cells (unless their cell membranes are destroyed) often retain antigens to which antibodies will bind, so most antibody-based assays will detect viable and non-viable cells indiscriminately.

The time required to carry out the biosensor assay (from sampling to detection) was approximately 70 min. This is a huge advantage over the standard (culture) method, which requires 24 h even for an initial positive/negative result (FDA 2009). Also, this assay time is competitive in comparison with other IMS-electrochemical detection sensors (Table 3), with assay times ranging from 35 min to 2 h. With automation of the washing steps required for IMS, this biosensor would be ideal for high-throughput initial screening of samples, after which any positive results could be confirmed by standard methods.

Another important advantage of this biosensor is its portability. The handheld potentiostat can be paired with a pocket PC, battery-operated, and transported easily. The SPCE sensors require no chemical or biological modification of the electrode surface, and therefore can be stored up to a year. All the other necessary equipment and reagents can also be transported and operated remotely, which enables the possibility of field-based testing with this biosensor.

4.3 Conclusion

Proof-of-concept has been demonstrated for a rapid electrochemical method for *E. coli* O157:H7 detection (Setterington and Alocilja 2010). Cells are isolated by immunomagnetic

separation, labeled with electroactive polyaniline, and detected by cyclic voltammetry on screen-printed carbon electrodes. Initial results show detection as low as 7 CFU (70 CFU/ml) in pure culture, with a linear range of 10^1 to 10^5 CFU/ml. The assay requires 70 min from sampling to result. The detection of low pathogen levels and the short assay time give this biosensor the potential to replace time-consuming culture methods as the means of initial screening for rapid qualitative results. Another major advantage of the biosensor is its portability. No surface modification of the SPCE sensor is required, making it stable for long term storage and transport. A handheld, battery-powered potentiostat and pocket PC make it feasible to perform this assay in the field. The biosensor could be adapted for other targets simply by use of different antibodies, and immunomagnetic separation of the target can be performed in a variety of sample matrices.

A limitation of the sensor is that linearity is only observed in data from individual experiments, but linearity disappears when data from multiple experiments is pooled. Therefore it is not yet clear whether this method will ever be truly quantitative. Also the biosensor's specificity, response to nonviable cells, and performance in complex matrices have not yet been determined. Future work will focus on optimization and validation of the biosensor, including detection from mixed bacterial cultures and complex matrices. Applications for this technology include routine monitoring or emergency detection of bacterial pathogens for food and water safety, environmental monitoring, healthcare, and biodefense.

CHAPTER 5

DEVELOPMENT OF A NEW IMMUNOMAGNETIC SEPARATION METHODOLOGY

The development and application of EAMNPs for IMS has been previously reported by this laboratory (Pal, Setterington et al. 2008; Pal and Alocilja 2009). The reported method was effective in isolating target cells from pure culture and food matrices even at low concentrations of the target, but when challenged with non-target organisms, it demonstrated inadequate specificity. The new IMS methodology reported in this work was able to isolate *E. coli* O157:H7 effectively, and discriminate against *E. coli* O55:H7 and *Shigella boydii*. Additionally, this methodology required a smaller volume of magnetic nanoparticles (MNPs) per extraction, and resulted in an MNP-antibody conjugate with a much longer storage life, as compared to our previous method. Both of these improvements contributed to a lower overall cost of the IMS assay. This IMS methodology was developed for two different types of MNPs which were already synthesized in this laboratory and available for use in these experiments, in order to allow for flexibility in coupling chemistries.

5.1 Materials and Methods

5.1.1 Reagents and Materials

Ferric chloride hexahydrate (EMD Chemicals), sodium acetate (CCI Chemicals), sodium acrylate, sodium chloride (NaCl), ethylene glycol, ethylenediamine, HCl, aniline, iron (III) oxide nanopowder, ammonium persulfate, methanol, and diethyl ether were used as received in the synthesis of the magnetic nanoparticles. Nanoparticles were immunofunctionalized with monoclonal anti-*E. coli* O157:H7 antibodies obtained from Meridian Life Science, Inc. (Saco, ME). *N*-Hydroxysuccinimide (NHS) and 1-ethyl-3-(3-dimethylaminopropyl) carbodiimide

hydrochloride (EDC), both from Pierce / Thermo Scientific (Rockford, IL) were used in the coupling of antibodies onto MNPs.

Polysorbate-20 (Tween-20), Triton X-100, phosphate buffered saline (PBS), trizma base, casein, and sodium phosphate (dibasic and monobasic) were used in the immunomagnetic separation procedure. All of the above reagents, unless otherwise noted, were purchased from Sigma-Aldrich (St. Louis, MO).

All solutions and buffers used in this study were prepared in DI water (from Millipore Direct-Q system) as follows: PBS buffer (10mM PBS, pH 7.4), wash buffer (10mM PBS, pH 7.4, with 0.05% Tween-20 or 0.05% Triton X-100), phosphate buffer (100mM sodium phosphate, pH 7.4), blocking buffer (100mM tris buffer, pH 7.6, with 0.01% w/v casein).

Magnetic separations were performed with a commercial magnetic separator (Promega Corporation, Madison, WI). Hybridization of biological materials was carried out at room temperature with rotation on a tube rotisserie (Labquake, Thermo Scientific, MA). Scanning electron micrographs were acquired using field-emission scanning electron microscopy (JOEL 7500F, acceleration voltage of 5 kV). A superconducting quantum interference device magnetometer (Quantum design MPMS SQUID) was used for magnetic characterization of MNPs.

5.1.2 Culturing and Plating of Microorganism

E. coli O157:H7 (Sakai strain), *E. coli* O55:H7, and *Shigella boydii* were obtained from the Food Safety and Toxicology collection at Michigan State University. From frozen purified culture stocks (stored at -70° C), colonies were isolated by streak-plate method on trypticase soy agar (BD Biosciences, MD) plates. A single colony was used to inoculate a vial of tryptic soy

broth (BD Biosciences, MD) and grown overnight at 37° C. An aliquot of the liquid culture was transferred to a new vial of broth and stored at 37° C for up to 6 days. This culture was used to inoculate a new vial of broth 14 to 24 h before each experiment, to produce fresh bacterial cells which were serially diluted in 0.1% w/v peptone water (Fluka-Biochemika, Switzerland) prior to their use in the immunomagnetic separation procedure. Viable cells were enumerated by microbial plating on MacConkey agar with sorbitol (BD Biosciences, MD), according to standard rules for plate counting (FDA 2009).

5.1.3 Synthesis and Characterization of Two Magnetic Nanoparticles

Carboxylate-functionalized magnetic nanoparticles (CMNPs) were synthesized separately in the lab using a published solvothermal procedure (Xuan, Wang et al. 2009), and were made available for this study. A brief description of the procedure is presented as follows: $FeCl_3 \cdot 6H_2O$ (1.08 g), sodium acetate (3.0 g) and sodium acrylate (3.0 g) were dissolved in 40 ml of ethylene glycol for 2 h at room temperature. The yellow-colored solution was transferred to a teflon-lined stainless-steel pressure vessel (container volume 125 ml, Parr Instrument Company), sealed, and heated at 200° C for 15 h. The pressure vessel was then cooled to room temperature and the synthesized nanoparticles were magnetically separated, washed with 20 ml of water three times and with 20 ml of ethanol three times, and dried overnight under vacuum. As reported in the lab, the resulting particles had an approximate average diameter of 180 nm, and displayed a room temperature saturation magnetization of 60 emu/g.

Similarly, amine-functionalized magnetic nanoparticles (AMNPs) were synthesized separately in the lab with slight modifications of a previously reported procedure (Barick, Aslam et al. 2009), and were made available for this study. A brief description of the procedure is

presented as follows: $FeCl_3 \cdot 6H_2O$ (1.08 g), sodium acetate (2.0 g) and ethylenediamine (7.0 ml) were dissolved in 30 ml of ethylene glycol for 2 h at room temperature. The solution was transferred to the teflon-lined stainless-steel pressure vessel (Parr Instrument Company), sealed, and heated at 200° C for 15 h. The pressure vessel was then cooled to room temperature and the synthesized nanoparticles were magnetically separated, washed with 20 ml of water three times and with 20 ml of ethanol three times, and dried overnight under vacuum. As reported in the lab, the resulting particles had an approximate average diameter of 20 to 30 nm, and displayed a room temperature saturation magnetization of 80 emu/g.

5.1.4 Immunofunctionalization of Magnetic Nanoparticles

Each type of MNP (AMNPs and CMNPs) was conjugated with monoclonal antibodies at an initial MNP concentration of 10 mg/ml (1% solids). Two different initial concentrations of monoclonal antibody were used during conjugation: 1.0 mg/ml antibody and 0.5 mg/ml antibody. Conjugation of antibodies onto MNPs was performed both with and without the addition of NaCl.

Conjugation of antibodies onto carboxylate- and amine-functionalized magnetic nanoparticles employed carbodiimide chemistry for covalent attachment of antibodies. First, 2.5 mg of dry MNPs were suspended in 135 µl of phosphate buffer, 10 µl of 0.1M NHS and 5 µl of 0.1M EDC, and dispersed by ultrasonication for 15 minutes. A volume of 100 µl of monoclonal anti-*E. coli* O157:H7 antibody (also suspended in phosphate buffer) was added, yielding a final antibody concentration of either 1.0 mg/ml or 0.5 mg/ml. The mixture was hybridized on a rotisserie-style rotator for 1 h at room temperature, with 25 µl of 10X PBS being added after the first 5 min of hybridization, to increase the NaCl content of the suspension to approximately

0.14M. (For select experiments, the 10X PBS was omitted). Following hybridization, the MNP-antibody conjugate was magnetically separated, the supernatant removed, and the conjugate resuspended in 250 µl of blocking buffer (tris buffer with casein) for 5 min. Again the conjugate was magnetically separated, the supernatant removed, and the conjugate resuspended in 250 µl of blocking buffer, this time for 1 h with rotation. Finally, the MNP-antibody conjugate was magnetically separated, the supernatant removed, and the conjugate resuspended in 2.5 ml of phosphate buffer.

The final concentration of MNPs in each solution was 1.0 mg/ml. Immuno-conjugated MNPs (immuno-MNPs) were stored at 4° C. Prior to experimental use, immuno-MNPs were either magnetically concentrated or further diluted in phosphate buffer, in order to obtain solutions of both immuno-CMNPs and immuno-AMNPs at the following concentrations: 1.5 mg/ml, 1.0 mg/ml, 0.5 mg/ml, and 0.1 mg/ml MNPs.

5.1.5 Immunomagnetic Separation of Microorganism

Serial dilutions of each bacteria (*E. coli* O157:H7, *E. coli* O55:H7, and *S. boydii)* were independently prepared in 0.1% w/v peptone water. Three or four of the pure dilutions of each bacteria were plated (100-µl aliquots) on sorbitol MacConkey agar and incubated at 37° C overnight. For IMS, 50 µl of immuno-MNPs and 50 µl of the appropriate bacterial dilution were combined with 400 µl of 10mM PBS (pH 7.4), and hybridized with rotation at room temperature for 30 minutes. After hybridization, the cell-immuno-MNP complexes were magnetically separated and the supernatant removed. Complexes were washed twice in wash buffer (PBS containing 0.05% Tween-20 or 0.05% Triton X-100), and finally resuspended in 0.5 ml of PBS. The IMS procedure required 35 min, and is depicted in Figure 17.

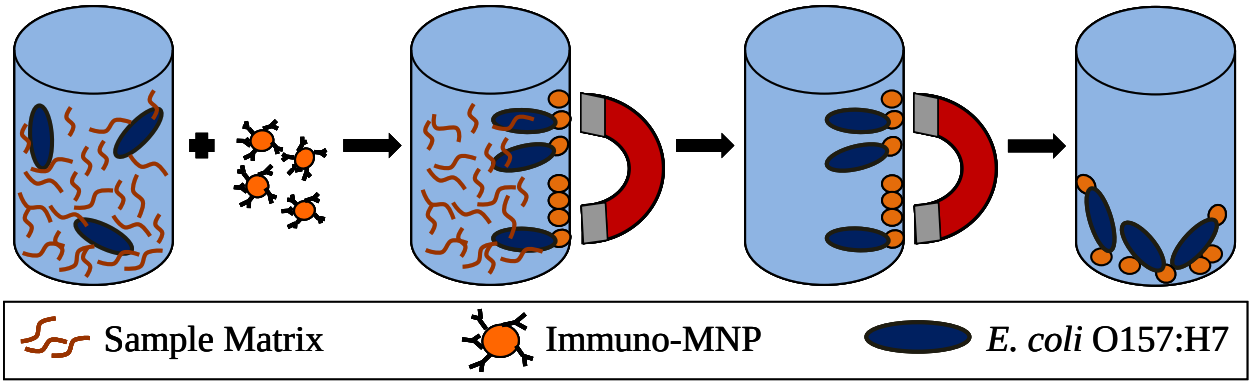

Figure 17. Immunomagnetic separation procedure: sample plus immuno-MNPs → magnetic separation of target cells → removal of sample matrix → purified *E. coli* O157:H7-immuno-MNP complexes.

A 100-µl aliquot was plated on sorbitol MacConkey agar and incubated at 37° C overnight. The number of colony-forming units (CFU) in the 100-µl aliquot was determined by manually counting the colonies on each plate. For every experimental case (i.e., particular combination of immuno-MNP type, immuno-MNP concentration, and bacterial species), a minimum of two bacterial dilutions underwent IMS and were plated.

Calculation of bacterial cell concentrations in both pure and immunomagnetically separated samples were carried out according to rules provided by the United States Food and Drug Administration's Bacteriological Analytical Manual (FDA 2009). Plate counts between 25 and 250 colonies were used to calculate the original cell concentrations in CFU/ml. If all plate counts for a given case fell outside of this range, estimates were made according to FDA rules.

5.1.6 Experimental Design

This study was designed to test four distinct hypotheses, which were developed using the previously reported methodology (Pal, Setterington et al. 2008; Pal and Alocilja 2009) as a

starting point, and with the goal of developing a new IMS methodology for *E. coli* O157:H7 which is able to discriminate against select non-target organisms.

It was hypothesized that the IMS performance would be affected by:

1. The addition of NaCl to a (physiological) concentration of about 0.14M during conjugation of antibodies onto MNPs;

   ($\mu_{salt} \neq \mu_{no\ salt}$; null hypothesis $\mu_{salt} = \mu_{no\ salt}$)

2. The concentration of antibodies present during conjugation of antibodies onto MNPs;

   ($\mu_{1.0\ mg/ml} \neq \mu_{0.5\ mg/ml}$; null hypothesis $\mu_{1.0\ mg/ml} = \mu_{0.5mg/ml}$)

3. The concentration of immuno-MNPs present during IMS;

   ($\mu_{0.1mg/ml} \neq \mu_{0.5\ mg/ml} \neq \mu_{1.0\ mg/ml} \neq \mu_{1.5\ mg/ml}$;

   null hypothesis $\mu_{0.1\ mg/ml} = \mu_{0.5\ mg/ml} = \mu_{1.0\ mg/ml} = \mu_{1.5\ mg/ml}$)

4. The number of days elapsed since conjugation of antibodies onto MNPs.

   ($\mu_{day\ 0} \neq \mu_{day\ x}$; null hypothesis $\mu_{day\ 0} = \mu_{day\ x}$)

In order to test the four hypotheses stated above, four factors (NaCl addition, antibody concentration, immuno-MNP concentration, and age of the immuno-MNP solution) were evaluated in terms of their effect on the ability of the proposed IMS methodology to capture *E. coli* O157:H7 and distinguish it from non-target species,. Therefore, every experiment was applied to three different bacterial species individually: *E. coli* O157:H7 (target species), *E. coli* O55:H7 and *Shigella boydii* (both non-target species). *E. coli* O55:H7 is another EHEC species, closely related to *E. coli* O157:H7. *S. boydii* bears less genotypic and phenotypic similarity to the target organism, but it is a commonly encountered foodborne pathogen, and also produces shiga-toxin like *E. coli* O157:H7. The non-target organisms chosen for this study correspond with the

recommendations made by the AOAC Task Force on Best Practices in Microbiological Methodology (AOAC 2006).

To test Hypothesis 1, immuno-MNPs made with the addition of NaCl were compared to those made without NaCl. (In either case, the initial concentration of antibody was 1.0 mg/ml). Both with and without NaCl, three concentrations (1.0 mg/ml, 0.5 mg/ml, and 0.1 mg/ml) of each type of immuno-MNP were used to perform IMS.

To test Hypothesis 2, immuno-MNPs made with an initial antibody concentration of 1.0 mg/ml were compared to those made with an initial antibody concentration of 0.5 mg/ml. (In either case, NaCl was added during conjugation). With both 1.0 mg/ml antibody and 0.5 mg/ml antibody, three concentrations (1.0 mg/ml, 0.5 mg/ml, and 0.1 mg/ml) of each type of immuno-MNP were used to perform IMS.

To test Hypothesis 3, immuno-MNPs were made with the addition of NaCl and with an initial antibody concentration of 1.0 mg/ml. Each of the four concentrations (1.5 mg/ml, 1.0 mg/ml, 0.5 mg/ml, and 0.1 mg/ml) of each type of immuno-MNPs was used to perform IMS.

To test Hypothesis 4, immuno-MNPs were made with the addition of NaCl, and with initial antibody concentrations of both 1.0 mg/ml and 0.5 mg/ml. Two concentrations (1.0 mg/ml and 0.5 mg/ml) of each type of immuno-MNPs were used to perform IMS at various points from 0 to 60 days after conjugation.

5.1.7 Statistical Analysis

The calculated concentrations of cells captured by IMS (in CFU/ml) were converted to their $\log_{10}$ values for ease of analysis. Statistical analysis was performed using SPSS software. Missing values were computed with hot-deck imputation or excluded analysis by analysis.

Independent, two-tailed T-tests were used to compare experiments in which NaCl was added during conjugation, to experiments in which NaCl was omitted. In the same way, experiments in which the antibody concentration was 1.0 mg/ml were compared to experiments in which the antibody concentration was 0.5 mg/ml. All experimental results were included for these two analyses.

Subsequent analysis was performed using both one-way ANOVA and independent two-tailed T-tests, to evaluate the effect of immuno-MNP concentration, for each type of MNPs. This analysis included only the results of experiments which had the 1.0 mg/ml antibody concentration and the addition of NaCl during conjugation. (In the previous analyses, these parameters were statistically determined to result in better overall IMS performance). Analyses which showed non-normal data distributions were re-evaluated with Kruskal-Wallis or Mann-Whitney U tests as needed. Longevity of the immuno-MNP solutions was also evaluated by one-way ANOVA and independent two-tailed T-tests. All analyses were calculated with 95% confidence ($\alpha = 0.05$).

5.2 Results and Discussion

5.2.1 Immunofunctionalization and Immunomagnetic Separation

Immunofunctionalization of the CMNPs and AMNPs is based on covalent attachment via carbodiimide chemistry. Successful conjugation of antibodies onto MNPs was confirmed by measuring the quantity of antibody in the post-hybridization supernatant with a commercial fluorescence-based protein quantification kit. The measured protein concentration in the supernatant was significantly lower than the concentration of antibodies initially added to the

MNPs (data not shown), indicating that antibodies were retained on the MNPs during hybridization. Immunomagnetic capture of *E. coli* O157:H7 cells was quantified by plate counts.

5.2.2 Hypothesis 1: Effect of NaCl Addition during Conjugation

Conjugation of antibodies onto MNPs was carried out in phosphate buffer at pH 7.4. A slightly basic pH such as this is recommended for optimal adsorption of the Fc (constant) portion of the antibody (Bangs Laboratories 2008), which positions the Fab (antigen-binding) portion outward for maximum target-binding capacity. Also, it has been reported that the addition of NaCl at or near physiological concentration (about 0.15M) increases adsorption efficiency of antibodies onto microspheres (Bangs Laboratories 2008).

Two-tailed independent T-tests performed on the mean concentrations of captured cells ($\log_{10}$ of CFU/ml) for all three bacteria showed that the addition of NaCl (compared with omitting NaCl) caused a significant decrease in capture of the negative control *S. boydii* ($p = 0.029$; CI = 0.05, 1.04), with no significant effect on the capture of the target *E. coli* O157:H7 or the other negative control *E. coli* O55:H7.

When separated according to MNP type, CMNPs showed the most significant decrease ($p = 0.047$; CI = 0.01, 2.07) in capture of *S. boydii* with addition of NaCl. This remained true when the data were separated according to MNP type and immuno-MNP concentration. At the 0.1 mg/ml MNP concentration, both AMNPs and CMNPs showed a significant increase in capture of negative control *E. coli* O55:H7 ($p = 0.021$; CI = -1.83, -0.18, and $p = 0.044$; CI = -2.62, -0.038, respectively).

Based on these statistical results, null hypothesis 1 is rejected. The addition of 0.14M NaCl during conjugation of antibodies onto MNPs increases the ability of both MNPs to

discriminate against non-target pathogens, at all immuno-MNP concentrations evaluated, but does not change the ability of the MNPs to recognize the target pathogen (Figure 18). Addition of NaCl during conjugation is a simple and inexpensive procedural change able to enhance IMS performance for any application.

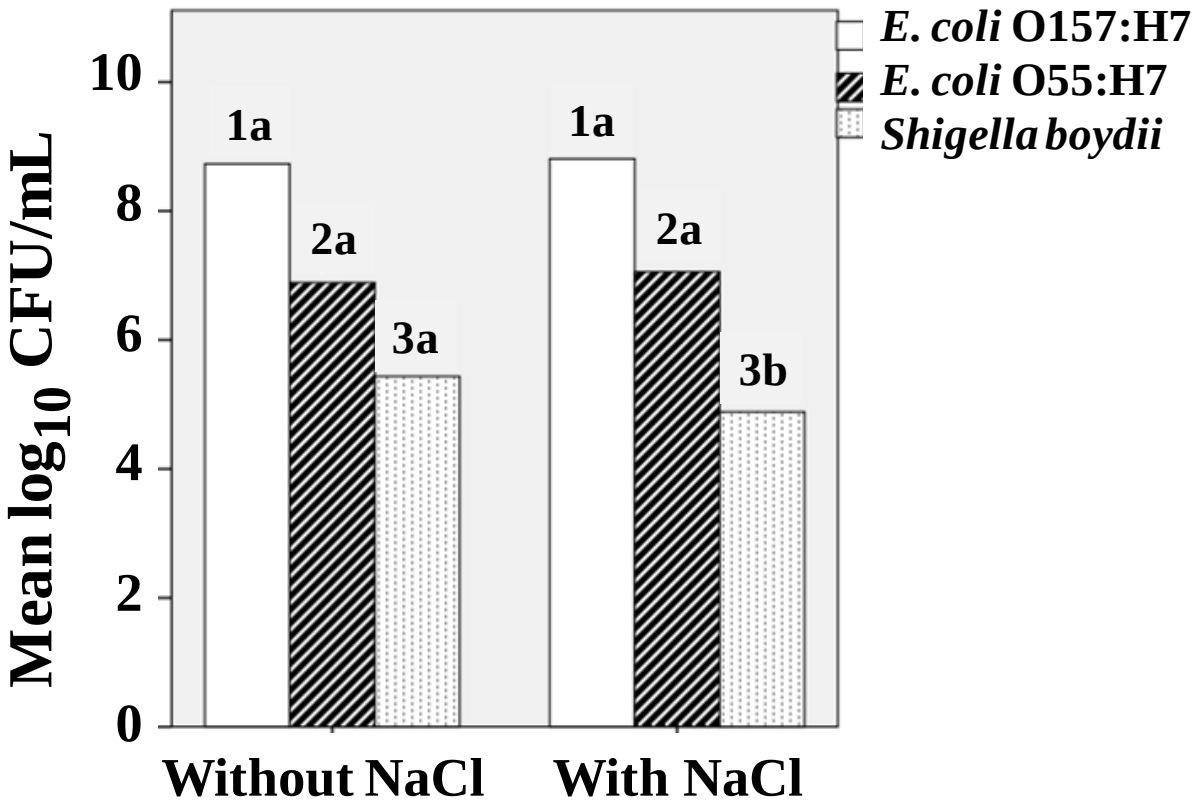

Figure 18. Mean concentration (log_{10} of CFU/ml) of each bacteria captured in IMS, using immuno-MNPs made with and without the addition of NaCl. Results from each type of immuno-MNP are included. Statistical comparisons were made within numbered groups (1-3), and letters (a or b) indicate significant differences ($\alpha = 0.05$).

5.2.3 Hypothesis 2: Effect of Antibody Concentration during Conjugation

During conjugation of antibodies onto MNPs, MNPs were present at a concentration of 10 mg/ml, or 1% solids. The solution volume was kept small (250 µl, until post-conjugation dilution) in order to increase the speed and frequency of interactions between antibodies and MNPs during conjugation. Monoclonal antibody was added at relatively high concentrations of 1.0 mg/ml or 0.5 mg/ml during conjugation, since the presence of excess antibody is thought to contribute to the correct orientation of adsorbed antibodies (Bangs Laboratories 2008; Bangs Laboratories 2008).

Two-tailed independent T-tests performed on the mean concentrations of captured cells ($\log_{10}$ of CFU/ml) for all three bacteria showed that the higher antibody concentration (1.0 mg/ml) caused a significant increase in capture of the target *E. coli* O157:H7 ($p = 0.018$; CI = -2.08, -0.23), with no significant effect on the capture of the negative control microorganisms.

When separated according to MNP type, CMNPs showed the most significant increase ($p = 0.000$, CI = -2.05, -0.75) in capture of *E. coli* O157:H7 with the higher antibody concentration. When separated according to both MNP type and immuno-MNP concentration, the number of data points per case was insufficient to draw conclusions on specificity.

Based on these statistical results, null hypothesis 2 was rejected. The higher antibody concentration (1.0 mg/ml) during conjugation increases the ability of both MNPs to recognize the target pathogen, at all immuno-MNP concentrations evaluated, but does not change the ability of the MNPs to discriminate against non-target pathogens (Figure 19). Although consumption of more antibodies increases the cost of the assay, it is worthwhile for some IMS applications. Since the infectious dose of *E. coli* O157:H7 is only 10 to 100 cells (FDA 2009), high sensitivity is a critical feature in any IMS assay for this organism. However if IMS is being

applied to a pathogen like *Bacillus cereus*, with an infectious dose greater than 10^6 cells (FDA 2009), then decreasing the cost of the assay would likely be of greater value than increasing the sensitivity, and a lower antibody concentration may be ideal.

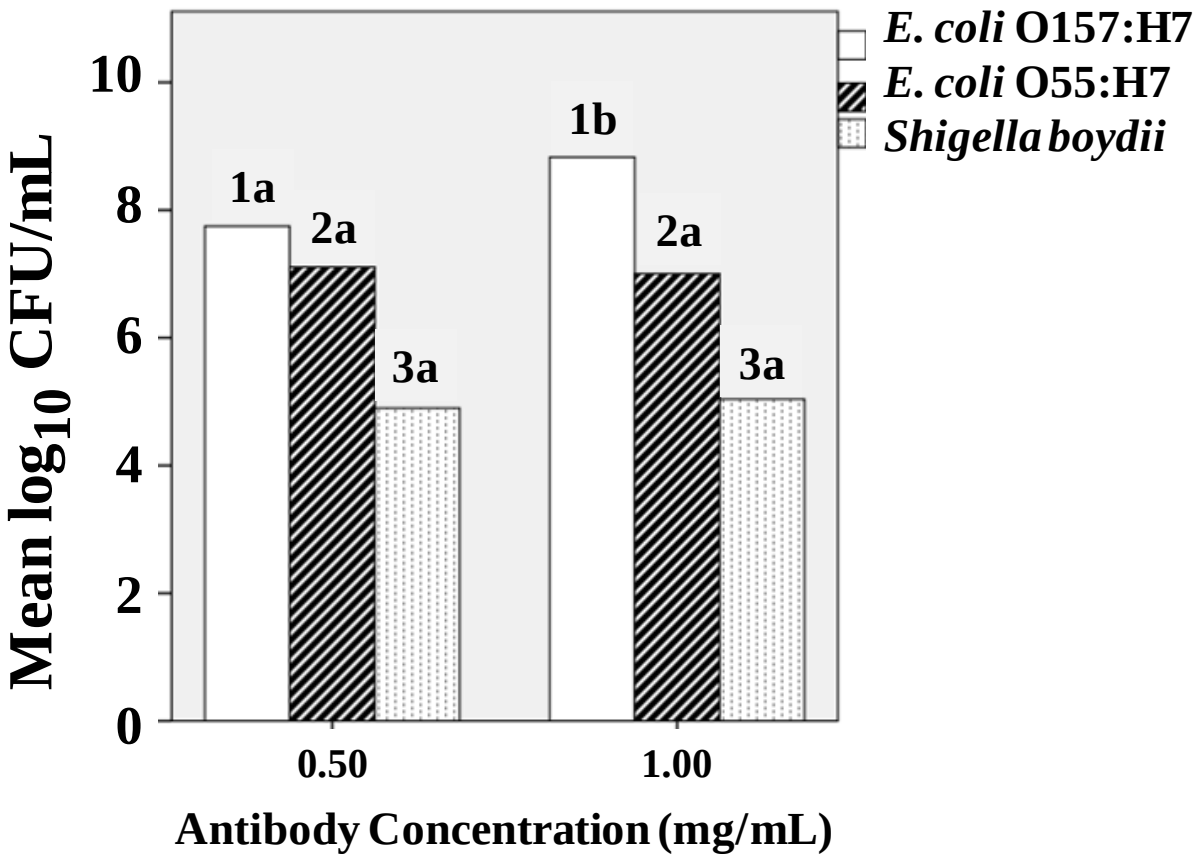

Figure 19. Mean concentration (log_{10} of CFU/ml) of each bacteria captured in IMS, using immuno-MNPs made with 1.0 mg/ml antibody and with 0.5 mg/ml antibody. Results from each type of immuno-MNP are included. Statistical comparisons were made within numbered groups (1-3), and letters (a or b) indicate significant differences ($\alpha = 0.05$).

5.2.4 Hypothesis 3: Effect of Immuno-MNP Concentration during IMS

With the objective of developing a practical and cost-effective IMS methodology, the concentration of immuno-MNPs employed in IMS was identified as an important parameter to be optimized.

One-way ANOVA was performed on the mean concentrations of captured cells ($\log_{10}$ of CFU/ml) for all three bacteria, separated according to MNP type and immuno-MNP concentration, using only the results of experiments which had the 1.0 mg/ml antibody concentration and the addition of NaCl during conjugation. No significant difference in the capture of the target *E. coli* O157:H7 was observed at any immuno-MNP concentration with this test (LDS and Bonferroni pairwise comparison). The only exception to this is that AMNPs at 1.0 mg/ml captured significantly more *E. coli* O157:H7 than AMNPs at 0.5 mg/ml (T-test, $p = 0.047$). However, the ANOVA homogeneity of variance test showed non-normal distributions for various MNP types and various bacteria. To account for the non-normality observed in the ANOVA, independent T-tests were also performed for each MNP type and for all three bacteria, and these did show some significant differences in medians, with the nonparametric comparison (using the Kruskal-Wallis test for median and distribution, or the Mann-Whitney two-sample comparison). From these statistical analyses, the following conclusions were drawn:

CMNPs at both 1.5 mg/ml and 0.1 mg/ml showed less ability to discriminate against non-target pathogens than CMNPs at either 1.0 mg/ml or 0.5 mg/ml. Concentration of CMNPs has no effect on their ability to recognize the target pathogen. There was no significant difference between CMNPs at 1.0 mg/ml and at 0.5 mg/ml.

AMNPs at 0.1 mg/ml showed less ability to discriminate against non-target pathogens than any other concentration of AMNPs. AMNPs at 1.0 mg/ml showed greater ability to

recognize the target pathogenthan AMNPs at 0.5 mg/ml. There are no other significant differences between any of the AMNP concentrations,

Based on these statistical results, null hypothesis 3 is rejected. The concentration of immuno-MNPs present during IMS influences their ability to recognize the target pathogen and to discriminate against non-target pathogens, for both types of immuno-MNPs (Figure 20). In most cases where the immuno-MNP concentration had a significant effect on bacterial capture, concentrations of 1.0 mg/ml and 0.5 mg/ml were optimal. Also, a very low immuno-MNP concentration (such as 0.1 mg/ml) could be employed to drastically decrease the cost of the assay in cases where performance need not be optimal (for example, high-throughput yes/no screening of food products, with tolerance levels greater than zero).

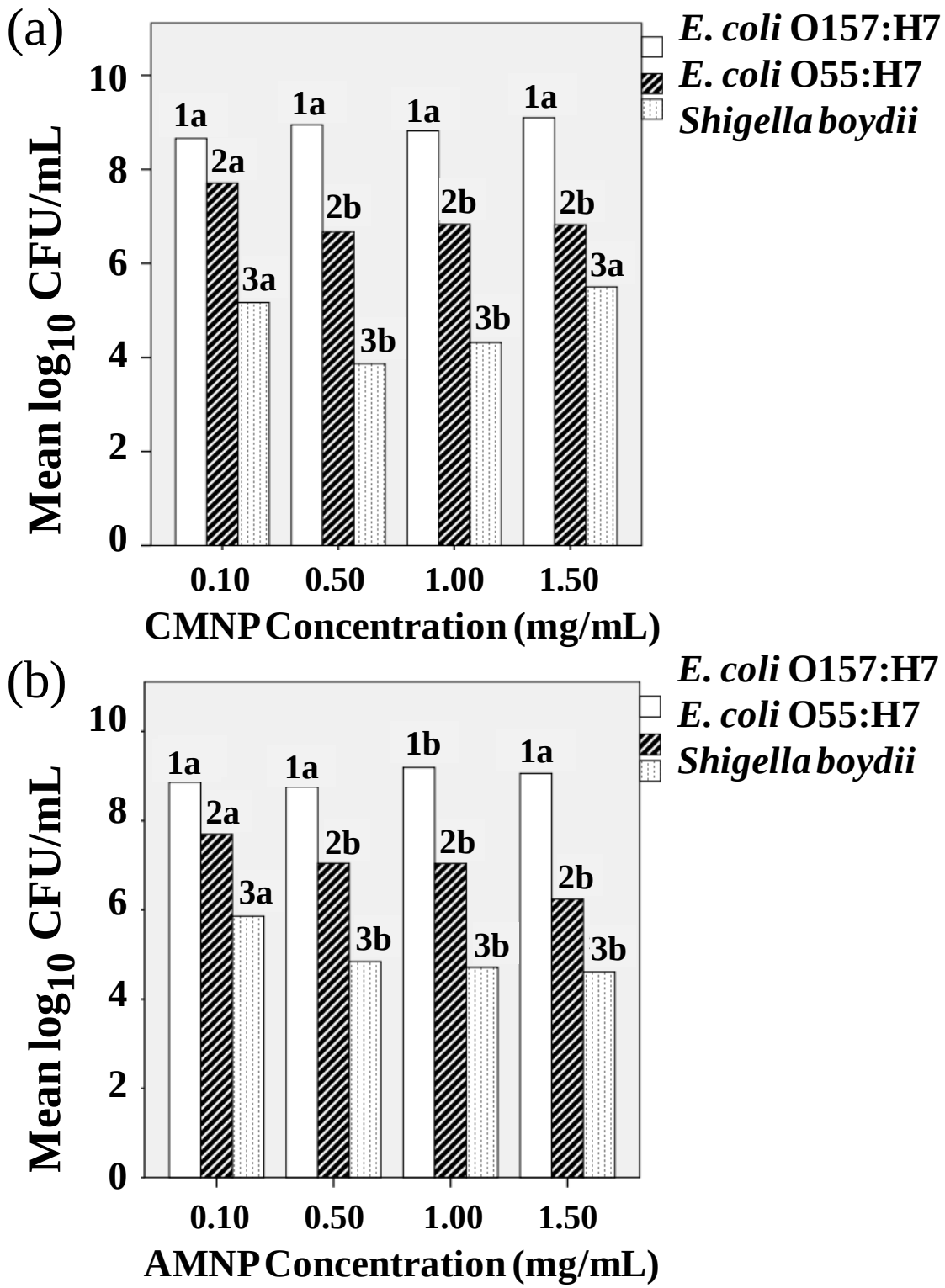

Figure 20. Mean concentration (log_{10} of CFU/ml) of each bacteria captured in IMS, using (a) immuno-CMNPs and (b) immuno-AMNPs, at concentrations of 1.5 mg/ml, 1.0 mg/ml, 0.5 mg/ml, and 0.1 mg/ml. Statistical comparisons were made within numbered groups (1-3), and letters (a or b) indicate significant differences ($\alpha = 0.05$).

5.2.5 Hypothesis 4: Effect of Age of Immuno-MNP Solution during IMS

With the previously reported method of conjugating antibodies onto MNPs (Pal, Setterington et al. 2008; Pal and Alocilja 2009), long term storage of immuno-MNP solutions (at 4° C) resulted in poorer IMS performance. This observation led to Hypothesis 4, that the number of days elapsed since conjugation of antibodies onto MNPs will affect IMS performance.

One-way ANOVA and independent two-tailed T-tests were performed on the mean concentration of captured cells ($\log_{10}$ of CFU/ml) for all three bacteria, comparing the experimental results obtained from immuno-MNP solutions ranging in age from 0 days to 60 days. Regardless of which statistical test was applied, no significant difference was observed in IMS capture of any of the three bacteria.

Based on these statistical results, null hypothesis 4 is retained. Days elapsed since conjugation of antibodies onto MNPs (stored at 4° C), from 0 to 60 days, has no effect on their ability to recognize the target pathogen or to discriminate against non-target pathogens. The excellent longevity of the immuno-MNPs makes the proposed IMS methodology more practical and cost-effective, by reducing both the labor and the materials required.

This study has laid the foundation for application of the IMS method to food samples. Future research will focus on quantifying sensitivity (in terms of LOD_{50} and false negatives), and specificity (in terms of false positives) of the IMS system when applied to food matrices. Additionally, the IMS methodology will be applied to various biosensor platforms for rapid detection of foodborne pathogens.

5.3 Conclusion

The experiments designed and executed in this study provided conclusive results, allowing the initial hypotheses to be either rejected or retained. Discrimination against non-target organisms was improved by adding 0.14M NaCl during conjugation of antibodies onto MNPs. Recognition of the target organism was improved by using a high initial concentration of monoclonal antibodies (1.0 mg/ml) during conjugation. In most cases where immuno-MNP concentration was significant, concentrations of 1.0 mg/ml and 0.5 mg/ml were optimal. The immuno-MNPs were proven to have excellent longevity, with no decline in performance up to 60 days after conjugation.

The IMS methodology presented here is sensitive, specific, rapid, and inexpensive. The entire IMS procedure requires only 35 min. It shows potential for extraction and concentration of microbial pathogens from food matrices, eliminating overnight enrichment steps, and could be paired with nearly any rapid detection method for practical applications in food defense, food and water safety, and clinical diagnostics.

CHAPTER 6

APPLICATION OF NEW IMMUNOMAGNETIC SEPARATION METHODOLOGY TO LABEL-BASED DETECTION OF *ESCHERICHIA COLI* O157:H7

The detection scheme presented here is a modification of the biosensor described in Chapter 4, in which carboxylate-functionalized magnetic nanoparticles (CMNPs) and the newly developed IMS methodology (Chapter 5) were utilized in place of commercial IMBs. This was done to prove the efficacy of the IMS methodology in conjunction with a rapid pathogen detection method. After immunomagnetic separation of *E. coli* O157:H7 cells, electrochemical detection was carried out by cyclic voltammetry on disposable SPCE sensors, based on a novel electroactive polyaniline label. An external magnetic field was employed to pull the labeled cells to the electrode surface, in order to amplify the electrochemical signal generated by the polyaniline.

6.1 Materials and Methods

6.1.1 Reagents and Materials

Aniline monomer, HCl, sodium dodecyl sulfate (SDS), ammonium persulfate, and methanol were used for the synthesis of polyaniline. Triton X-100, phosphate buffered saline (PBS), trizma base, casein, sodium phosphate (dibasic and monobasic), and sodium chloride were used in immunomagnetic separation and polyaniline labeling of bacteria. All of the above reagents were purchased from Sigma-Aldrich (St. Louis, MO) except SDS, which was purchased from Pierce/Thermo Scientific (Rockford, IL). Monoclonal and polyclonal anti-*E. coli* O157:H7 antibodies were obtained from Meridian Life Science, Inc. (Saco, ME).

All solutions and buffers used in this study were prepared in DI water from the Millipore Direct-Q system. Magnetic separations were performed with a commercial magnetic separator (Promega Corporation, Madison, WI). Centrifugation was performed with an Eppendorf 5415 R microcentrifuge. Hybridization of biological materials was carried out at room temperature with rotation on a tube rotisserie (Labquake, Thermo Scientific, MA).

6.1.2 Detection Apparatus

Cyclic voltammetric measurements were performed with a PalmSens handheld potentiostat connected to a personal computer equipped with PSLite software (PalmSens, Houten, Netherlands). SPCE sensors (Gwent Inc., UK) are shown in Figure 1. Every SPCE sensor was rinsed with sterile DI water and allowed to dry before test solution was applied. Sensors were disposed of after single use.

6.1.3 Culturing and Plating of Microorganism

E. coli O157:H7 (Sakai strain) was obtained from the Food Safety and Toxicology collection at Michigan State University. From frozen purified culture stocks (stored at -70° C), colonies were isolated by streak-plate method on trypticase soy agar (BD Biosciences, MD) plates. A single colony was used to inoculate a vial of tryptic soy broth (BD Biosciences, MD) and grown overnight at 37° C. An aliquot of the liquid culture was transferred to a new vial of broth and stored at 37° C for up to 6 days. This culture was used to inoculate a new vial of broth 14 to 24 h before each experiment, to produce fresh bacterial cells which were serially diluted in 0.1% w/v peptone water (Fluka-Biochemika, Switzerland) prior to their use in the IMS

procedure. Viable cells were enumerated by microbial plating on MacConkey agar with sorbitol (BD Biosciences, MD), according to standard rules for plate counting (FDA 2009).

6.1.4 Synthesis and Immunofunctionalization of Magnetic Nanoparticle

The CMNPs were synthesized exactly as described in Chapter 5 (section 5.1.3). Conjugation of antibodies onto CMNPs employed carbodiimide chemistry for covalent attachment of antibodies. CMNPs were present at an initial concentration of 10 mg/ml (1% solids) and monoclonal antibodies were present at an initial concentration of 1.0 mg/ml. First, 2.5 mg of dry CMNPs were suspended in 135 µl of 100mM phosphate buffer (pH 7.4), 10 µl of 0.1M NHS and 5 µl of 0.1M EDC, and dispersed by ultrasonication for 15 minutes. A volume of 100 µl of monoclonal anti-*E. coli* O157:H7 antibody was added, yielding a final antibody concentration of 1.0 mg/ml. The mixture was hybridized on a rotisserie-style rotator for 1 h at room temperature, with 25 µl of 10X PBS being added after the first 5 min of hybridization, to increase the NaCl content of the suspension to approximately 0.14M. Following hybridization, the CMNP-antibody conjugate was magnetically separated, the supernatant removed, and the conjugate resuspended in 250 µl of blocking buffer (10mM PBS buffer with 0.01% w/v casein to block unoccupied reactive sites on the CMNPs) for 5 min. Again the conjugate was magnetically separated, the supernatant removed, and the conjugate resuspended in 250 µl of blocking buffer, this time for 1 h with rotation. Finally, the CMNP-antibody conjugate was magnetically separated, the supernatant removed, and the conjugate resuspended in 2.5 ml of 10mM PBS buffer. The final concentration of CMNPs was 1.0 mg/ml. Immuno-conjugated CMNPs (immuno-CMNPs) were stored at 4° C.

6.1.5 Synthesis and Immunofunctionalization of Conductive Polymer for Target Labeling

Polyaniline nanostructures (nano-PANI) were synthesized and characterized exactly as described in Chapter 4 (section 4.1.3). Polyclonal anti-*E. coli* O157:H7 antibodies were coated onto nano-PANI by direct physical adsorption (Pal and Alocilja 2009). Antibodies were added to nano-PANI (at sufficient volume to achieve an antibody concentration of 1.0 mg/ml) suspended in 10mM PBS (0.15M NaCl) containing 0.01% Triton X-100 for dispersion. The mixture was hybridized on a rotisserie-style rotator for 1 h at room temperature. Following adsorption of antibody, the bio-modified polyaniline (immuno-PANI) was centrifuged (3 min at 10,200 rpm), the supernatant removed, and the immuno-PANI resuspended in blocking buffer (100mM tris buffer containing 0.15M NaCl, and 0.01% w/v casein to block unoccupied reactive sites on polyaniline), and hybridized for another 1 h with rotation. Finally the solution was centrifuged again (3 min at 10,400 rpm), the supernatant removed, and the immuno-PANI resuspended in 1 ml of 10mM PBS containing 0.02% Triton X-100 for dispersion. The immuno-PANI solution was blue-green in color, stayed well-dispersed (i.e., did not precipitate out during storage), and was stored at 4° C.

6.1.6 Immunomagnetic Separation and Electroactive Labeling of Microorganism

E. coli O157:H7 in pure culture was serially diluted in 0.1% w/v peptone water. A volume of 50 µl of the appropriate bacterial dilution was combined with 50µl of immuno-CMNPs (at 1.0 mg/ml) in 400 µl of 10mM PBS (pH 7.4), and hybridized with rotation at room temperature for 15 minutes. At this point, 55 µl of 10mM PBS (pH 7.4) containing 0.1% w/v casein was added and the solution hybridized for another 5 min with rotation, to block the unoccupied active sites on cells and CMNPs. After blocking, the cell-immuno-CMNP complexes

were magnetically separated and the supernatant removed. Complexes were resuspended in 450 μl of 10mM PBS (pH 7.4) and 50 μl of immuno-PANI, and hybridized with rotation at room temperature for 15 min. After labeling with immuno-PANI, the complexes were again magnetically separated and the supernatant removed. The PANI-cell-CMNP complexes were washed once in 10mM PBS containing 0.05% Triton X-100, and finally resuspended in 500 μl of 10mM PBS. Immunomagnetic separation and polyaniline labeling *E. coli* O157:H7 cells is depicted in Figure 11.

6.1.7 Electrochemical Detection of Microorganism

The IMB-*E.coli*-immuno-PANI complexes were magnetically separated and suspended in 0.1M HCl for 10 min in order to electrically activate the polyaniline by acid doping. The volume of acid in which complexes were suspended was one-third of the original solution volume, so that the concentration of IMB-*E.coli*-immuno-PANI complexes was tripled prior to detection. Immediately following the incubation period, a volume of 100 μl of IMB-*E.coli*-immuno-PANI in 0.1M HCl was added to the sample well of the SPCE sensor, and the sensor was placed on a magnetic field in order to attract and position the complexes tightly onto the sensor surface (Figure 1), to amplify the electrochemical signal generated by the polyaniline. The SPCE sensor was connected to the potentiostat/galvanostat, and a voltammetric cycle between +1.0 V and -0.4 V was applied at a scan rate of 100 mV/s. Each sensor was scanned with four complete, consecutive cycles, and for each cycle the response current data was recorded. The fourth cycle was chosen for analysis because it showed the most pronounced differences in current flow for different samples.

6.2 Results and Discussion

6.2.1 Immunomagnetic Separation and Electroactive Labeling of Microorganism

Successful immunomagnetic extraction of *E. coli* O157:H7 was confirmed by microbial plating of the IMB-*E.coli*-immuno-PANI solutions. Percent capture efficiency was calculated as (captured viable cell concentration / original viable cell concentration) x 100. The concentration of captured viable cells (CFU/ml) was also used to estimate the number of cells present in the 100-µl sample which was deposited onto the SPCE. Table 4 shows the original and captured cell concentrations, the capture efficiency, the estimated number of cells present on the SPCE during detection, and the minimum electrical current signal obtained during detection. Reported values are the mean of three identical trials ± 1 standard deviation.

Table 4. Original and captured cell concentrations, capture efficiencies, estimated cell numbers on SPCE sensor for detection, and electrical current signals obtained for an *E. coli* O157:H7 sample.

Original Viable Cell Concentration (CFU/ml)	Mean Captured Viable Cell Concentration (CFU/ml) ± S.D. (n = 3)	Capture Efficiency (%)	Mean Viable Cell Number (CFU) on SPCE ± S.D. (n = 3)	Mean Maximum Current Signal (µA) ± S.D. (n = 3)
0 (Blank)	0	---	0	12.8 ± 1.57
8.6×10^3	$(2.6 \pm 0.83) \times 10^3$	30. ± 9.7	$(7.8 \pm 2.5) \times 10^2$	39.9 ± 9.03

The capture efficiency attained here (30%) was slightly lower than the capture efficiency (40 to 50%) attained in this assay using commercial IMBs (Setterington and Alocilja 2010). However, during development of the IMS methodology (Chapter 5) for the CMNPs used here, many of the experiments exhibited capture efficiencies near or greater than 100%. Therefore the immuno-CMNPs employed in this detection assay have the potential to capture much more than

30% of the target bacteria present. However, in this detection assay the hybridization time of immuno-CMNPs with bacteria was shortened to 15 min (versus 30 min in the IMS methodology), in order to keep the total assay time as short as possible (since 20 min of additional incubation time is required for blocking and polyaniline labeling). The lower observed capture efficiency may be due to the shorter hybridization period. Perhaps increasing the hybridization time of immuno-CMNPs with bacteria in this detection assay will increase the capture efficiency. Regardless, more experimental data are necessary before any conclusive statements can be made on the quantitative abililty of immuno-CMNPs to capture target bacteria in this assay. The data reported here merely demonstrate proof-of-concept for the detection method.

The maximum current signals displayed in the last column of Table 4 demonstrated that the electrochemical detection results agreed with microbial plating results (higher cell concentration corresponds to significantly higher maximum current signal).

6.2.2 Electrochemical Detection of Electroactively-Labeled Microorganism

From each electrochemical test, cyclic voltammograms (plot of response current vs. applied potential) were recorded for each of the four consecutive scans performed. Figure 21 depicts cyclic voltammograms of three identical blank tests (no cells) and three identical tests in which approximately 7.8×10^2 CFU of *E. coli* O157:H7 cells, complexed with immno-CMNPs and immuno-PANI, were deposited onto the SPCE sensor for detection. (For a discussion of the oxidation and reduction peaks exhibited in a cyclic voltammogram of polyaniline, see section 4.2.2). It is evident from Figure 21 that the cyclic voltammograms generated by all three positive tests are much larger than those generated by the blank tests.

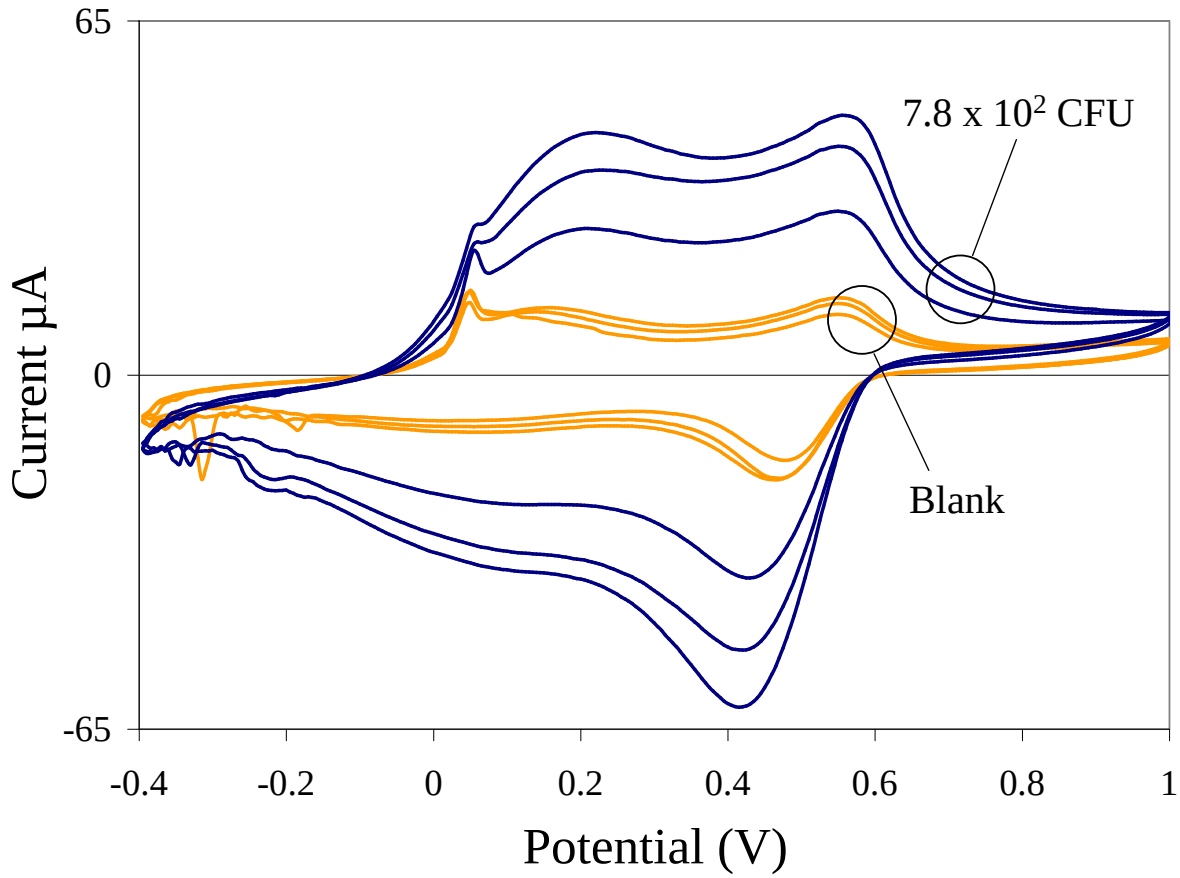

Figure 21. Cyclic voltammograms of three identical blank tests (0 CFU) and three identical tests containing 7.8 x 10^2 CFU *E. coli* O157:H7 (in the form of IMB-*E.coli*-immuno-PANI complexes), each suspended in 0.1M HCl.

For simplicity of comparison, each cyclic voltammogram (plot of response current vs. applied potential) can be represented by a single numeric parameter. Three parameters were evaluated for each voltammogram: the quantity of charge transferred (ΔQ), the maximum current value, and the minimum current value. Charge transfer ΔQ is computed as the integral of the current with respect to time. Maximum current is taken as the *positive* current value occurring at +0.220 V on the cyclic voltammogram (approximate location of the left-most oxidation peak). Minimum current is taken as the *negative* current value occurring at +0.420 V on the cyclic voltammogram (approximate location of the lowest reduction peak).

Figure 22 displays the charge transfer values and the maximum and minimum current values obtained from the cyclic voltammograms of test solutions containing 0 (blank) and 7.8 x 10^2 CFU. Values plotted are the mean of three replicate trials, and error bars represent ± 1 standard deviation. All data was collected in a single experiment. For all three sensor response parameters (ΔQ, maximum current, minimum current), the average parameter value for the positive tests is significantly higher than the average parameter value for the blank tests. Signal to blank ratios for each parameter are displayed on the chart. Maximum current is the parameter which yields the best signal: blank ratio (3.69), followed by minimum current (3.35) and ΔQ (2.94). A two-sample, two-tailed T-test assuming unequal variances indicated that the ΔQ values obtained for the blank tests are statistically different from the ΔQ values obtained for the positive tests, with 95% confidence ($\alpha = 0.05$). The same result was obtained in T-tests comparing the maximum current or minimum current values of the blank tests with those of the positive tests.

The data displayed in Figures 21 and 22 indicated that 7.8 x 10^2 CFU of *E. coli* O157:H7 present on the SPCE sensor (corresponding to an original cell concentration of 8.6 x 10^3 CFU/ml) could be detected with a signal: blank ratio >3. Only one cell concentration was tested, and it is unknown whether or not the sensor response is linear. However since this detection assay was very similar to the one described in Chapter 4 (the only difference is the immunomagnetic nanoparticle employed) which produced a linear response and detection as low as 7 CFU, it is expected that further experimentation will show this assay to perform similarly.

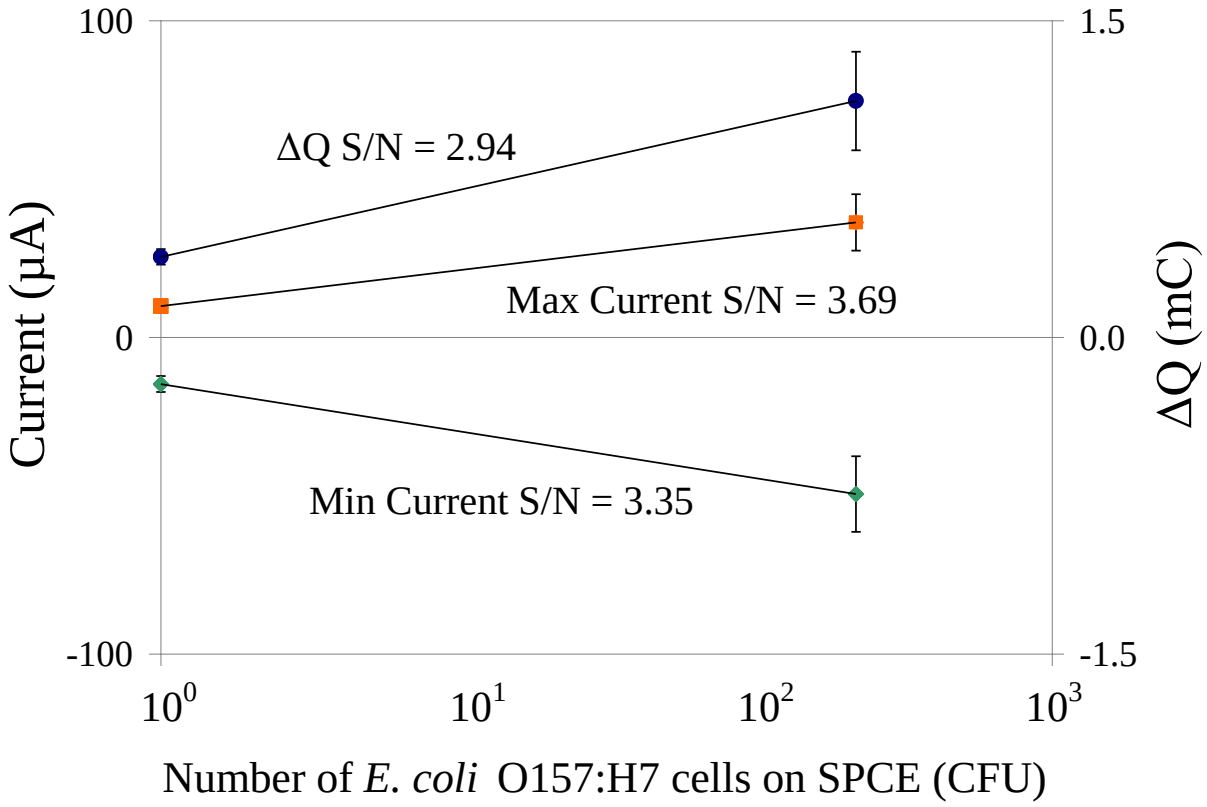

Figure 22. Average ΔQ (●), average maximum current (■), and average minimum current (◆) values obtained in cyclic voltammetry of IMB-*E.coli*-immuno-PANI solutions with cell counts of 0 (blank) and 7.8 x 10^2 CFU. Error bars represent ± 1 standard deviation (n = 3). Signal to blank ratios for each parameter are displayed on the chart.

Just as in Chapter 4, the IMB-*E.coli*-immuno-PANI complexes were immuno-magnetically concentrated prior to detection. The two-fold concentration employed in Chapter 4 yielded good results, and in this case, three-fold concentration was employed (i.e., the complexes were magnetically separated and resuspended in one-third of the original volume, in order to triple the concentration being applied to the SPCE sensor). This presumably amplified the signal even further, although the precise effect of pre-detection concentration of test solutions on signal magnitude or signal" blank ratio was not evaluated. If larger sample volumes were employed, samples could be immunomagnetically concentrated by more than three-fold before detection.

Also as in Chapter 4, an external magnetic field was used to draw IMB-*E.coli*-immuno-

PANI complexes to the sensor surface prior to detection (Figure 11), where the electric field is most concentrated (Radke and Alocilja 2004). Magnetically positioning the polyaniline as near as possible to the electrode is a simple way of amplifying the electrochemical signal.

The time required to carry out the biosensor assay (from sampling to detection) was approximately 55 min. The time has been reduced by 15 min in comparison to the similar assay described in Chapter 4, mainly by reducing the hybridization time of immunomagnetic nanoparticles with bacteria. Further optimization studies are needed to confirm whether the reduced hybridization time adversely affects capture efficiency. Either way, this time requirement is a huge advantage over the standard (culture) method, which requires 24 h even for an initial positive/negative result (FDA 2009). Also, this assay time is competitive in comparison with other IMS-electrochemical detection sensors (Table 3), with assay times ranging from 35 min to 2 h.

6.3 Conclusion

Proof-of-concept has been demonstrated for a rapid electrochemical method for *E. coli* O157:H7 detection. Cells are isolated by immunomagnetic separation, labeled with electroactive polyaniline, and detected by cyclic voltammetry on screen-printed carbon electrodes. Further experimentation is necessary to determine the detection limit and linearity of the sensor. Also the biosensor's specificity, response to nonviable cells, and performance in complex matrices have not yet been determined. Future work will focus on optimization and validation of the biosensor, including detection from mixed bacterial cultures and complex matrices. The assay required 55 min from sampling to result. The low detection limit and short assay time give this biosensor the potential to replace time-consuming culture methods as the means of initial screening for rapid

qualitative results. Another major advantage of the biosensor is its portability. No surface modification of the SPCE sensor is required, making it stable for long term storage and transport. A handheld, battery-powered potentiostat and pocket PC make it feasible to perform this assay in the field. The biosensor could be adapted for other targets simply by use of different antibodies, and immunomagnetic separation of the target can be performed in a variety of sample matrices. Applications for this technology include routine monitoring or emergency detection of bacterial pathogens for food and water safety, environmental monitoring, healthcare, and biodefense.

CONCLUSION

Biodefense, food safety, and water quality require the means to efficiently screen large volumes of samples for microbial pathogens. Rapid, sensitive, and field-ready detection methods are essential, but must also include a means to specifically extract and concentrate the target pathogen from a complex matrix. In this thesis, three proof-of-concept approaches to rapid electrochemical detection of microbial pathogens have been presented, each beginning with immunomagnetic separation (IMS) of the target organism. Additionally, the development of an improved IMS methodology and its use in a rapid electrochemical detection method was described. The detection methods are summarized and compared in Table 5.

Table 5. Comparison of electrochemical detection methods in terms of detection principle, target organism(s), lowest concentration detected, total time required, and key advantages.

Detection Principle	Target Organism(s)	Lowest Concentration Detected	Total Time Required	Key Advantages
IMS; Impedance of target applied to SPCE	*Bacillus cereus*, *E. coli* O157:H7	40 CFU/ml, 6 CFU/ml	65 min	Simple; no SPCE modification; only one antibody required
IMS; Electroactive label of target captured on modified SPCE	BVDV	Unknown	80 min	EAMNP functions both in IMS and as label; method applied to real serum samples
IMS; Electroactive label on target applied to SPCE	*E. coli* O157:H7	70 CFU/ml (7 CFU)	70 min	No SPCE modification; method demonstrated with new IMS procedure

In the first proof-of-concept, target cells in pure culture were detected directly by means of their ability to impede electrical current. An electrically active magnetic nanoparticle

(EAMNP) was employed for IMS and magnetic positioning of target cells on an unmodified screen-printed carbon electrode (SPCE) sensor. The presence of target cells significantly inhibited current flow as measured by cyclic voltammetry. *Bacillus cereus* (as a surrogate for *B. anthracis*) and *E. coli* O157:H7 were detected from pure culture at lower levels of 40 CFU/ml and 6 CFU/ml, respectively, in 65 min.

In the second proof-of-concept, EAMNPs were employed for separation of Bovine Viral Diarrhea Virus (BVDV) from bovine serum samples, and also as an electroactive label. EAMNP-virus complexes were captured on an antibody-functionalized SPCE sensor, and excess EAMNPs were rinsed away. The current flow enabled by BVDV-bound EAMNPs was measured by cyclic voltammetry. The method required 80 min from sampling to detection.

In the third proof-of-concept, target cells in pure culture were isolated via IMS with a non-conductive immunomagnetic bead, and labeled with immunofunctionalized electroactive polyaniline. Labeled cell complexes were magnetically positioned on an unmodified SPCE sensor and detected via cyclic voltammetry. *E. coli* O157:H7 was detected from pure culture with a limit of 7 CFU (or 70 CFU/ml) in 70 min.

Finally, an improved IMS methodology was developed for *E. coli* O157:H7 in pure culture, using two magnetic nanoparticle (MNP) types, and its specificity was initially evaluated against *E. coli* O55:H7 and *Shigella boydii*. The method, optimized in terms of antibody concentration, MNP concentration, and conjugation conditions, required only 35 min and yielded antibody-conjugated MNPs that were stable for up to 60 days. The IMS methodology was demonstrated in conjunction with label-based electrochemical detection of *E. coli* O157:H7.

More research is required in order to determine sensitivity, specificity, and dynamic range for each of the electrochemical detection methods and the IMS methodology, using

complex matrices. Potential applications for these techniques include biosecurity and biodefense, food and water safety, agriculture, animal health, environmental protection, and point-of-care medical diagnostics.

APPENDICES

APPENDIX A

Data Presented in Chapter 2

Table 6. Data referenced in Chapter 2, Table 1.

***B. cereus* Capture:**

Volume plated (µl)	Plate	Dilution	Count	CFU/ml		Original		
50	10^-4 pure	1.0E-04	18	3.6E+02		3.6E+06		
50	10^-4 pure	1.0E-04	21	4.2E+02		4.2E+06		
					AVERAGE:	**3.9E+06**		
Volume plated (µl)	Plate	Dilution	Count	Captured CFU/ml	Actual CFU/ml	Projected Original	Capture Efficiency	(100 µl) CFU/SPCE
100	Blank 1	---	0	---	---	---	---	0
100	Blank 2	---	0	---	---	---	---	0
100	Blank 3	---	0	---	---	---	---	0
100	10^-4 (1)	1.0E-04	9	9.0E+01	390	9.0E+05	23%	9
100	10^-4 (2)	1.0E-04	15	1.5E+02	390	1.5E+06	38%	15
100	10^-4 (3)	1.0E-04	13	1.3E+02	390	1.3E+06	33%	13
AVERAGE:				**1.2E+02**		**1.2E+06**	**32%**	**12**
STD DEV:				**3.1E+01**		**3.1E+05**	**8%**	**3**
100	10^-5 (1)	1.0E-05	2	2.0E+01	39	2.0E+06	51%	2
100	10^-5 (2)	1.0E-05	0	0.0E+00	39	0.0E+00	0%	0
100	10^-5 (3)	1.0E-05	1	1.0E+01	39	1.0E+06	26%	1
AVERAGE:				**1.0E+01**		**1.0E+06**	**26%**	**1**
STD DEV:				**1.0E+01**		**1.0E+06**	**26%**	**1**
100	10^-6 (1)	1.0E-06	0	0.0E+00	3.9	0.0E+00	0%	0
100	10^-6 (2)	1.0E-06	0	0.0E+00	3.9	0.0E+00	0%	0
100	10^-6 (3)	1.0E-06	0	0.0E+00	3.9	0.0E+00	0%	0
AVERAGE:				**0.0E+00**		**0.0E+00**	**0%**	**0**
STD DEV:				**0.0E+00**		**0.0E+00**	**0%**	**0**

***E. coli* Capture:**

Volume plated (µl)	Plate	Dilution	Count	CFU/ml		Original		
100	10^-6 pure	1.E-06	37	3.7E+02		3.7E+08		
50	10^-5 pure	1.E-05	306	6.12E+03		6.12E+08		
					AVERAGE:	**5.9E+08**		
Volume plated (µl)	Plate	Dilution	Count	Captured CFU/ml	Actual CFU/ml	Projected Original	Capture Efficiency	(100 µl) CFU/SPCE
100	Blank 1		0	---	0	---	---	0
100	Blank 2		0	---	0	---	---	0
100	Blank 3		0	---	0	---	---	0
100	10^-8 (1)	1.E-08	1	1.00E+01	5.9	1.E+09	169%	1
100	10^-8 (2)	1.E-08	1	1.00E+01	5.9	1.E+09	169%	1
100	10^-8 (3)	1.E-08	0	0.00E+00	5.9	0.E+00	0%	0
AVERAGE:				**6.67E+00**		**7.E+08**	**113%**	**1**
STD DEV:				**5.77E+00**		**6.E+08**	**98%**	**1**
100	10^-7 (1)	1.E-07	1	1.00E+01	59	1.E+08	17%	1
100	10^-7 (2)	1.E-07	1	1.00E+01	59	1.E+08	17%	1
100	10^-7 (3)	1.E-07	2	2.00E+01	59	2.E+08	34%	2
AVERAGE:				**1.33E+01**		**1.E+08**	**23%**	**1**
STD DEV:				**5.77E+00**		**6.E+07**	**10%**	**1**
100	10^-6 (1)	1.E-06	18	1.80E+02	590	1.8E+08	31%	18
100	10^-6 (2)	1.E-06	16	1.60E+02	590	1.6E+08	27%	16
100	10^-6 (3)	1.E-06	16	1.60E+02	590	1.6E+08	27%	16
AVERAGE:				**1.67E+02**		**1.7E+08**	**28%**	**17**
STD DEV:				**1.15E+01**		**1.2E+07**	**2%**	**1**
50	10^-5 (1)	1.E-05	107	2.14E+03	5900	2.14E+08	36%	214
50	10^-5 (2)	1.E-05	104	2.08E+03	5900	2.08E+08	35%	208
50	10^-5 (3)	1.E-05	35	7.00E+02	5900	7.0E+07	12%	70
AVERAGE:				**1.64E+03**		**1.6E+08**	**28%**	**164**
STD DEV:				**8.15E+02**		**8.1E+07**	**14%**	**81**
50	10^-4 (1)*	1.E-04	51	1.02E+04	59000	1.0E+08	17%	1020
50	10^-4 (2)*	1.E-04	86	1.72E+04	59000	1.7E+08	29%	1720
50	10^-4 (3)*	1.E-04	60	1.20E+04	59000	1.2E+08	20%	1200

AVERAGE:	*diluted by 1/10	**1.31E+04**	**1.3E+08**	**22%**	**1313**
STD DEV:	before plating	**3.64E+03**	**3.6E+07**	**6%**	**364**

Table 7. Data referenced in Chapter 2, Figure 5.

ΔQ (mC)	***E. coli* Concentration (CFU/ml)**
0.0534	HCl only
0.1132	10^6
0.0581	10^4
0.0584	10^2
0.0605	10^0

ΔQ (mC)	***B. cereus* Concentration (CFU/ml)**
0.0534	HCl only
0.2746	10^7
0.0547	10^3
0.0504	10^3
0.0548	10^1

Table 8. Data referenced in Chapter 2, Figure 7.

ΔQ (mC)	***B. cereus*** Concentration (CFU/ml)	Average	Std Dev	ΔQ (mC)	***E. coli*** Concentration (CFU/ml)	Average	Std Dev
0.9588	4.0E+00			1.2760	6.0E+00		
1.2600	4.0E+00			1.0500	6.0E+00		
1.0650	4.0E+00	1.0946	0.1528	1.2520	6.0E+00	1.1927	0.1241
1.1160	4.0E+01			0.9605	6.0E+01		
1.1660	4.0E+01			0.9128	6.0E+01	0.9367	0.0337
1.1230	4.0E+01	1.1350	0.0271	1.2590	5.9E+02		
1.0740	3.9E+02			0.8778	5.9E+02		
0.9868	3.9E+02			0.7593	5.9E+02	0.9654	0.2611
0.9679	3.9E+02	1.0096	0.0566	3.1360	5.9E+03		
1.1750	Blank (1)			2.4480	5.9E+03		
1.4100	Blank (2)			2.1370	5.9E+03	2.5737	0.5112
1.5650	Blank (3)	1.3833	0.1964	2.6460	5.9E+04		
				2.1340	5.9E+04		
				1.9280	5.9E+04	2.2360	0.3697
				1.6080	Blank (1)		
				1.4850	Blank (2)		
				1.4770	Blank (3)	1.5233	0.0734

APPENDIX B

Data Presented in Chapter 3

Table 9. Data referenced in Chapter 3, Figure 10.

BVDV serum	ΔQ (mC)	Average (mC)	Std Dev (mC)
Negative 1	0.6185		
Negative 2	0.6519		
Negative 3	0.6318	0.6341	0.0168
Positive 1	0.7349		
Positive 2	0.7802		
Positive 3	0.721	0.7454	0.0310

BVDV serum	Max Current (A)	Max Current (μA)	Average (μA)	Std Dev (μA)	Variance
Negative 1	0.00001245	12.45			
Negative 2	0.00001647	16.47			
Negative 3	0.00001578	15.78	14.9	2.1496	4.62
Positive 1	0.0000461	46.1			
Positive 2	0.0000421	42.1			
Positive 3	0.0000384	38.4	42.2	3.8510	14.83

APPENDIX C

Data Presented in Chapter 4

Table 10. Data referenced in Chapter 4, Table 2.

***E. coli* Capture:** (Concentrated 2X before applying to SPCE)

Volume plated (µl)	Plate	Dilution	Count	CFU/ml	CFU/SPCE	Original	Capture Efficiency
50	10^-6 pure	1.0E-06	29	5.80E+02	---	5.80E+08	---
50	10^-6 pure	1.0E-06	39	7.80E+02	---	7.80E+08	---
50	10^-6 pure	1.0E-06	38	7.60E+02	---	7.60E+08	---
		AVERAGE:	**35**	**7.07E+02**	**---**	**7.07E+08**	**---**
		STD DEV:	**6**	**1.10E+02**	**---**	**1.10E+08**	**---**
50 each	Blank 1 / 2 / 3	---	0 / 0 / 0	---	---	---	---
25 each	10^-3* 1 / 2 / 3	1.0E-03	78	3.12E+05	6.24E+04	3.12E+08	44.15%
	*diluted by 1/100	1.0E-03	103	4.12E+05	8.24E+04	4.12E+08	58.30%
	before plating	1.0E-03	75	3.00E+05	6.00E+04	3.00E+08	42.45%
	AVERAGE:		**85**	**3.41E+05**	**6.83E+04**	**3.41E+08**	**48.30%**
	STD DEV:		**15**	**6.15E+04**	**1.23E+04**	**6.15E+07**	**8.70%**
25 each	10^-5 1 / 2 / 3	1.0E-05	78	3.12E+03	6.24E+02	3.12E+08	44.15%
		1.0E-05	68	2.72E+03	5.44E+02	2.72E+08	38.49%
		1.0E-05	78	3.12E+03	6.24E+02	3.12E+08	44.15%
	AVERAGE:		**75**	**2.99E+03**	**5.97E+02**	**2.99E+08**	**42.26%**
	STD DEV:		**6**	**2.31E+02**	**4.62E+01**	**2.31E+07**	**3.27%**
50 each	10^-7 1 / 2 / 3	1.0E-07	1	2.00E+01	4.00E+00	2.00E+08	28.30%
		1.0E-07	1	2.00E+01	4.00E+00	2.00E+08	28.30%
		1.0E-07	3	6.00E+01	1.20E+01	6.00E+08	84.91%
	AVERAGE:		**2**	**3.33E+01**	**6.67E+00**	**3.33E+08**	**47.17%**
	STD DEV:		**1**	**2.31E+01**	**4.62E+00**	**2.31E+08**	**32.68%**

Table 11. Data referenced in Chapter 4, Figure 14.

	Total Charge Transfer	With ALL Data		Without Outliers
CFU *E. coli*	**DELTA Q (mC)**	**Average**	**Std Dev**	**DELTA Q (mC)**
0	0.1246			0.1246
0	0.1449	**Blank**		0.1449
0	0.1835	0.1510	0.0299	0.1835
7	0.2325			0.2325
7	0.1924	**10^-7**		0.1924
7	0.1990	0.2080	0.0215	0.1990
600	0.7396			
600	0.2227	**10^-5**		0.2227
600	0.2647	0.2437	0.0297	0.2647
68000	0.2229			
68000	0.3188	**10^-3**		0.3188
68000	0.3128	0.3158	0.0042	0.3128
10^-5 (1) IS an outlier.	10^-3 (1) IS an outlier.	No other outliers.		
	Max Current at 0.245 V	With ALL Data		Without Outliers
CFU *E. coli*	**MAX CURRENT (µA)**	**Average**	**Std Dev**	**MAX CURRENT (µA)**
0	2.1383			2.1383
0	3.5949	**Blank**		3.5949
0	2.8546	2.8626	0.7283	2.8546
7	5.9826			5.9826
7	5.0445	**10^-7**		5.0445
7	4.7244	5.2505	0.6539	4.7244
600	24.0413			
600	5.8537	**10^-5**		5.8537
600	7.6402	6.7469	1.2633	7.6402
68000	7.3653			7.3653
68000	7.7140	**10^-3**		7.7140
68000	8.2350	7.7714	0.4377	8.2350
10^-5 (1) IS an outlier.	10^-3 (1) is NOT an outlier.	No other outliers.		

	Min Current at 0.420 V	With ALL Data		Without Outliers
CFU *E. coli*	**MIN CURRENT (µA)**	**Average**	**Std Dev**	**MIN CURRENT (µA)**
0	-2.0148			-2.0148
0	-3.5186	**Blank**		-3.5186
0	-2.7758	-2.7697	0.7520	-2.7758
7	-5.4494			-5.4494
7	-4.8231	**10^-7**		-4.8231
7	-4.6956	-4.9893	0.4035	-4.6956
600	-21.6264			
600	-5.3419	**10^-5**		-5.3419
600	-6.8949	-6.1184	1.0982	-6.8949
68000	-6.9136			-6.9136
68000	-7.7200	**10^-3**		-7.7200
68000	-7.4899	-7.3745	0.4154	-7.4899
10^-5 (1) IS an outlier.	10^-3 (1) is NOT an outlier.	No other outliers.		

Table 12. Data referenced in Chapter 4, Figure 15.

First Expt: CFU *E. coli*	**MAX CURRENT (µA) at 0.245 V**	**Average**	**Std Dev**	**Signal:Noise**
0	5.3870			
0	5.9924	**Blank**		
0	4.2001	5.1932	0.9117	
500	12.9040			2.4848
500	10.1246	**10^-5**		1.9496
500	21.5523	14.8603	5.9598	4.1501
47000	8.3300			1.6040
47000	7.5478	**10^-3**		1.4534
47000	15.1623	10.3467	4.1887	2.9197

Second Expt: CFU *E. coli*	**MAX CURRENT (µA) at 0.245 V**	**Average**	**Std Dev**	**Signal:Noise**
0	3.0457			
0	4.7785	**Blank**		
0	3.5689	4.1737	0.8553	
7	8.5369			2.0454
7	6.9840	**10^-7**		1.6733
7	7.2428	7.5879	0.8320	1.7353
600	31.2838			7.4954
600	7.3895	**10^-5**		1.7705
600	10.4011	16.3581	13.0134	2.4920
68000	8.9183			2.1368
68000	11.1053	**10^-3**		2.6608
68000	11.3191	10.4475	1.3287	2.7120

Third Expt: CFU *E. coli*	**MAX CURRENT (µA) at 0.245 V**	**Average**	**Std Dev**	**Signal:Noise**
0	2.3663			
0	3.4329	**Blank**		
0	2.7912	2.8635	0.5370	

285000	5.5174			1.9268
285000	4.2828	**10^-2**		1.4957
285000	10.9154	6.9052	3.5274	3.8120

Fourth Expt: CFU *E. coli*	**MAX CURRENT (µA) at 0.245 V**	**Average**	**Std Dev**	**Signal:Noise**
0	4.1175			
50400	11.7545			2.8548
50400	12.4862			3.0324

Table 13. Data referenced in Chapter 4, Figure 16.

Current (µA) at 0.42 V		-Current (µA) at 0.42 V	
-13.60	(0.42 V)	13.6	5x10^4 CFU, Magnet
-2.68	(0.42 V)	2.7	5x10^4 CFU, No Magnet
-4.22	(0.42 V)	4.2	Blank test, Magnet
-0.85	(0.42 V)	0.9	Blank test, No Magnet

APPENDIX D

Data Presented in Chapter 5

Table 14. Data referenced in Chapter 5, Figures 18, 19, and 20.

***E. coli* O157:H7 Sakai strain** Trial (Date/#)	Ab conc (mg/ml)	Add NaCl?	Conj age (days)	Bead type	Bead conc (mg/ml)		Sakai Proj CFU/ml Captured	Sakai Original CFU/ml	Sakai Actual CFU/ml Captured	Sakai Actual CFU/ml Present
07/30/2010 #1	1.0	yes	2	Amine	1.5		2.76E+08	9.43E+09	1.05E+03	9.43E+03
07/30/2010 #2	1.0	yes	2	Amine	1.5		2.06E+09	1.56E+10	2.06E+03	1.56E+04
07/30/2010 #3	1.0	yes	2	Amine	1.5					
07/30/2010 #4	1.0	yes	2	Amine	1.5		8.00E+08	8.80E+07	8.00E+02	8.80E+01
07/30/2010 #5	1.0	yes	2	Amine	1.5		2.86E+09	8.80E+07	2.86E+03	8.80E+01
07/16/2010	1.0	no	1	Amine	1.0		2.78E+08	1.52E+09	2.46E+03	1.52E+04
07/19/2010 AM	1.0	no	3	Amine	1.0		4.70E+08	2.63E+10	4.70E+02	2.63E+04
07/19/2010 PM	1.0	no	3	Amine	1.0		9.70E+08	7.50E+09	9.70E+02	7.50E+03
07/20/2010 AM	1.0	no	4	Amine	1.0		3.00E+08	1.90E+09	3.00E+02	1.90E+03
07/20/2010 PM	1.0	no	4	Amine	1.0		6.10E+08	1.80E+09	6.10E+02	1.80E+03
07/09/2010	1.0	yes	1	Amine	1.0		2.44E+09	9.10E+08	2.44E+03	9.10E+02
07/14/2010	0.5	yes	2	Amine	1.0	<	2.50E+08	7.90E+08	5.00E+01	7.90E+02
07/21/2010	1.0	yes	1	Amine	1.0		3.62E+10	1.08E+10	3.62E+04	1.08E+04
07/22/2010 AM	1.0	yes	2	Amine	1.0		4.40E+08	2.70E+09	4.40E+02	2.70E+03
07/22/2010 PM	1.0	yes	2	Amine	1.0		3.40E+08	3.90E+09	3.40E+02	3.90E+03
07/23/2010 AM	1.0	yes	3	Amine	1.0		1.04E+09	1.58E+10	1.04E+03	1.58E+04
07/23/2010 PM	1.0	yes	3	Amine	1.0		6.70E+08	8.50E+08	6.70E+02	8.50E+02
07/28/2010 #1	1.0	yes	2	Amine	1.0		1.69E+09	2.50E+09	1.69E+04	2.50E+04
07/28/2010 #2	1.0	yes	2	Amine	1.0		1.05E+09	1.51E+09	1.05E+03	1.51E+03

07/28/2010 #3	1.0	yes	2	Amine	1.0		2.02E+09	1.84E+09	2.19E+04	1.84E+04
07/29/2010 #1	1.0	yes	3	Amine	1.0		1.86E+09	8.10E+09	1.86E+03	8.10E+03
07/29/2010 #2	1.0	yes	3	Amine	1.0		1.98E+09	1.12E+11	1.98E+03	1.12E+05
07/16/2010	1.0	no	1	Amine	0.5		5.70E+08	1.52E+09	5.70E+02	1.52E+03
07/19/2010 AM	1.0	no	4	Amine	0.5		1.80E+09	2.63E+10	1.80E+03	2.63E+04
07/19/2010 PM	1.0	no	4	Amine	0.5		8.30E+08	7.50E+09	8.30E+02	7.50E+03
07/20/2010 AM	1.0	no	5	Amine	0.5		9.59E+08	1.90E+09	9.59E+03	1.90E+04
07/20/2010 PM	1.0	no	5	Amine	0.5		2.70E+08	1.80E+09	2.70E+02	1.80E+03
07/12/2010	1.0	yes	4	Amine	0.5		3.70E+08	3.90E+08	3.70E+02	3.90E+02
07/21/2010	1.0	yes	1	Amine	0.5		1.25E+10	1.08E+10	1.25E+03	1.08E+03
07/22/2010 AM	1.0	yes	2	Amine	0.5		5.10E+08	2.70E+09	5.10E+02	2.70E+03
07/22/2010 PM	1.0	yes	2	Amine	0.5	<	2.50E+08	3.90E+09	6.00E+01	3.90E+03
07/23/2010 AM	1.0	yes	3	Amine	0.5		1.21E+08	1.58E+10	5.10E+02	1.58E+05
07/23/2010 PM	1.0	yes	3	Amine	0.5		5.50E+08	8.50E+08	5.50E+02	8.50E+02
07/28/2010 #1	1.0	yes	2	Amine	0.5		1.38E+08	2.50E+09	1.38E+03	2.50E+04
07/28/2010 #2	1.0	yes	2	Amine	0.5		2.60E+08	1.51E+09	2.60E+02	1.51E+03
07/28/2010 #3	1.0	yes	2	Amine	0.5		1.30E+09	1.84E+09	1.30E+04	1.84E+04
07/29/2010 #1	1.0	yes	3	Amine	0.5		1.89E+09	8.10E+09	1.89E+03	8.10E+03
07/29/2010 #2	1.0	yes	3	Amine	0.5		6.10E+08	1.12E+11	6.10E+02	1.12E+05
07/16/2010	1.0	no	1	Amine	0.1	<	2.50E+07	1.52E+09	4.00E+01	1.52E+04
07/19/2010 AM	1.0	no	4	Amine	0.1		1.64E+10	2.63E+10	1.64E+04	2.63E+04
07/19/2010 PM	1.0	no	4	Amine	0.1		9.91E+07	7.50E+09	6.60E+02	7.50E+04
07/20/2010 AM	1.0	no	5	Amine	0.1		5.69E+09	1.90E+09	5.69E+03	1.90E+03
07/20/2010 PM	1.0	no	5	Amine	0.1		1.53E+08	1.80E+09	8.60E+02	1.80E+04
07/13/2010	1.0	yes	5	Amine	0.1	<	2.50E+08	1.72E+09	3.00E+01	1.72E+03
07/09/2010	1.0	yes	1	Amine	0.1		8.80E+08	9.10E+08	8.80E+02	9.10E+02
07/12/2010	1.0	yes	4	Amine	0.1	<	1.00E+07	3.90E+08	0.00E+00	3.90E+02
07/14/2010	0.5	yes	2	Amine	0.1	<	2.50E+08	7.90E+08	8.00E+01	7.90E+02

07/21/2010	1.0	yes	1	Amine	0.1		2.21E+09	1.08E+10	2.12E+03	1.08E+04
07/22/2010 AM	1.0	yes	2	Amine	0.1		1.11E+09	2.70E+09	1.11E+03	2.70E+03
07/22/2010 PM	1.0	yes	2	Amine	0.1	<	2.50E+08	3.90E+09	7.00E+01	3.90E+03
07/23/2010 AM	1.0	yes	3	Amine	0.1	<	2.50E+07	1.58E+10	7.00E+01	1.58E+05
07/23/2010 PM	1.0	yes	3	Amine	0.1		7.09E+07	8.50E+08	5.30E+02	8.50E+03
08/03/2010 #1	1.0	yes	5	Amine	0.1		2.30E+09	4.55E+09	1.99E+02	4.55E+02
08/03/2010 #2	1.0	yes	5	Amine	0.1		2.16E+09	4.55E+09	2.00E+02	4.55E+02
08/03/2010 #3	1.0	yes	5	Amine	0.1		1.70E+10	4.55E+09	1.43E+03	4.55E+02
08/03/2010 #4	1.0	yes	5	Amine	0.1		9.90E+09	6.39E+09	3.37E+02	6.39E+02
08/03/2010 #5	1.0	yes	5	Amine	0.1		7.20E+09	6.39E+09	2.80E+02	6.39E+02
07/30/2010 #1	1.0	yes	2	Carboxyl	1.5		1.84E+09	9.43E+09	1.84E+03	9.43E+03
07/30/2010 #2	1.0	yes	2	Carboxyl	1.5		2.25E+09	1.56E+10	2.25E+03	1.56E+04
07/30/2010 #3	1.0	yes	2	Carboxyl	1.5					
07/30/2010 #4	1.0	yes	2	Carboxyl	1.5		6.80E+08	8.80E+07	6.80E+02	8.80E+01
07/30/2010 #5	1.0	yes	2	Carboxyl	1.5		8.00E+08	8.80E+07	8.00E+02	8.80E+01
07/16/2010	1.0	no	1	Carboxyl	1.0		7.70E+08	1.52E+09	7.70E+02	1.52E+03
07/19/2010 AM	1.0	no	4	Carboxyl	1.0		1.15E+09	2.63E+10	1.15E+03	2.63E+04
07/19/2010 PM	1.0	no	4	Carboxyl	1.0		7.10E+08	7.50E+09	7.10E+02	7.50E+03
07/20/2010 AM	1.0	no	5	Carboxyl	1.0		2.33E+09	1.90E+09	2.33E+03	1.90E+03
07/20/2010 PM	1.0	no	5	Carboxyl	1.0		9.50E+08	1.80E+09	9.50E+02	1.80E+03
07/09/2010	1.0	yes	1	Carboxyl	1.0		7.30E+08	9.10E+08	7.30E+02	9.10E+02
07/12/2010	1.0	yes	4	Carboxyl	1.0		4.30E+08	3.90E+08	4.30E+02	3.90E+02
07/14/2010	0.5	yes	2	Carboxyl	1.0		2.00E+08	7.90E+08	2.00E+03	7.90E+03
07/21/2010	1.0	yes	1	Carboxyl	1.0		2.68E+09	1.08E+10	2.47E+03	1.08E+04
07/22/2010 AM	1.0	yes	2	Carboxyl	1.0	<	2.50E+08	2.70E+09	1.90E+02	2.70E+03
07/22/2010 PM	1.0	yes	2	Carboxyl	1.0		5.50E+08	3.90E+09	5.50E+02	3.90E+03
07/23/2010 AM	1.0	yes	3	Carboxyl	1.0		8.60E+08	1.58E+10	8.60E+02	1.58E+04
07/23/2010 PM	1.0	yes	3	Carboxyl	1.0		5.50E+08	8.50E+08	5.50E+02	8.50E+02

07/28/2010 #1	1.0	yes	2	Carboxyl	1.0		3.60E+08	2.50E+09	3.60E+02	2.50E+03
07/28/2010 #2	1.0	yes	2	Carboxyl	1.0		6.30E+08	1.51E+09	6.30E+02	1.51E+03
07/28/2010 #3	1.0	yes	2	Carboxyl	1.0		7.10E+08	1.84E+09	7.10E+02	1.84E+03
07/29/2010 #1	1.0	yes	3	Carboxyl	1.0		1.92E+09	8.10E+09	1.92E+03	8.10E+03
07/29/2010 #2	1.0	yes	3	Carboxyl	1.0		3.90E+08	1.12E+11	3.90E+02	1.12E+05
07/16/2010	1.0	no	1	Carboxyl	0.5		1.37E+09	1.52E+09	1.37E+03	1.52E+03
07/19/2010 AM	1.0	no	4	Carboxyl	0.5		1.05E+09	2.63E+10	1.05E+03	2.63E+04
07/19/2010 PM	1.0	no	4	Carboxyl	0.5		1.66E+09	7.50E+09	1.66E+03	7.50E+03
07/20/2010 AM	1.0	no	5	Carboxyl	0.5		1.66E+09	1.90E+09	1.66E+03	1.90E+03
07/20/2010 PM	1.0	no	5	Carboxyl	0.5		3.50E+08	1.80E+09	3.50E+02	1.80E+03
07/12/2010	1.0	yes	4	Carboxyl	0.5		2.49E+08	3.90E+08	2.49E+03	3.90E+03
07/14/2010	0.5	yes	2	Carboxyl	0.5	<	1.00E+06	7.90E+08	0.00E+00	7.90E+03
07/21/2010	1.0	yes	1	Carboxyl	0.5		9.10E+08	1.08E+10	9.10E+02	1.08E+04
07/22/2010 AM	1.0	yes	2	Carboxyl	0.5		6.00E+09	2.70E+09	6.00E+02	2.70E+02
07/22/2010 PM	1.0	yes	2	Carboxyl	0.5		2.50E+09	3.90E+09	2.50E+02	3.90E+02
07/23/2010 AM	1.0	yes	3	Carboxyl	0.5		9.70E+08	1.58E+10	9.70E+02	1.58E+04
07/23/2010 PM	1.0	yes	3	Carboxyl	0.5		8.64E+07	8.50E+08	6.10E+02	8.50E+03
07/28/2010 #1	1.0	yes	2	Carboxyl	0.5		5.10E+08	2.50E+09	5.10E+02	2.50E+03
07/28/2010 #2	1.0	yes	2	Carboxyl	0.5		5.10E+08	1.51E+09	5.10E+02	1.51E+03
07/28/2010 #3	1.0	yes	2	Carboxyl	0.5		2.80E+08	1.84E+09	2.80E+02	1.84E+03
07/29/2010 #1	1.0	yes	3	Carboxyl	0.5		1.04E+10	8.10E+09	1.04E+04	8.10E+03
07/29/2010 #2	1.0	yes	3	Carboxyl	0.5		1.25E+09	1.12E+11	1.25E+04	1.12E+06
07/16/2010	1.0	no	1	Carboxyl	0.1		2.39E+08	1.52E+09	2.39E+03	1.52E+04
07/19/2010 AM	1.0	no	4	Carboxyl	0.1		8.64E+07	2.63E+10	4.50E+02	2.63E+05
07/19/2010 PM	1.0	no	4	Carboxyl	0.1		7.15E+08	7.50E+09	7.15E+03	7.50E+04
07/20/2010 AM	1.0	no	5	Carboxyl	0.1		2.70E+08	1.90E+09	2.70E+02	1.90E+03
07/20/2010 PM	1.0	no	5	Carboxyl	0.1		1.09E+09	1.80E+09	1.09E+04	1.80E+04
07/09/2010	1.0	yes	1	Carboxyl	0.1		5.70E+08	9.10E+08	5.70E+02	9.10E+02

07/21/2010	1.0	yes	1	Carboxyl	0.1		4.90E+08	1.08E+10	4.90E+02	1.08E+04
07/22/2010 AM	1.0	yes	2	Carboxyl	0.1	<	2.50E+08	2.70E+09	1.00E+01	2.70E+03
07/22/2010 PM	1.0	yes	2	Carboxyl	0.1	<	1.00E+07	3.90E+09	0.00E+00	3.90E+03
07/23/2010 AM	1.0	yes	3	Carboxyl	0.1		3.00E+07	1.58E+10	3.00E+02	1.58E+05
07/23/2010 PM	1.0	yes	3	Carboxyl	0.1	<	2.50E+07	8.50E+08	8.00E+01	8.50E+03
08/03/2010 #1	1.0	yes	5	Carboxyl	0.1		3.05E+09	4.55E+09	1.72E+02	4.55E+02
08/03/2010 #2	1.0	yes	5	Carboxyl	0.1		1.39E+10	4.55E+09	3.05E+02	4.55E+02
08/03/2010 #3	1.0	yes	5	Carboxyl	0.1		2.50E+09	4.55E+09	1.51E+02	4.55E+02
08/03/2010 #4	1.0	yes	5	Carboxyl	0.1		1.86E+09	6.39E+09	1.54E+02	6.39E+02
08/03/2010 #5	1.0	yes	5	Carboxyl	0.1		1.59E+09	6.39E+09	1.05E+02	6.39E+02
07/30/2010 #1	1.0	yes	2	Pani	1.5		1.96E+09	9.43E+09	1.96E+03	9.43E+03
07/30/2010 #2	1.0	yes	2	Pani	1.5		2.65E+09	1.56E+10	2.65E+03	1.56E+04
07/30/2010 #3	1.0	yes	2	Pani	1.5					
07/30/2010 #4	1.0	yes	2	Pani	1.5		2.29E+09	8.80E+07	2.29E+03	8.80E+01
07/30/2010 #5	1.0	yes	2	Pani	1.5		7.80E+08	8.80E+07	7.80E+03	8.80E+02
07/16/2010	1.0	no	1	Pani	1.0		2.19E+09	1.52E+09	2.19E+03	1.52E+03
07/19/2010 AM	1.0	no	3	Pani	1.0		2.40E+07	2.63E+10	2.40E+02	2.63E+04
07/19/2010 PM	1.0	no	3	Pani	1.0		6.50E+08	7.50E+09	6.50E+02	7.50E+03
07/20/2010 AM	1.0	no	4	Pani	1.0		1.17E+09	1.90E+09	1.17E+04	1.90E+04
07/20/2010 PM	1.0	no	4	Pani	1.0		7.80E+08	1.80E+09	7.80E+03	1.80E+04
07/09/2010	1.0	yes	1	Pani	1.0		9.80E+08	9.10E+08	9.80E+02	9.10E+02
07/12/2010	1.0	yes	4	Pani	1.0		3.40E+08	3.90E+08	3.40E+02	3.90E+02
07/14/2010	0.5	yes	2	Pani	1.0	<	2.50E+08	7.90E+08	3.00E+01	7.90E+02
07/21/2010	1.0	yes	1	Pani	1.0		6.30E+08	1.08E+10	6.30E+02	1.08E+04
07/22/2010 AM	1.0	yes	2	Pani	1.0	<	2.50E+08	2.70E+09	1.60E+02	2.70E+03
07/22/2010 PM	1.0	yes	2	Pani	1.0		1.59E+09	3.90E+09	1.50E+03	3.90E+03
07/23/2010 AM	1.0	yes	3	Pani	1.0		3.00E+08	1.58E+10	3.00E+02	1.58E+04
07/23/2010 PM	1.0	yes	3	Pani	1.0		2.60E+08	8.50E+08	2.60E+02	8.50E+02

07/28/2010 #1	1.0	yes	2	Pani	1.0		5.50E+08	2.50E+09	5.50E+02	2.50E+03
07/28/2010 #2	1.0	yes	2	Pani	1.0		3.57E+09	1.51E+09	3.57E+03	1.51E+03
07/28/2010 #3	1.0	yes	2	Pani	1.0		2.42E+09	1.84E+09	2.42E+03	1.84E+03
07/29/2010 #1	1.0	yes	3	Pani	1.0		2.44E+09	8.10E+09	2.44E+03	8.10E+03
07/29/2010 #2	1.0	yes	3	Pani	1.0		7.90E+08	1.12E+11	7.90E+02	1.12E+05
07/16/2010	1.0	no	1	Pani	0.5		1.63E+09	1.52E+09	1.63E+03	1.52E+03
07/19/2010 AM	1.0	no	4	Pani	0.5		1.54E+08	2.63E+10	7.70E+02	2.63E+05
07/19/2010 PM	1.0	no	4	Pani	0.5		1.25E+09	7.50E+09	1.25E+03	7.50E+03
07/20/2010 AM	1.0	no	5	Pani	0.5	<	2.50E+08	1.90E+09	1.80E+02	1.90E+03
07/20/2010 PM	1.0	no	5	Pani	0.5		3.42E+08	1.80E+09	2.61E+03	1.80E+04
07/12/2010	1.0	yes	4	Pani	0.5		1.58E+08	3.90E+08	1.58E+03	3.90E+03
07/14/2010	0.5	yes	2	Pani	0.5	<	1.00E+07	7.90E+08	0.00E+00	7.90E+02
07/21/2010	1.0	yes	1	Pani	0.5		4.80E+08	1.08E+10	4.80E+02	1.08E+04
07/22/2010 AM	1.0	yes	2	Pani	0.5		7.90E+08	2.70E+09	7.90E+02	2.70E+03
07/22/2010 PM	1.0	yes	2	Pani	0.5		7.60E+08	3.90E+09	7.60E+02	3.90E+03
07/23/2010 AM	1.0	yes	3	Pani	0.5		1.82E+08	1.58E+10	1.69E+03	1.58E+05
07/23/2010 PM	1.0	yes	3	Pani	0.5		3.40E+07	8.50E+08	3.40E+02	8.50E+03
07/28/2010 #1	1.0	yes	2	Pani	0.5		5.40E+08	2.50E+09	5.40E+02	2.50E+03
07/28/2010 #2	1.0	yes	2	Pani	0.5		1.20E+09	1.51E+09	1.20E+03	1.51E+03
07/28/2010 #3	1.0	yes	2	Pani	0.5		1.01E+09	1.84E+09	1.01E+03	1.84E+03
07/29/2010 #1	1.0	yes	3	Pani	0.5		2.27E+09	8.10E+09	2.27E+03	8.10E+03
07/29/2010 #2	1.0	yes	3	Pani	0.5		1.25E+09	1.12E+11	1.25E+04	1.12E+06
07/16/2010	1.0	no	1	Pani	0.1		1.25E+08	1.52E+09	1.12E+03	1.52E+04
07/19/2010 AM	1.0	no	4	Pani	0.1		3.40E+08	2.63E+10	3.40E+02	2.63E+04
07/19/2010 PM	1.0	no	4	Pani	0.1		1.54E+08	7.50E+09	8.70E+02	7.50E+04
07/20/2010 AM	1.0	no	5	Pani	0.1		1.87E+08	1.90E+09	1.87E+03	1.90E+04
07/20/2010 PM	1.0	no	5	Pani	0.1		5.30E+08	1.80E+09	9.10E+03	1.80E+04
07/09/2010	1.0	yes	1	Pani	0.1	<	2.50E+08	9.10E+08	1.10E+02	9.10E+02

07/21/2010	1.0	yes	1	Pani	0.1		6.20E+08	1.08E+10	6.20E+02	1.08E+04
07/22/2010 AM	1.0	yes	2	Pani	0.1	<	2.50E+08	2.70E+09	3.00E+01	2.70E+03
07/22/2010 PM	1.0	yes	2	Pani	0.1	<	2.50E+08	3.90E+09	4.00E+01	3.90E+03
07/23/2010 AM	1.0	yes	3	Pani	0.1		3.10E+07	1.58E+10	3.10E+02	1.58E+05
07/23/2010 PM	1.0	yes	3	Pani	0.1	<	2.50E+07	8.50E+08	2.00E+01	8.50E+02
08/03/2010 #1	1.0	yes	5	Pani	0.1		7.70E+08	4.55E+09	7.70E+01	4.55E+02
08/03/2010 #2	1.0	yes	5	Pani	0.1		1.79E+09	4.55E+09	1.08E+02	4.55E+02
08/03/2010 #3	1.0	yes	5	Pani	0.1		2.50E+08	4.55E+09	2.50E+01	4.55E+02
08/03/2010 #4	1.0	yes	5	Pani	0.1		2.86E+09	6.39E+09	1.19E+02	6.39E+02
08/03/2010 #5	1.0	yes	5	Pani	0.1		3.72E+09	6.39E+09	2.46E+02	6.39E+02

***E. coli* O55:H7** Trial (Date/#)	Ab conc (mg/ml)	Add NaCl?	Conj age (days)	Bead type	Bead conc (mg/ml)		O55 Proj CFU/ml Captured	O55 Original CFU/ml	O55 Actual CFU/ml Captured	O55 Actual CFU/ml Present
07/30/2010 #1	1.0	yes	2	Amine	1.5		2.50E+05	1.64E+09	2.50E+02	1.64E+06
07/30/2010 #2	1.0	yes	2	Amine	1.5		1.17E+06	1.64E+09	1.17E+03	1.64E+06
07/30/2010 #3	1.0	yes	2	Amine	1.5		1.86E+06	1.64E+09	1.86E+03	1.64E+06
07/30/2010 #4	1.0	yes	2	Amine	1.5		1.10E+07	2.15E+09	1.10E+03	2.15E+05
07/30/2010 #5	1.0	yes	2	Amine	1.5		2.60E+06	2.15E+09	2.60E+02	2.15E+05
07/16/2010	1.0	no	1	Amine	1.0		1.79E+07	9.00E+08	1.79E+03	9.00E+04
07/19/2010 AM	1.0	no	3	Amine	1.0		1.19E+07	8.50E+08	1.19E+03	8.50E+04
07/19/2010 PM	1.0	no	3	Amine	1.0		6.30E+06	1.30E+09	6.30E+02	1.30E+05
07/20/2010 AM	1.0	no	4	Amine	1.0		2.18E+07	4.20E+09	2.18E+04	4.20E+06
07/20/2010 PM	1.0	no	4	Amine	1.0		4.39E+06	1.45E+09	4.39E+03	1.45E+06
07/09/2010	1.0	yes	1	Amine	1.0	<	1.00E+07	9.70E+08	0.00E+00	9.70E+02
07/14/2010	0.5	yes	2	Amine	1.0	<	2.50E+07	1.32E+11	7.00E+01	1.32E+06

07/21/2010	1.0	yes	1	Amine	1.0	<	2.50E+06	1.83E+10	1.80E+02	1.83E+06
07/22/2010 AM	1.0	yes	2	Amine	1.0		1.55E+08	2.70E+09	1.55E+03	2.70E+04
07/22/2010 PM	1.0	yes	2	Amine	1.0		9.10E+08	1.13E+10	9.10E+03	1.13E+05
07/23/2010 AM	1.0	yes	3	Amine	1.0		1.56E+07	1.75E+10	1.56E+03	1.75E+06
07/23/2010 PM	1.0	yes	3	Amine	1.0		2.40E+06	9.90E+08	2.40E+03	9.90E+05
07/28/2010 #1	1.0	yes	2	Amine	1.0	<	2.50E+05	4.00E+09	1.80E+02	4.00E+06
07/28/2010 #2	1.0	yes	2	Amine	1.0		6.80E+06	1.70E+09	6.80E+02	1.70E+05
07/28/2010 #3	1.0	yes	2	Amine	1.0		1.39E+07	2.22E+09	1.39E+03	2.22E+05
07/29/2010 #1	1.0	yes	3	Amine	1.0		1.04E+07	2.08E+10	1.04E+03	2.08E+06
07/29/2010 #2	1.0	yes	3	Amine	1.0		8.00E+06	2.47E+11	8.00E+02	2.47E+07
07/16/2010	1.0	no	1	Amine	0.5		1.26E+06	9.00E+08	1.26E+03	9.00E+05
07/19/2010 AM	1.0	no	4	Amine	0.5		1.84E+07	8.50E+08	1.84E+03	8.50E+04
07/19/2010 PM	1.0	no	4	Amine	0.5		7.48E+06	1.30E+09	7.48E+03	1.30E+06
07/20/2010 AM	1.0	no	5	Amine	0.5		9.30E+06	4.20E+09	9.30E+02	4.20E+05
07/20/2010 PM	1.0	no	5	Amine	0.5		1.93E+08	1.45E+09	1.93E+04	1.45E+05
07/12/2010	1.0	yes	4	Amine	0.5	<	2.50E+07	1.82E+09	2.00E+01	1.82E+04
07/21/2010	1.0	yes	1	Amine	0.5	<	2.50E+06	1.83E+10	1.20E+02	1.83E+06
07/22/2010 AM	1.0	yes	2	Amine	0.5		7.15E+07	2.70E+09	7.15E+03	2.70E+05
07/22/2010 PM	1.0	yes	2	Amine	0.5		2.26E+08	1.13E+10	2.26E+03	1.13E+05
07/23/2010 AM	1.0	yes	3	Amine	0.5		1.77E+08	1.75E+10	1.77E+04	1.75E+06
07/23/2010 PM	1.0	yes	3	Amine	0.5	<	2.50E+05	9.90E+08	1.50E+02	9.90E+05
07/28/2010 #1	1.0	yes	2	Amine	0.5		5.36E+06	4.00E+09	5.36E+03	4.00E+06
07/28/2010 #2	1.0	yes	2	Amine	0.5		6.20E+06	1.70E+09	6.20E+02	1.70E+05
07/28/2010 #3	1.0	yes	2	Amine	0.5		1.41E+07	2.22E+09	1.41E+04	2.22E+06
07/29/2010 #1	1.0	yes	3	Amine	0.5		7.00E+05	2.08E+10	7.00E+02	2.08E+07
07/29/2010 #2	1.0	yes	3	Amine	0.5		2.11E+07	2.47E+11	2.11E+03	2.47E+07
07/16/2010	1.0	no	1	Amine	0.1		2.96E+07	9.00E+08	2.96E+03	9.00E+04
07/19/2010 AM	1.0	no	4	Amine	0.1		7.00E+06	8.50E+08	7.00E+02	8.50E+04

07/19/2010 PM	1.0	no	4	Amine	0.1		5.40E+06	1.30E+09	5.40E+02	1.30E+05
07/20/2010 AM	1.0	no	5	Amine	0.1		9.30E+05	4.20E+09	9.30E+02	4.20E+06
07/20/2010 PM	1.0	no	5	Amine	0.1		2.33E+06	1.45E+09	2.33E+03	1.45E+06
07/13/2010	1.0	yes	5	Amine	0.1	<	2.50E+07	4.60E+09	1.00E+01	4.60E+04
07/09/2010	1.0	yes	1	Amine	0.1	<	2.50E+08	9.70E+08	1.00E+01	9.70E+02
07/12/2010	1.0	yes	4	Amine	0.1	<	1.00E+06	1.82E+09	0.00E+00	1.82E+04
07/14/2010	0.5	yes	2	Amine	0.1	<	2.50E+07	1.32E+11	3.00E+01	1.32E+06
07/21/2010	1.0	yes	1	Amine	0.1	<	2.50E+06	1.83E+10	4.00E+01	1.83E+06
07/22/2010 AM	1.0	yes	2	Amine	0.1		1.14E+08	2.70E+09	1.14E+04	2.70E+05
07/22/2010 PM	1.0	yes	2	Amine	0.1		2.05E+07	1.13E+10	2.05E+03	1.13E+06
07/23/2010 AM	1.0	yes	3	Amine	0.1		2.39E+07	1.75E+10	2.39E+04	1.75E+07
07/23/2010 PM	1.0	yes	3	Amine	0.1		1.40E+07	9.90E+08	1.40E+03	9.90E+04
08/03/2010 #1	1.0	yes	5	Amine	0.1		---	---	---	---
08/03/2010 #2	1.0	yes	5	Amine	0.1		---	---	---	---
08/03/2010 #3	1.0	yes	5	Amine	0.1		---	---	---	---
08/03/2010 #4	1.0	yes	5	Amine	0.1		---	---	---	---
08/03/2010 #5	1.0	yes	5	Amine	0.1		---	---	---	---
07/30/2010 #1	1.0	yes	2	Carboxyl	1.5		6.90E+05	1.64E+09	6.90E+02	1.64E+06
07/30/2010 #2	1.0	yes	2	Carboxyl	1.5		1.11E+07	1.64E+09	1.11E+04	1.64E+06
07/30/2010 #3	1.0	yes	2	Carboxyl	1.5		3.08E+06	1.64E+09	3.08E+03	1.64E+06
07/30/2010 #4	1.0	yes	2	Carboxyl	1.5		6.01E+07	2.15E+09	6.01E+03	2.15E+05
07/30/2010 #5	1.0	yes	2	Carboxyl	1.5		9.10E+06	2.15E+09	9.10E+02	2.15E+05
07/16/2010	1.0	no	1	Carboxyl	1.0	<	2.50E+05	9.00E+08	1.30E+02	9.00E+04
07/19/2010 AM	1.0	no	4	Carboxyl	1.0		6.00E+06	8.50E+08	6.00E+02	8.50E+04
07/19/2010 PM	1.0	no	4	Carboxyl	1.0		9.70E+05	1.30E+09	9.70E+02	1.30E+05
07/20/2010 AM	1.0	no	5	Carboxyl	1.0		1.15E+07	4.20E+09	1.15E+04	4.20E+05
07/20/2010 PM	1.0	no	5	Carboxyl	1.0		1.01E+07	1.45E+09	1.01E+04	1.45E+05
07/09/2010	1.0	yes	1	Carboxyl	1.0	<	2.50E+07	9.70E+08	2.00E+01	9.70E+03

07/12/2010	1.0	yes	4	Carboxyl	1.0		6.40E+06	1.82E+09	6.40E+02	1.82E+05
07/14/2010	0.5	yes	2	Carboxyl	1.0	<	2.50E+06	1.32E+11	1.00E+01	1.32E+07
07/21/2010	1.0	yes	1	Carboxyl	1.0	<	2.50E+06	1.83E+10	6.00E+01	1.83E+06
07/22/2010 AM	1.0	yes	2	Carboxyl	1.0		6.70E+07	2.70E+09	6.70E+02	2.70E+04
07/22/2010 PM	1.0	yes	2	Carboxyl	1.0		2.42E+08	1.13E+10	2.42E+03	1.13E+05
07/23/2010 AM	1.0	yes	3	Carboxyl	1.0		8.00E+06	1.75E+10	8.00E+02	1.75E+06
07/23/2010 PM	1.0	yes	3	Carboxyl	1.0		8.60E+05	9.90E+08	8.60E+02	9.90E+05
07/28/2010 #1	1.0	yes	2	Carboxyl	1.0		1.56E+07	4.00E+09	1.56E+04	4.00E+06
07/28/2010 #2	1.0	yes	2	Carboxyl	1.0		1.80E+06	1.70E+09	1.80E+03	1.70E+06
07/28/2010 #3	1.0	yes	2	Carboxyl	1.0		2.40E+06	2.22E+09	2.40E+03	2.22E+06
07/29/2010 #1	1.0	yes	3	Carboxyl	1.0		1.00E+06	2.08E+10	1.00E+03	2.08E+07
07/29/2010 #2	1.0	yes	3	Carboxyl	1.0		3.10E+06	2.47E+11	3.10E+02	2.47E+07
07/16/2010	1.0	no	1	Carboxyl	0.5		1.26E+06	9.00E+08	1.26E+03	9.00E+05
07/19/2010 AM	1.0	no	4	Carboxyl	0.5		8.40E+06	8.50E+08	8.40E+02	8.50E+04
07/19/2010 PM	1.0	no	4	Carboxyl	0.5		1.63E+07	1.30E+09	1.63E+04	1.30E+06
07/20/2010 AM	1.0	no	5	Carboxyl	0.5		9.91E+07	4.20E+09	9.91E+03	4.20E+05
07/20/2010 PM	1.0	no	5	Carboxyl	0.5		8.94E+07	1.45E+09	8.94E+03	1.45E+05
07/12/2010	1.0	yes	4	Carboxyl	0.5		8.30E+06	1.82E+09	8.30E+02	1.82E+05
07/14/2010	0.5	yes	2	Carboxyl	0.5		2.80E+06	1.32E+11	2.80E+02	1.32E+07
07/21/2010	1.0	yes	1	Carboxyl	0.5		5.80E+06	1.83E+10	5.80E+02	1.83E+06
07/22/2010 AM	1.0	yes	2	Carboxyl	0.5		2.22E+07	2.70E+09	2.22E+03	2.70E+05
07/22/2010 PM	1.0	yes	2	Carboxyl	0.5		5.40E+07	1.13E+10	5.40E+02	1.13E+05
07/23/2010 AM	1.0	yes	3	Carboxyl	0.5		8.90E+06	1.75E+10	8.90E+02	1.75E+06
07/23/2010 PM	1.0	yes	3	Carboxyl	0.5	<	2.50E+05	9.90E+08	6.00E+01	9.90E+05
07/28/2010 #1	1.0	yes	2	Carboxyl	0.5		8.50E+06	4.00E+09	8.50E+02	4.00E+05
07/28/2010 #2	1.0	yes	2	Carboxyl	0.5		1.84E+06	1.84E+06	1.84E+03	1.70E+06
07/28/2010 #3	1.0	yes	2	Carboxyl	0.5		7.80E+06	2.22E+09	7.80E+02	2.22E+05
07/29/2010 #1	1.0	yes	3	Carboxyl	0.5		1.00E+06	2.08E+10	1.00E+03	2.08E+07

07/29/2010 #2	1.0	yes	3	Carboxyl	0.5		1.62E+06	2.47E+11	1.62E+03	2.47E+08
07/16/2010	1.0	no	1	Carboxyl	0.1		3.20E+05	9.00E+08	3.20E+02	9.00E+05
07/19/2010 AM	1.0	no	4	Carboxyl	0.1		2.80E+06	8.50E+08	2.80E+02	8.50E+04
07/19/2010 PM	1.0	no	4	Carboxyl	0.1		1.05E+06	1.30E+09	1.05E+03	1.30E+06
07/20/2010 AM	1.0	no	5	Carboxyl	0.1		8.13E+06	4.20E+09	8.13E+03	4.20E+06
07/20/2010 PM	1.0	no	5	Carboxyl	0.1		1.06E+07	1.45E+09	1.06E+04	1.45E+06
07/09/2010	1.0	yes	1	Carboxyl	0.1	<	2.50E+08	9.70E+08	2.00E+01	9.70E+02
07/21/2010	1.0	yes	1	Carboxyl	0.1	<	1.00E+05	1.83E+10	0.00E+00	1.83E+06
07/22/2010 AM	1.0	yes	2	Carboxyl	0.1		9.75E+07	2.70E+09	9.75E+03	2.70E+05
07/22/2010 PM	1.0	yes	2	Carboxyl	0.1		8.45E+07	1.13E+10	8.45E+03	1.13E+06
07/23/2010 AM	1.0	yes	3	Carboxyl	0.1		1.27E+08	1.75E+10	1.27E+04	1.75E+06
07/23/2010 PM	1.0	yes	3	Carboxyl	0.1	<	2.50E+05	9.90E+08	1.20E+02	9.90E+05
08/03/2010 #1	1.0	yes	5	Carboxyl	0.1		---	---	---	---
08/03/2010 #2	1.0	yes	5	Carboxyl	0.1		---	---	---	---
08/03/2010 #3	1.0	yes	5	Carboxyl	0.1		---	---	---	---
08/03/2010 #4	1.0	yes	5	Carboxyl	0.1		---	---	---	---
08/03/2010 #5	1.0	yes	5	Carboxyl	0.1		---	---	---	---
07/30/2010 #1	1.0	yes	2	Pani	1.5		4.06E+06	1.64E+09	4.06E+03	1.64E+06
07/30/2010 #2	1.0	yes	2	Pani	1.5		2.46E+06	1.64E+09	2.46E+03	1.64E+06
07/30/2010 #3	1.0	yes	2	Pani	1.5		2.50E+06	1.64E+09	2.50E+03	1.64E+06
07/30/2010 #4	1.0	yes	2	Pani	1.5		2.09E+07	2.15E+09	2.09E+03	2.15E+05
07/30/2010 #5	1.0	yes	2	Pani	1.5		1.07E+07	2.15E+09	1.07E+03	2.15E+05
07/16/2010	1.0	no	1	Pani	1.0		1.11E+07	9.00E+08	1.11E+04	9.00E+05
07/19/2010 AM	1.0	no	3	Pani	1.0		1.74E+07	8.50E+08	1.74E+04	8.50E+05
07/19/2010 PM	1.0	no	3	Pani	1.0		9.26E+06	1.30E+09	9.26E+03	1.30E+06
07/20/2010 AM	1.0	no	4	Pani	1.0		1.30E+07	4.20E+09	1.30E+04	4.20E+06
07/20/2010 PM	1.0	no	4	Pani	1.0		1.35E+07	1.45E+09	1.35E+04	1.45E+06
07/09/2010	1.0	yes	1	Pani	1.0	<	2.50E+08	9.70E+08	1.00E+01	9.70E+02

07/12/2010	1.0	yes	4	Pani	1.0		4.00E+07	1.82E+09	4.00E+02	1.82E+04
07/14/2010	0.5	yes	2	Pani	1.0		2.80E+07	1.32E+11	2.80E+02	1.32E+06
07/21/2010	1.0	yes	1	Pani	1.0	<	2.50E+06	1.83E+10	2.10E+02	1.83E+06
07/22/2010 AM	1.0	yes	2	Pani	1.0		9.30E+07	2.70E+09	9.30E+02	2.70E+04
07/22/2010 PM	1.0	yes	2	Pani	1.0		9.75E+08	1.13E+10	9.75E+03	1.13E+05
07/23/2010 AM	1.0	yes	3	Pani	1.0		5.40E+06	1.75E+10	5.40E+02	1.75E+06
07/23/2010 PM	1.0	yes	3	Pani	1.0		9.40E+05	9.90E+08	9.40E+02	9.90E+05
07/28/2010 #1	1.0	yes	2	Pani	1.0	<	2.50E+05	4.00E+09	2.10E+02	4.00E+06
07/28/2010 #2	1.0	yes	2	Pani	1.0		8.20E+06	1.70E+09	8.20E+02	1.70E+05
07/28/2010 #3	1.0	yes	2	Pani	1.0		1.17E+07	2.22E+09	1.17E+03	2.22E+05
07/29/2010 #1	1.0	yes	3	Pani	1.0		1.30E+08	2.08E+10	1.30E+04	2.08E+06
07/29/2010 #2	1.0	yes	3	Pani	1.0		9.70E+05	2.47E+11	9.70E+02	2.47E+08
07/16/2010	1.0	no	1	Pani	0.5		9.91E+06	9.00E+08	9.91E+03	9.00E+05
07/19/2010 AM	1.0	no	4	Pani	0.5		1.85E+06	8.50E+08	1.85E+03	8.50E+05
07/19/2010 PM	1.0	no	4	Pani	0.5		7.40E+06	1.30E+09	7.40E+02	1.30E+05
07/20/2010 AM	1.0	no	5	Pani	0.5		6.40E+05	4.20E+09	6.40E+02	4.20E+06
07/20/2010 PM	1.0	no	5	Pani	0.5		1.59E+07	1.45E+09	1.59E+03	1.45E+05
07/12/2010	1.0	yes	4	Pani	0.5		1.78E+08	1.82E+09	1.78E+03	1.82E+04
07/14/2010	0.5	yes	2	Pani	0.5		3.70E+07	1.32E+11	3.70E+02	1.32E+06
07/21/2010	1.0	yes	1	Pani	0.5	<	2.50E+06	1.83E+10	2.20E+02	1.83E+06
07/22/2010 AM	1.0	yes	2	Pani	0.5		6.01E+07	2.70E+09	6.01E+03	2.70E+05
07/22/2010 PM	1.0	yes	2	Pani	0.5		6.34E+07	1.13E+10	6.34E+03	1.13E+06
07/23/2010 AM	1.0	yes	3	Pani	0.5		2.94E+07	1.75E+10	2.94E+03	1.75E+06
07/23/2010 PM	1.0	yes	3	Pani	0.5	<	2.50E+05	9.90E+08	2.00E+02	9.90E+05
07/28/2010 #1	1.0	yes	2	Pani	0.5		2.55E+06	4.00E+09	2.55E+03	4.00E+06
07/28/2010 #2	1.0	yes	2	Pani	0.5		3.09E+06	1.70E+09	3.09E+03	1.70E+06
07/28/2010 #3	1.0	yes	2	Pani	0.5		2.52E+07	2.22E+09	2.52E+03	2.22E+05
07/29/2010 #1	1.0	yes	3	Pani	0.5		2.76E+07	2.08E+10	2.76E+03	2.08E+06

07/29/2010 #2	1.0	yes	3	Pani	0.5		5.20E+06	2.47E+11	5.20E+02	2.47E+07
07/16/2010	1.0	no	1	Pani	0.1		1.51E+07	9.00E+08	1.51E+04	9.00E+05
07/19/2010 AM	1.0	no	4	Pani	0.1		1.41E+07	8.50E+08	1.41E+04	8.50E+05
07/19/2010 PM	1.0	no	4	Pani	0.1		1.79E+07	1.30E+09	1.79E+04	1.30E+06
07/20/2010 AM	1.0	no	5	Pani	0.1		7.96E+06	4.20E+09	7.96E+03	4.20E+06
07/20/2010 PM	1.0	no	5	Pani	0.1		3.82E+08	1.45E+09	3.82E+04	1.45E+05
07/09/2010	1.0	yes	1	Pani	0.1	<	1.00E+07	9.70E+08	0.00E+00	9.70E+02
07/21/2010	1.0	yes	1	Pani	0.1	<	2.50E+06	1.83E+10	1.30E+02	1.83E+06
07/22/2010 AM	1.0	yes	2	Pani	0.1		7.15E+07	2.70E+09	7.15E+03	2.70E+05
07/22/2010 PM	1.0	yes	2	Pani	0.1		4.23E+07	1.13E+10	4.23E+03	1.13E+06
07/23/2010 AM	1.0	yes	3	Pani	0.1		8.50E+06	1.75E+10	8.50E+02	1.75E+06
07/23/2010 PM	1.0	yes	3	Pani	0.1	<	1.00E+04	9.90E+08	0.00E+00	9.90E+05
08/03/2010 #1	1.0	yes	5	Pani	0.1		---	---	---	---
08/03/2010 #2	1.0	yes	5	Pani	0.1		---	---	---	---
08/03/2010 #3	1.0	yes	5	Pani	0.1		---	---	---	---
08/03/2010 #4	1.0	yes	5	Pani	0.1		---	---	---	---
08/03/2010 #5	1.0	yes	5	Pani	0.1		---	---	---	---

Shigella boydii Trial (Date/#)	Ab conc (mg/ml)	Add NaCl?	Conj age (days)	Bead type	Bead conc (mg/ml)		Shig Proj CFU/ml Captured	Shigella Original CFU/ml	Shig Actual CFU/ml Captured	Shig Actual CFU/ml Present
07/30/2010 #1	1.0	yes	2	Amine	1.5		3.50E+04	1.62E+08	3.50E+02	1.62E+06
07/30/2010 #2	1.0	yes	2	Amine	1.5		4.60E+04	1.62E+08	4.60E+02	1.62E+06
07/30/2010 #3	1.0	yes	2	Amine	1.5		6.90E+04	1.62E+08	6.90E+02	1.62E+06
07/30/2010 #4	1.0	yes	2	Amine	1.5	<	2.50E+04	1.90E+08	2.00E+01	1.90E+06
07/30/2010 #5	1.0	yes	2	Amine	1.5		4.20E+04	1.90E+08	4.20E+02	1.90E+06

07/16/2010	1.0	no	1	Amine	1.0		1.22E+06	6.70E+07	1.22E+04	6.70E+05
07/19/2010 AM	1.0	no	3	Amine	1.0		4.06E+07	2.55E+09	4.06E+04	2.55E+06
07/19/2010 PM	1.0	no	3	Amine	1.0		6.20E+05	1.48E+08	6.20E+02	1.48E+05
07/20/2010 AM	1.0	no	4	Amine	1.0		2.03E+05	2.87E+08	2.03E+03	2.87E+06
07/20/2010 PM	1.0	no	4	Amine	1.0		7.20E+04	2.18E+08	7.20E+02	2.18E+06
07/09/2010	1.0	yes	1	Amine	1.0	<	1.00E+07	2.50E+08	0.00E+00	2.50E+02
07/14/2010	0.5	yes	2	Amine	1.0	<	1.00E+05	3.69E+10	0.00E+00	3.69E+06
07/21/2010	1.0	yes	1	Amine	1.0		3.20E+04	1.81E+08	3.20E+02	1.81E+06
07/22/2010 AM	1.0	yes	2	Amine	1.0		2.50E+04	1.38E+08	2.50E+02	1.38E+06
07/22/2010 PM	1.0	yes	2	Amine	1.0		4.30E+04	2.25E+08	4.30E+02	2.25E+06
07/23/2010 AM	1.0	yes	3	Amine	1.0	<	2.50E+04	2.50E+08	6.00E+01	2.50E+06
07/23/2010 PM	1.0	yes	3	Amine	1.0		3.90E+04	1.26E+08	3.90E+02	1.26E+06
07/28/2010 #1	1.0	yes	2	Amine	1.0		3.20E+04	1.44E+08	3.20E+02	1.44E+06
07/28/2010 #2	1.0	yes	2	Amine	1.0		1.02E+05	1.51E+09	1.02E+03	1.51E+07
07/28/2010 #3	1.0	yes	2	Amine	1.0	<	1.00E+03	1.30E+08	0.00E+00	1.30E+06
07/29/2010 #1	1.0	yes	3	Amine	1.0	<	2.50E+04	2.76E+09	1.00E+02	2.76E+07
07/29/2010 #2	1.0	yes	3	Amine	1.0	<	2.50E+05	2.50E+09	2.20E+02	2.50E+06
07/16/2010	1.0	no	1	Amine	0.5		3.62E+06	6.70E+07	3.62E+04	6.70E+05
07/19/2010 AM	1.0	no	4	Amine	0.5		1.95E+07	2.55E+09	1.95E+04	2.55E+06
07/19/2010 PM	1.0	no	4	Amine	0.5	<	2.50E+04	1.48E+08	9.00E+01	1.48E+06
07/20/2010 AM	1.0	no	5	Amine	0.5		5.10E+05	2.87E+08	5.10E+02	2.87E+05
07/20/2010 PM	1.0	no	5	Amine	0.5	<	2.50E+04	2.18E+08	1.60E+02	2.18E+06
07/12/2010	1.0	yes	4	Amine	0.5	<	1.00E+06	1.60E+07	0.00E+00	1.60E+02
07/21/2010	1.0	yes	1	Amine	0.5		6.30E+04	1.81E+08	6.30E+02	1.81E+06
07/22/2010 AM	1.0	yes	2	Amine	0.5		3.20E+04	1.38E+08	3.20E+02	1.38E+06
07/22/2010 PM	1.0	yes	2	Amine	0.5		8.30E+04	2.25E+08	8.30E+02	2.25E+06
07/23/2010 AM	1.0	yes	3	Amine	0.5		3.50E+04	2.50E+08	3.50E+02	2.50E+06
07/23/2010 PM	1.0	yes	3	Amine	0.5		3.70E+04	1.26E+08	3.70E+02	1.26E+06

07/28/2010 #1	1.0	yes	2	Amine	0.5		1.74E+05	1.44E+08	1.74E+03	1.44E+06
07/28/2010 #2	1.0	yes	2	Amine	0.5	<	2.50E+05	1.51E+09	1.70E+02	1.51E+06
07/28/2010 #3	1.0	yes	2	Amine	0.5	<	1.00E+03	1.30E+08	0.00E+00	1.30E+06
07/29/2010 #1	1.0	yes	3	Amine	0.5		8.00E+04	2.76E+09	8.00E+02	2.76E+07
07/29/2010 #2	1.0	yes	3	Amine	0.5	<	2.50E+05	2.50E+09	2.10E+02	2.50E+06
07/16/2010	1.0	no	1	Amine	0.1		8.40E+05	6.70E+07	8.40E+02	6.70E+04
07/19/2010 AM	1.0	no	4	Amine	0.1		2.18E+05	2.55E+09	2.18E+03	2.55E+07
07/19/2010 PM	1.0	no	4	Amine	0.1	<	1.00E+03	1.48E+08	0.00E+00	1.48E+06
07/20/2010 AM	1.0	no	5	Amine	0.1		2.55E+06	2.87E+08	2.55E+04	2.87E+06
07/20/2010 PM	1.0	no	5	Amine	0.1	<	2.50E+04	2.18E+08	1.70E+02	2.18E+06
07/13/2010	1.0	yes	5	Amine	0.1	<	1.00E+06	4.66E+07	0.00E+00	4.66E+02
07/09/2010	1.0	yes	1	Amine	0.1	<	1.00E+07	2.50E+08	0.00E+00	2.50E+02
07/12/2010	1.0	yes	4	Amine	0.1	<	1.00E+06	1.60E+07	0.00E+00	1.60E+02
07/14/2010	0.5	yes	2	Amine	0.1	<	2.50E+06	3.69E+10	1.10E+02	3.69E+06
07/21/2010	1.0	yes	1	Amine	0.1		3.00E+04	1.81E+08	3.00E+02	1.81E+06
07/22/2010 AM	1.0	yes	2	Amine	0.1	<	1.00E+03	1.38E+08	0.00E+00	1.38E+06
07/22/2010 PM	1.0	yes	2	Amine	0.1		2.27E+05	2.25E+08	2.27E+03	2.25E+06
07/23/2010 AM	1.0	yes	3	Amine	0.1		9.20E+04	2.50E+08	9.20E+02	2.50E+06
07/23/2010 PM	1.0	yes	3	Amine	0.1	<	2.50E+04	1.26E+08	9.00E+01	1.26E+06
08/03/2010 #1	1.0	yes	5	Amine	0.1		---	---	---	---
08/03/2010 #2	1.0	yes	5	Amine	0.1		---	---	---	---
08/03/2010 #3	1.0	yes	5	Amine	0.1		---	---	---	---
08/03/2010 #4	1.0	yes	5	Amine	0.1		---	---	---	---
08/03/2010 #5	1.0	yes	5	Amine	0.1		---	---	---	---
07/30/2010 #1	1.0	yes	2	Carboxyl	1.5		1.19E+05	1.62E+08	1.19E+03	1.62E+06
07/30/2010 #2	1.0	yes	2	Carboxyl	1.5		1.20E+06	1.62E+08	1.20E+04	1.62E+06
07/30/2010 #3	1.0	yes	2	Carboxyl	1.5		3.14E+05	1.62E+08	3.14E+03	1.62E+06
07/30/2010 #4	1.0	yes	2	Carboxyl	1.5		1.41E+06	1.90E+08	1.41E+04	1.90E+06

07/30/2010 #5	1.0	yes	2	Carboxyl	1.5		5.00E+04	1.90E+08	5.00E+02	1.90E+06
07/16/2010	1.0	no	1	Carboxyl	1.0		1.72E+06	6.70E+07	1.72E+03	6.70E+04
07/19/2010 AM	1.0	no	4	Carboxyl	1.0		3.93E+07	2.55E+09	3.93E+04	2.55E+06
07/19/2010 PM	1.0	no	4	Carboxyl	1.0	<	1.00E+03	1.48E+08	0.00E+00	1.48E+05
07/20/2010 AM	1.0	no	5	Carboxyl	1.0		3.10E+05	2.87E+08	3.10E+02	2.87E+05
07/20/2010 PM	1.0	no	5	Carboxyl	1.0		1.06E+05	2.18E+08	1.06E+03	2.18E+05
07/09/2010	1.0	yes	1	Carboxyl	1.0	<	1.00E+06	2.50E+08	0.00E+00	2.50E+03
07/12/2010	1.0	yes	4	Carboxyl	1.0	<	1.00E+05	1.60E+07	0.00E+00	1.60E+03
07/14/2010	0.5	yes	2	Carboxyl	1.0	<	1.00E+04	3.69E+10	0.00E+00	3.69E+07
07/21/2010	1.0	yes	1	Carboxyl	1.0	<	1.00E+03	1.81E+08	0.00E+00	1.81E+06
07/22/2010 AM	1.0	yes	2	Carboxyl	1.0	<	1.00E+03	1.38E+08	0.00E+00	1.38E+06
07/22/2010 PM	1.0	yes	2	Carboxyl	1.0		8.13E+05	2.25E+08	8.13E+03	2.25E+06
07/23/2010 AM	1.0	yes	3	Carboxyl	1.0		6.80E+04	2.50E+08	6.80E+02	2.50E+06
07/23/2010 PM	1.0	yes	3	Carboxyl	1.0		1.32E+05	1.26E+08	1.32E+03	1.26E+06
07/28/2010 #1	1.0	yes	2	Carboxyl	1.0	<	1.00E+03	1.44E+08	0.00E+00	1.44E+06
07/28/2010 #2	1.0	yes	2	Carboxyl	1.0		3.50E+04	1.51E+09	3.50E+02	1.51E+07
07/28/2010 #3	1.0	yes	2	Carboxyl	1.0	<	1.00E+03	1.30E+08	0.00E+00	1.30E+06
07/29/2010 #1	1.0	yes	3	Carboxyl	1.0	<	1.00E+03	2.76E+09	0.00E+00	2.76E+07
07/29/2010 #2	1.0	yes	3	Carboxyl	1.0	<	2.50E+05	2.50E+09	4.00E+01	2.50E+06
07/16/2010	1.0	no	1	Carboxyl	0.5		1.51E+07	6.70E+07	1.51E+04	6.70E+04
07/19/2010 AM	1.0	no	4	Carboxyl	0.5		3.27E+07	2.55E+09	3.27E+04	2.55E+06
07/19/2010 PM	1.0	no	4	Carboxyl	0.5	<	1.00E+03	1.48E+08	0.00E+00	1.48E+05
07/20/2010 AM	1.0	no	5	Carboxyl	0.5		3.04E+07	2.87E+08	3.04E+04	2.87E+05
07/20/2010 PM	1.0	no	5	Carboxyl	0.5		4.40E+04	2.18E+08	4.40E+02	2.18E+06
07/12/2010	1.0	yes	4	Carboxyl	0.5	<	1.00E+05	1.60E+07	0.00E+00	1.60E+03
07/14/2010	0.5	yes	2	Carboxyl	0.5	<	1.00E+04	3.69E+10	0.00E+00	3.69E+07
07/21/2010	1.0	yes	1	Carboxyl	0.5	<	1.00E+03	1.81E+08	0.00E+00	1.81E+06
07/22/2010 AM	1.0	yes	2	Carboxyl	0.5	<	1.00E+03	1.38E+08	0.00E+00	1.38E+06

07/22/2010 PM	1.0	yes	2	Carboxyl	0.5		4.40E+04	2.25E+08	4.40E+02	2.25E+06
07/23/2010 AM	1.0	yes	3	Carboxyl	0.5		4.00E+04	2.50E+08	4.00E+02	2.50E+06
07/23/2010 PM	1.0	yes	3	Carboxyl	0.5		7.80E+04	1.26E+08	7.80E+02	1.26E+06
07/28/2010 #1	1.0	yes	2	Carboxyl	0.5	<	1.00E+03	1.44E+08	0.00E+00	1.44E+06
07/28/2010 #2	1.0	yes	2	Carboxyl	0.5	<	2.50E+04	1.51E+09	2.00E+02	1.51E+07
07/28/2010 #3	1.0	yes	2	Carboxyl	0.5	<	1.00E+03	1.30E+08	0.00E+00	1.30E+06
07/29/2010 #1	1.0	yes	3	Carboxyl	0.5	<	1.00E+03	2.76E+09	0.00E+00	2.76E+07
07/29/2010 #2	1.0	yes	3	Carboxyl	0.5	<	1.00E+04	2.50E+09	0.00E+00	2.50E+06
07/16/2010	1.0	no	1	Carboxyl	0.1		6.10E+04	6.70E+07	6.10E+02	6.70E+05
07/19/2010 AM	1.0	no	4	Carboxyl	0.1		1.54E+07	2.55E+09	1.54E+04	2.55E+06
07/19/2010 PM	1.0	no	4	Carboxyl	0.1	<	1.00E+03	1.48E+08	0.00E+00	1.48E+06
07/20/2010 AM	1.0	no	5	Carboxyl	0.1		2.52E+07	2.87E+08	2.52E+04	2.87E+05
07/20/2010 PM	1.0	no	5	Carboxyl	0.1	<	2.50E+04	2.18E+08	1.30E+02	2.18E+06
07/09/2010	1.0	yes	1	Carboxyl	0.1	<	1.00E+06	2.50E+08	0.00E+00	2.50E+03
07/21/2010	1.0	yes	1	Carboxyl	0.1	<	1.00E+03	1.81E+08	0.00E+00	1.81E+06
07/22/2010 AM	1.0	yes	2	Carboxyl	0.1	<	1.00E+03	1.38E+08	0.00E+00	1.38E+06
07/22/2010 PM	1.0	yes	2	Carboxyl	0.1		5.20E+05	2.25E+08	5.20E+03	2.25E+06
07/23/2010 AM	1.0	yes	3	Carboxyl	0.1		5.60E+04	2.50E+08	5.60E+02	2.50E+06
07/23/2010 PM	1.0	yes	3	Carboxyl	0.1	<	2.50E+04	1.26E+08	5.00E+01	1.26E+06
08/03/2010 #1	1.0	yes	5	Carboxyl	0.1		---	---	---	---
08/03/2010 #2	1.0	yes	5	Carboxyl	0.1		---	---	---	---
08/03/2010 #3	1.0	yes	5	Carboxyl	0.1		---	---	---	---
08/03/2010 #4	1.0	yes	5	Carboxyl	0.1		---	---	---	---
08/03/2010 #5	1.0	yes	5	Carboxyl	0.1		---	---	---	---
07/30/2010 #1	1.0	yes	2	Pani	1.5	<	2.50E+04	1.62E+08	7.00E+01	1.62E+06
07/30/2010 #2	1.0	yes	2	Pani	1.5	<	2.50E+04	1.62E+08	1.80E+02	1.62E+06
07/30/2010 #3	1.0	yes	2	Pani	1.5	<	2.50E+04	1.62E+08	9.00E+01	1.62E+06
07/30/2010 #4	1.0	yes	2	Pani	1.5	<	2.50E+04	1.90E+08	5.00E+01	1.90E+06

07/30/2010 #5	1.0	yes	2	Pani	1.5	<	2.50E+04	1.90E+08	1.00E+01	1.90E+06
07/16/2010	1.0	no	1	Pani	1.0	<	1.00E+03	6.70E+07	0.00E+00	6.70E+05
07/19/2010 AM	1.0	no	3	Pani	1.0		3.87E+06	2.55E+09	3.87E+04	2.55E+07
07/19/2010 PM	1.0	no	3	Pani	1.0		6.00E+04	1.48E+08	6.00E+02	1.48E+06
07/20/2010 AM	1.0	no	4	Pani	1.0		2.88E+06	2.87E+08	2.88E+04	2.87E+06
07/20/2010 PM	1.0	no	4	Pani	1.0	<	2.50E+04	2.18E+08	4.00E+01	2.18E+06
07/09/2010	1.0	yes	1	Pani	1.0	<	1.00E+07	2.50E+08	0.00E+00	2.50E+02
07/12/2010	1.0	yes	4	Pani	1.0	<	1.00E+06	1.60E+07	0.00E+00	1.60E+02
07/14/2010	0.5	yes	2	Pani	1.0	<	1.00E+05	3.69E+10	0.00E+00	3.69E+06
07/21/2010	1.0	yes	1	Pani	1.0	<	1.00E+03	1.81E+08	0.00E+00	1.81E+06
07/22/2010 AM	1.0	yes	2	Pani	1.0	<	1.00E+03	1.38E+08	0.00E+00	1.38E+06
07/22/2010 PM	1.0	yes	2	Pani	1.0		2.07E+05	2.25E+08	2.07E+03	2.25E+06
07/23/2010 AM	1.0	yes	3	Pani	1.0		5.90E+05	2.50E+08	5.90E+02	2.50E+05
07/23/2010 PM	1.0	yes	3	Pani	1.0		1.25E+05	1.26E+08	1.25E+03	1.26E+06
07/28/2010 #1	1.0	yes	2	Pani	1.0	<	1.00E+03	1.44E+08	0.00E+00	1.44E+06
07/28/2010 #2	1.0	yes	2	Pani	1.0		1.37E+06	1.51E+09	1.37E+03	1.51E+06
07/28/2010 #3	1.0	yes	2	Pani	1.0	<	1.00E+03	1.30E+08	0.00E+00	1.30E+06
07/29/2010 #1	1.0	yes	3	Pani	1.0		4.20E+05	2.76E+09	4.20E+02	2.76E+06
07/29/2010 #2	1.0	yes	3	Pani	1.0		2.53E+06	2.53E+06	2.53E+03	2.50E+06
07/16/2010	1.0	no	1	Pani	0.5	<	1.00E+03	6.70E+07	0.00E+00	6.70E+05
07/19/2010 AM	1.0	no	4	Pani	0.5		5.20E+06	2.55E+09	5.20E+04	2.55E+07
07/19/2010 PM	1.0	no	4	Pani	0.5		1.16E+05	1.48E+08	1.16E+03	1.48E+06
07/20/2010 AM	1.0	no	5	Pani	0.5		2.78E+07	2.87E+08	2.78E+04	2.87E+05
07/20/2010 PM	1.0	no	5	Pani	0.5		5.60E+04	2.18E+08	5.60E+02	2.18E+06
07/12/2010	1.0	yes	4	Pani	0.5	<	1.00E+06	1.60E+07	0.00E+00	1.60E+02
07/14/2010	0.5	yes	2	Pani	0.5	<	1.00E+05	3.69E+10	0.00E+00	3.69E+06
07/21/2010	1.0	yes	1	Pani	0.5		5.20E+04	1.81E+08	5.20E+02	1.81E+06
07/22/2010 AM	1.0	yes	2	Pani	0.5	<	1.00E+03	1.38E+08	0.00E+00	1.38E+06

07/22/2010 PM	1.0	yes	2	Pani	0.5		1.00E+05	2.25E+08	1.00E+03	2.25E+06
07/23/2010 AM	1.0	yes	3	Pani	0.5	<	1.00E+03	2.50E+08	0.00E+00	2.50E+06
07/23/2010 PM	1.0	yes	3	Pani	0.5	<	2.50E+04	1.26E+08	1.80E+02	1.26E+06
07/28/2010 #1	1.0	yes	2	Pani	0.5	<	1.00E+03	1.44E+08	0.00E+00	1.44E+06
07/28/2010 #2	1.0	yes	2	Pani	0.5	<	2.50E+04	1.51E+09	1.00E+01	1.51E+07
07/28/2010 #3	1.0	yes	2	Pani	0.5	<	1.00E+03	1.30E+08	0.00E+00	1.30E+06
07/29/2010 #1	1.0	yes	3	Pani	0.5		2.80E+05	2.76E+09	2.80E+02	2.76E+06
07/29/2010 #2	1.0	yes	3	Pani	0.5		3.80E+05	2.50E+09	3.80E+02	2.50E+06
07/16/2010	1.0	no	1	Pani	0.1	<	1.00E+03	6.70E+07	0.00E+00	6.70E+04
07/19/2010 AM	1.0	no	4	Pani	0.1		2.15E+06	2.55E+09	2.15E+04	2.55E+07
07/19/2010 PM	1.0	no	4	Pani	0.1	<	2.50E+04	1.48E+08	1.50E+02	1.48E+06
07/20/2010 AM	1.0	no	5	Pani	0.1		6.83E+06	2.87E+08	6.83E+03	2.87E+05
07/20/2010 PM	1.0	no	5	Pani	0.1		6.00E+04	2.18E+08	6.00E+02	2.18E+06
07/09/2010	1.0	yes	1	Pani	0.1	<	1.00E+07	2.50E+08	0.00E+00	2.50E+02
07/21/2010	1.0	yes	1	Pani	0.1		2.60E+04	1.81E+08	2.60E+02	1.81E+06
07/22/2010 AM	1.0	yes	2	Pani	0.1	<	2.50E+04	1.38E+08	3.00E+01	1.38E+06
07/22/2010 PM	1.0	yes	2	Pani	0.1		5.20E+04	2.25E+08	5.20E+02	2.25E+06
07/23/2010 AM	1.0	yes	3	Pani	0.1	<	2.50E+04	2.50E+08	1.10E+02	2.50E+06
07/23/2010 PM	1.0	yes	3	Pani	0.1	<	2.50E+04	1.26E+08	8.00E+01	1.26E+06
08/03/2010 #1	1.0	yes	5	Pani	0.1		---	---	---	---
08/03/2010 #2	1.0	yes	5	Pani	0.1		---	---	---	---
08/03/2010 #3	1.0	yes	5	Pani	0.1		---	---	---	---
08/03/2010 #4	1.0	yes	5	Pani	0.1		---	---	---	---
08/03/2010 #5	1.0	yes	5	Pani	0.1		---	---	---	---

APPENDIX E

Data Presented in Chapter 6

Table 15. Data referenced in Chapter 6, Table 4.

***E. coli* Capture:**

Volume plated (µl)	Plate	Dilution	Count	CFU/ml		Original		
50	10^-5 pure	1.0E-05	468	9.4E+03		don't use		
50	10^-6 pure	1.0E-06	43	8.6E+08		8.6E+08		
					AVERAGE:	**8.6E+08**		
						(Concentrated 3X before applying to SPCE)		
				Captured CFU/ml	Actual CFU/ml	Projected Original	Capture Efficiency	CFU/SPCE
50 each	Blank 1/2/3	---	0/0/0	---	---	---	---	---
50	10^-5 (1)	1.0E-05	102	2.04E+03	8.6E+03	2.0E+08	23.72%	6.12E+02
50	10^-5 (2)	1.0E-05	111	2.22E+03	8.6E+03	2.2E+08	25.81%	6.66E+02
50	10^-5 (3)	1.0E-05	178	3.56E+03	8.6E+03	3.6E+08	41.40%	1.07E+03
		AVERAGE:	**130**	**2.6E+03**	**8.6E+03**	**2.6E+08**	**30.31%**	**7.8E+02**
		STD DEV:	**42**	**8.3E+02**	**0.0E+00**	**8.3E+07**	**9.66%**	**2.5E+02**

Table 16. Data referenced in Chapter 6, Figure 22.

		(0 CFU)					(780 CFU)					
		Blank 1	**Blank 2**	**Blank 3**	**AVE**	**STDEV**	**10^-5 (1)**	**10^-5 (2)**	**10^-5 (3)**	**AVE**	**STDEV**	**S/N:**
Maximum Current:	**Potential (V):**	0.22	0.22	0.22			0.22	0.22	0.22			
	Current (µA):	-1.27	-1.47	-0.58	-1.11	0.47	-0.64	-0.59	-0.62	-0.62	0.02	**0.56**
Minimum Current:	**Potential (V):**	0.42	0.42	0.42			0.42	0.42	0.42			
	Current (µA):	4.44	4.12	0.67	3.08	2.09	0.62	0.75	0.70	0.69	0.07	**0.22**
Charge Transfer:	**ΔQ**	0.35	0.38	0.42	0.38	0.04	0.87	1.33	1.17	1.12	0.23	**2.94**

REFERENCES

REFERENCES

AOAC (2006). Final Report and Executive Summaries from the AOAC International Presidential Task Force on Best Practices in Microbiological Methodology, AOAC International**:** Appendix 9, pages 1-2 of 3; Appendix E, page 5 of 10.

Aybay, C. (2003). "Differential binding characteristics of protein G and protein A for Fc fragments of papain-digested mouse IgG." Immunology Letters **85(**3): 231-235.

Bangs Laboratories, I. (2008). TechNote 201: Working with Microspheres**:** pg 9 of 20.

Bangs Laboratories, I. (2008). TechNote 204: Adsorption to Microspheres**:** pgs 1-3 of 6.

Barick, K. C., M. Aslam, et al. (2009). "Nanoscale assembly of amine-functionalized colloidal iron oxide." Journal of Magnetism and Magnetic Materials **321**(10): 1529-1532.

Barreiros dos Santos, M., C. Sporer, et al. (2009). "Detection of pathogenic Bacteria by Electrochemical Impedance Spectroscopy: Influence of the immobilization strategies on the sensor performance." Procedia Chemistry **1**(1): 1291-1294.

Barton, A. C., S. D. Collyer, et al. (2009). "Labeless AC impedimetric antibody-based sensors with pg ml-1 sensitivities for point-of-care biomedical applications." Biosensors and Bioelectronics **24(**5): 1090-1095.

Barton, A. C., F. Davis, et al. (2008). "Labeless Immunosensor Assay for Prostate Specific Antigen with Picogram per Milliliter Limits of Detection Based upon an ac Impedance Protocol." Analytical Chemistry **80**(16): 6198-6205.

CDC (2001). Bacillus anthracis, Centers for Disease Control and Prevention.

CDC. (2008). "*Escherichia coli*." Retrieved July 7 2009, from www.cdc.gov/nczved/dfbmd/disease_listing/stec_gi.html.

CDC. (2010). "Bioterrorism Agents/Diseases." Retrieved 7 October 2010, from http://www.bt.cdc.gov/agent/agentlist-category.asp.

CDC. (2010). "*E. coli* Outbreak Investigations." Retrieved 12 October 2010, from http://www.cdc.gov/ecoli/outbreaks.html.

Cheng, Y., Y. Liu, et al. (2009). "Combining biofunctional magnetic nanoparticles and ATP bioluminescence for rapid detection of Escherichia coli." Talanta **77**(4): 1332-1336.

Daniels, J. S. and N. Pourmand (2007). "Label-Free Impedance Biosensors: Opportunities and Challenges." Electroanalysis **19**(12): 1239-1257.

Edwards, K., H. Clancy, et al. (2006). "Bacillus anthracis: toxicology, epidemiology and current rapid-detection methods." Analytical and Bioanalytical Chemistry **384**(1): 73-84.

ELISHA. (2010). "Sensitive Detection of Bacteria." Retrieved 6 November, 2010, from http://www.immunosensors.com/?i=140&s=1111.

Escamilla-Gómez, V., S. Campuzano, et al. (2009). "Gold screen-printed-based impedimetric immunobiosensors for direct and sensitive Escherichia coli quantisation." Biosensors and Bioelectronics **24**(11): 3365-3371.

FDA (2009). Bacteriological Analytical Manual (BAM), U.S. Food & Drug Administration**:** Chapter 4a: Diarrheagenic Escherichia coli; Appendix 1: Rapid Methods for Detecting Foodborne Pathogens.

FDA (2009). Bad Bug Book: Foodborne Pathogenic Microorganisms and Natural Toxins Handbook, U.S. Food and Drug Administration**:** Bacillus cereus and other Bacillus spp.

Gamella, M., S. Campuzano, et al. (2009). "Microorganisms recognition and quantification by lectin adsorptive affinity impedance." Talanta **78**(4-5): 1303-1309.

Garifallou, G. Z., G. Tsekenis, et al. (2007). Labeless Immunosensor Assay for Fluoroquinolone Antibiotics Based Upon an AC Impedance Protocol, Taylor & Francis. **40:** 1412 - 1422.

Gehring, A. G., J. D. Brewster, et al. (1999). "1-Naphthyl phosphate as an enzymatic substrate for enzyme-linked immunomagnetic electrochemistry." Journal of Electroanalytical Chemistry **469**(1): 27-33.

Gehring, A. G. and S. I. Tu (2005). "Enzyme-Linked Immunomagnetic Electrochemical Detection of Live Escherichia coli O157:H7 in Apple Juice." Journal of Food Protection **68**: 146-149.

Geng, P., X. Zhang, et al. (2008). "Self-assembled monolayers-based immunosensor for detection of Escherichia coli using electrochemical impedance spectroscopy." Electrochimica Acta **53**(14): 4663-4668.

Grant, S., F. Davis, et al. (2005). "Label-free and reversible immunosensor based upon an ac impedance interrogation protocol." Analytica Chimica Acta **537**(1-2): 163-168.

Hill, H. D. and C. A. Mirkin (2006). "The bio-barcode assay for the detection of protein and nucleic acid targets using DTT-induced ligand exchange." Nat. Protocols **1**(1): 324-336.

Hnaiein, M., W. M. Hassen, et al. (2008). "A conductometric immunosensor based on functionalized magnetite nanoparticles for E. coli detection." Electrochemistry Communications **10**(8): 1152-1154.

ICTVdB - The Universal Virus Database, version 4. Retrieved 11 December 2010, from http://www.ncbi.nlm.nih.gov/ICTVdb/ICTVdB/.

Jaffrezic-Renault, N., C. Martelet, et al. (2007). "Biosensors and Bio-Bar Code Assays Based on Biofunctionalized Magnetic Microbeads." Sensors **7**(4): 589-614.

Kim, B.-J., S.-G. Oh, et al. (2000). "Preparation of Polyaniline Nanoparticles in Micellar Solutions as Polymerization Medium." Langmuir **16**(14): 5841-5845.

Kim, G., M. Morgan, et al. (2008). "Interdigitated microelectrode based impedance biosensor for detection of *Salmonella enteriditis* in food samples." Journal of Physics: Conference Series **100**(052044).

Laczka, O., E. Baldrich, et al. (2008). "Detection of Escherichia coli and Salmonella typhimurium Using Interdigitated Microelectrode Capacitive Immunosensors: The Importance of Transducer Geometry." Analytical Chemistry **80**(19): 7239-7247.

Li, D., J. Wang, et al. (2007). Rapid Detection of *Escherichia coli* O157:H7 Using Electrochemical Impedance Immunosensor. 2007 ASABE Annual International Meeting. Minneapolis, MN, American Society of Agricultural and Biological Engineers.

Li, D., J. Wang, et al. (2008). Development of a Capacitative Immunosensor for Detection of *Eschericha coli* O157:H7. 2008 ASABE Annual International Meeting. Providence, Rhode Island, American Society of Agricultural and Biological Engineers.

Lin, Y. H., S. H. Chen, et al. (2008). "Disposable amperometric immunosensing strips fabricated by Au nanoparticles-modified screen-printed carbon electrodes for the detection of foodborne pathogen Escherichia coli O157:H7." Biosens Bioelectron **23**(12): 1832-7.

Liu, R. H., J. Yang, et al. (2004). "Self-Contained, Fully Integrated Biochip for Sample Preparation, Polymerase Chain Reaction Amplification, and DNA Microarray Detection." Analytical Chemistry **76**(7): 1824-1831.

Liu, W., J. Kumar, et al. (1998). "Enzymatically Synthesized Conducting Polyaniline." Journal of the American Chemical Society **121**(1): 71-78.

Maalouf, R., C. Fournier-Wirth, et al. (2007). "Label-Free Detection of Bacteria by Electrochemical Impedance Spectroscopy: Comparison to Surface Plasmon Resonance." Analytical Chemistry **79**(13): 4879-4886.

Maalouf, R., W. Hassen, et al. (2008). "Comparison of two innovatives approaches for bacterial detection: paramagnetic nanoparticles and self-assembled multilayer processes." Microchimica Acta **163**(3): 157-161.

Mantzila, A. G., V. Maipa, et al. (2008). "Development of a Faradic Impedimetric Immunosensor for the Detection of Salmonella typhimurium in Milk." Analytical Chemistry **80**(4): 1169-1175.

Marquis, R. E. and E. L. Carstensen (1973). "Electric Conductivity and Internal Osmolality of Intact Bacterial Cells." Journal of Bacteriology **113**(3): 1198-1206.

Muhammad-Tahir, Z., E. C. Alocilja, et al. (2005). "Rapid detection of bovine viral diarrhea virus as surrogate of bioterrorism agents." Sensors Journal, IEEE **5**(4): 757-762.

NIAID. (2009, 9 December 2009). "Biodefense: NIAID Category A, B, and C Priority Pathogens." Retrieved 7 October 2010, from www3.niaid.nih.gov/topics/BiodefenseRelated/Biodefense/research/CatA.htm.

Obuchowska, A. (2008). "Quantitation of bacteria through adsorption of intracellular biomolecules on carbon paste and screen-printed carbon electrodes and voltammetry of redox-active probes." Analytical and Bioanalytical Chemistry **390**(5): 1361-1371.

Pal, S. and E. C. Alocilja (2009). "Electrically active polyaniline coated magnetic (EAPM) nanoparticle as novel transducer in biosensor for detection of Bacillus anthracis spores in food samples." Biosens Bioelectron **24**(5): 1437-44.

Pal, S., E. B. Setterington, et al. (2008). "Electrically Active Magnetic Nanoparticles for Concentrating and Detecting Bacillus anthracis Spores in a Direct-Charge Transfer Biosensor." IEEE Sensors Journal **8**(6): 647-654.

Palchetti, I. and M. Mascini (2008). "Electroanalytical biosensors and their potential for food pathogen and toxin detection." Analytical and Bioanalytical Chemistry **391**(2): 455-471.

Perez, F. G., M. Mascini, et al. (1998). "Immunomagnetic Separation with Mediated Flow Injection Analysis Amperometric Detection of Viable *Escherichia coli* O157." Analytical Chemistry **70**(11): 2380-2386.

Prakash, R. (2002). "Electrochemistry of polyaniline: Study of the pH effect and electrochromism." Journal of Applied Polymer Science **83**(2): 378-385.

Pruneanu, S., E. Veress, et al. (1999). "Characterization of polyaniline by cyclic voltammetry and UV-Vis absorption spectroscopy." Journal of Materials Science **34**(11): 2733-2739.

Radke, S. M. and E. C. Alocilja (2004). "Design and fabrication of a microimpedance biosensor for bacterial detection." Sensors Journal, IEEE **4**(4): 434-440.

Radke, S. M. and E. C. Alocilja (2005). "A high density microelectrode array biosensor for detection of E. coli O157:H7." Biosens Bioelectron **20**(8): 1662-7.

Radke, S. M. and E. C. Alocilja (2005). "A microfabricated biosensor for detecting foodborne bioterrorism agents." Sensors Journal, IEEE **5**(4): 744-750.

Rahman, M., P. Kumar, et al. (2008). "Electrochemical Sensors Based on Organic Conjugated Polymers." Sensors **8**(1): 118-141.

Ridpath, J. F. (2010). Bvdv: Detection, Risk Management and Control. Proceedings of Texas Veterinary Medical Association, p. 151-158.

Ruan, C., H. Wang, et al. (2002). "A bienzyme electrochemical biosensor coupled with immunomagnetic separation for rapid detection of Escherichia coli O157:H7 in food samples " Transactions of the ASAE **45**(1): 249–255

Ruan, C., L. Yang, et al. (2002). "Immunobiosensor Chips for Detection of Escherichia coli O157:H7 Using Electrochemical Impedance Spectroscopy." Analytical Chemistry **74**(18): 4814-4820.

Saliki, J. T., R. W. Fulton, et al. (1997). "Microtiter virus isolation and enzyme immunoassays for detection of bovine viral diarrhea virus in cattle serum." J Clinical Microbiol. **35**: 803-807.

Sarno, D. M., S. K. Manohar, et al. (2005). "Controlled interconversion of semiconducting and metallic forms of polyaniline nanofibers." Synthetic Metals **148**(3): 237-243.

Setterington, E. B. and E. C. Alocilja (2010). "Rapid electrochemical detection of polyaniline-labeled Escherichia coli O157:H7." Biosensors and Bioelectronics **In Press, Corrected Proof**.

Shabani, A., M. Zourob, et al. (2008). "Bacteriophage-Modified Microarrays for the Direct Impedimetric Detection of Bacteria." Analytical Chemistry **80**(24): 9475-9482.

Sharma, R., S. Lamba, et al. (2005). "Composition dependent magnetic properties of iron oxide-polyaniline nanoclusters." Journal of Applied Physics **97**(1): 014311-6.

Suehiro, J., T. Hatano, et al. (2005). "Improvement of electric pulse shape for electropermeabilization-assisted dielectrophoretic impedance measurement for high sensitive bacteria detection." Sensors and Actuators B: Chemical **109**(2): 209-215.

Suehiro, J., A. Ohtsubo, et al. (2006). "Selective detection of bacteria by a dielectrophoretic impedance measurement method using an antibody-immobilized electrode chip." Sensors and Actuators B: Chemical **119**(1): 319-326.

Susmel, S., G. G. Guilbault, et al. (2003). "Demonstration of labeless detection of food pathogens using electrochemical redox probe and screen printed gold electrodes." Biosensors and Bioelectronics **18**(7): 881-889.

Tsekenis, G., G.-Z. Garifallou, et al. (2008). "Detection of Fluoroquinolone Antibiotics in Milk via a Labeless Immunoassay Based upon an Alternating Current Impedance Protocol." Analytical Chemistry **80**(23): 9233-9239.

Tu, S.-I., M. Golden, et al. (2005). "Detection of *Escherichia coli* O157:H7 through the formation of sandiwiched complexes with immunomagnetic and fluorescent beads." Journal of Rapid Methods & Automation in Microbiology **13**(4): 269-282.

Varshney, M. and Y. Li (2007). "Interdigitated array microelectrode based impedance biosensor coupled with magnetic nanoparticle-antibody conjugates for detection of Escherichia coli O157:H7 in food samples." Biosens Bioelectron **22**(11): 2408-14.

Varshney, M., Y. Li, et al. (2003). "A chemiluminescence biosensor coupled with immunomagnetic separation for rapid detection of *Salmonella typhimurium*." Journal of Rapid Methods & Automation in Microbiology **11**(2): 111-131.

Varshney, M., Y. Li, et al. (2007). "A label-free, microfluidics and interdigitated array microelectrode-based impedance biosensor in combination with nanoparticles immunoseparation for detection of Escherichia coli O157:H7 in food samples." Sensors and Actuators B: Chemical **128**(1): 99-107.

Varshney, M., L. Yang, et al. (2005). "Magnetic nanoparticle-antibody conjugates for the separation of Escherichia coli O157:H7 in ground beef." J Food Prot **68**(9): 1804-11.

Wang, F. and S. Hu (2009). "Electrochemical sensors based on metal and semiconductor nanoparticles." Microchimica Acta **165**(1): 1-22.

Wang, Z. and G. Jin (2003). "Feasibility of protein A for the oriented immobilization of immunoglobulin on silicon surface for a biosensor with imaging ellipsometry." Journal of Biochemical and Biophysical Methods **57**(3): 203-211.

WHO (2006). Guidelines for drinking-water quality, third edition. World Health Organization**:** 142 -143, 229a - 230, 284 - 285.

Widjojoatmodjo, M. N., A. C. Fluit, et al. (1993). "Comparison of immunomagnetic beads coated with protein A, protein G, or goat anti-mouse immunoglobulins Applications in enzyme immunoassays and immunomagnetic separations." Journal of Immunological Methods **165**(1): 11-19.

Xuan, S., Y.-X. J. Wang, et al. (2009). "Preparation, Characterization, and Catalytic Activity of Core/Shell Fe3O4@Polyaniline@Au Nanocomposites." Langmuir **25**(19): 11835-11843.

Yang, H., H. Li, et al. (2008). "Detection of foodborne pathogens using bioconjugated nanomaterials." Microfluidics and Nanofluidics **5**(5): 571-583.

Yang, H., L. Qu, et al. (2007). "Rapid detection of Listeria monocytogenes by nanoparticle-based immunomagnetic separation and real-time PCR." International Journal of Food Microbiology **118**(2): 132-138.

Yang, L. and Y. Li (2005). "AFM and impedance spectroscopy characterization of the immobilization of antibodies on indium-tin oxide electrode through self-assembled monolayer of epoxysilane and their capture of Escherichia coli O157:H7." Biosensors and Bioelectronics **20**(7): 1407-1416.

Yang, L., Y. Li, et al. (2004). "Interdigitated Array Microelectrode-Based Electrochemical Impedance Immunosensor for Detection of Escherichia coli O157:H7." Analytical Chemistry **76**(4): 1107-1113.

Zhang, D., D. J. Carr, et al. (2009). "Fluorescent bio-barcode DNA assay for the detection of Salmonella enterica serovar Enteritidis." Biosensors and Bioelectronics **24**(5): 1377-1381.

Zourob, M., S. Elwary, et al., Eds. (2008). Principles of Bacterial Detection: Biosensors, Recognition Receptors, and Microsystems. New York NY, Springer.